Morphoelastic models for burn contraction

D. Smits

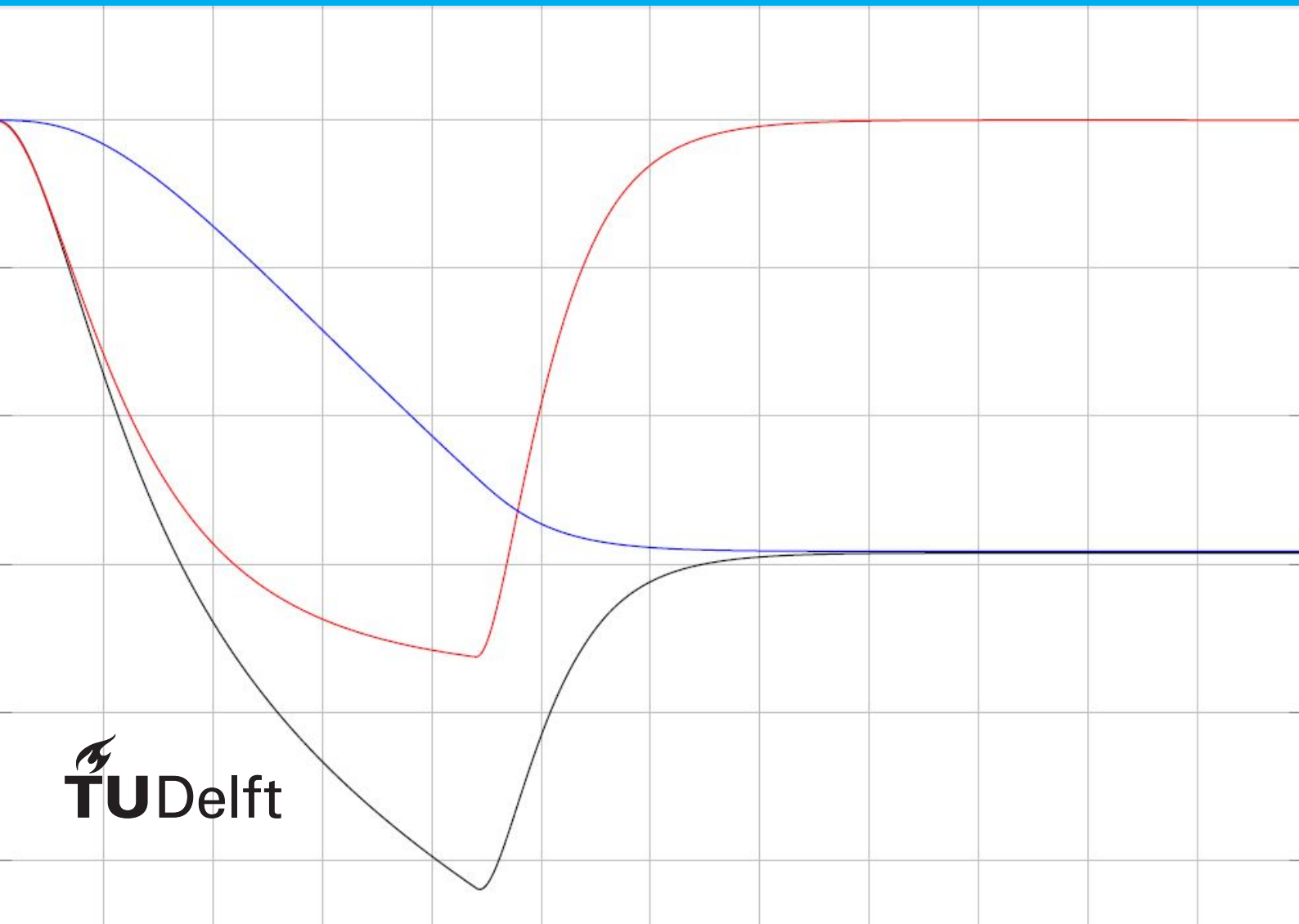

TU Delft

Morphoelastic models for burn contraction

by

D. Smits

to obtain the degree of Master of Science
at the Delft University of Technology,
to be defended publicly on Tuesday September 24, 2019 at 3:00 PM.

Student number:	4092171	
Project duration:	October 23, 2018 – September 24, 2019	
Thesis committee:	Dr. ir. F. J. Vermolen,	TU Delft, supervisor
	Dr. J. L. A. Dubbeldam,	TU Delft
	Dr. H. M. Schuttelaars,	TU Delft

An electronic version of this thesis is available at http://repository.tudelft.nl/.

TU Delft

Contents

1 Introduction

A burn is a type of injury to the skin that may be caused by heat, electricity, radiation, lasers or chemical substances. After a burn has healed, mechanical tension remains. A *contracture* can be defined as a tightening of the skin caused by a burn. Symptoms may include restriction of movement, a feeling of tightness, and pain [1].

Insight in the mechanics involved in the wound healing process that occurs after a burn, results in a better understanding of contractures. Eventually, this could lead to improved treatment. One could, for example, think of splinting a limb in order to minimize the final tightness of the skin.

To describe the mechanical behavior of skin during wound healing, a so-called *morphoelastic* model has been used in [12], [14] and [11]. The idea is to split deformations up into an *elastic* and a *plastic* part.

At the start of this graduation project my supervisor Fred Vermolen told me that he wanted to gain more understanding in how the morphoelasticity models applied to burns work. To do so, in this thesis we will loosely reconstruct some of the models from [12] and [11]. We will start with very rudimentary models, and build on them towards more complicated ones. We will try to understand how most of the models work by walking through derivations. Additionally, we will present results that will highlight the most important features of every model. We will also construct a framework to include a means of heterogeneity in some of the models. Moreover, we will allow for this heterogeneity to be stochastic.

In chapter 2 we will walk through the biology relevant to this project. We will introduce some necessary terminology and we will discuss the effects at play that will be captured by the models.

In chapter 3 we will present some prerequisite theory on stress and strain. Although there are plenty of books that cover this, the models will rely heavily on this theory. For that reason, it is important for the reader to be familiar with it. Also, a chapter on stress and strain gives us the opportunity to introduce some of the notation we will use throughout this thesis.

In chapter 4 we will provide a mathematical derivation or substantiation for each of the models around which this thesis revolves. We will start off fairly easy, so that the reader can finish the chapter with a profound understanding of morphoelasticity.

In chapter 5 we will walk through the Finite Element Method applied to some of the more advanced models. With this chapter, it should be clear how the Finite Element Method can be applied to the simpler models.

In chapter 6, we present results for the models introduced in chapter 4. Some of these results will aim at gaining even more understanding in the models. Others will contain relevant quantitative outputs of the models.

Finally, in chapter **??**, we will briefly summarize the findings of the thesis, and provide some recommendations for future work.

2

Biological background

In this chapter we will walk through the relevant biological background. We will discuss burns, wound healing, contraction and contractures. We will also provide a timeline for wound healing and contraction. This timeline will be helpful in the chapters that follow.

2.1. Layers of the skin

Human skin consists of three layers. See figure 2.1.

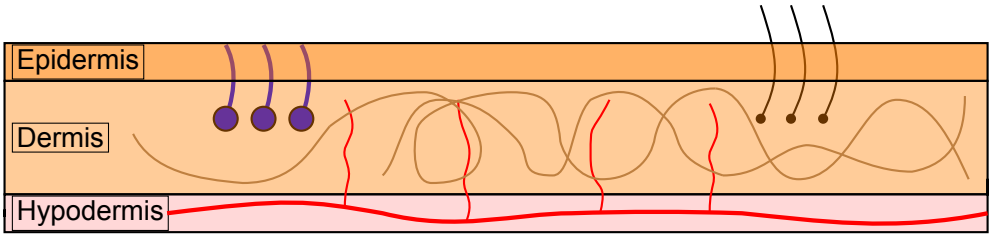

Figure 2.1: A simplified representation of the skin, including sweat glands (blue), hair follicles (black), blood vessels (red), and collagen fibres (brown).

The *epidermis* is the outermost layer, and is relatively thin. Its main functions are providing protection against infection from pathogens, regulating perspiration, and the production of melanin to form a barrier to ultraviolet radiation.

The *dermis* is the middle layer, and is the thickest of the three. It houses biological structures like sweat glands, hair follicles, and blood vessels. The dermis itself consists of cells, such as endothelial cells, immune cells and fibroblasts, and an extracellular matrix. In turn, the extracellular matrix is made up of components such as collagen and elastin. In figure 2.1 the brown strings running through the dermis are collagen fibres. It turns out that the arrangement of these fibres strongly affects the mechanical properties of the skin. In healthy, uninjured skin, the arrangement seems to be random ([12]).

The *hypodermis*, also refered to as the subcutis, connects the dermis to the tissues underneath the skin.

2.2. Burns

A burn is an injury to the skin that can be classified as [2]:

- thermal,
- electrical,
- radiation-induced,

- laser-induced,
- chemical.

All of these types of burns are slightly different from each other. Burns as a class of wound in turn have different characteristics compared to wounds caused by, for example, cuts or infections. Consequently every type of wound will heal in its own way. However, to a large extent the process is always the same, and for that reason in this thesis it will be reasonable to build upon the general wound healing theory.

2.3. Healing of dermal wounds

Superficial wounds, that only affect the epidermis, do usually not cause scars [3]. Therefore the focus will be on wounds involving damage to the dermis, so-called *dermal wounds*. The morphoelastic model, that we will present later in this thesis, will only capture part of the healing process. Also, it will have a rudimentary character, i.e. only the processes that are known to have a large influence will be taken into account. In [1] an elaborate description of the healing process of dermal wounds is given. Here we will essentially give a simplified summary of this description, refraining from introducing too much terminology that is ultimately not reflected by the morphoelastic model.

The body's healing response to dermal wounds can be subdivided into four phases, i.e. *hemostasis*, *inflammation*, *proliferation* and *maturation*. It is important to note that these phases overlap partially.

2.3.1. Hemostasis and inflammation

Upon injury, the hemostasis phase commences. Reactions in the blood lead to the production of fibrin, which forms a clot. See figure 2.2. This stops the bleeding, and, additionally, the clot serves as a

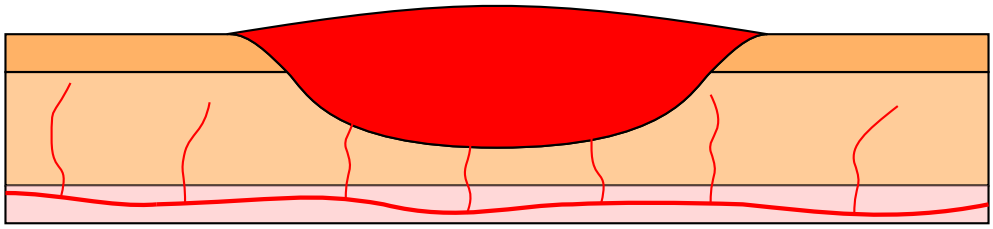

Figure 2.2: Injured skin. A blood cloth (red) has formed during hemostasis.

scaffold for cells to migrate in the absence of an ECM. In the inflammatory phase, blood vessels become more permeable, and white blood cells make their way into the wounded area. Their main function is to prevent infection from pathogens, and to remove dead cells, damaged cells and other debris.

2.3.2. Proliferation

In the proliferation phase *granulation tissue* is formed. Three cell types that play an important role are macrophages, endothelial cells and fibroblasts.

Through the proliferation phase, macrophages continue the removal of debris from the wound, and the protection against pathogenic infection.

Fibroblasts are an important type of cell. The two most important phenotypes are the 'normal' fibroblast, and the *myofibroblast*. It is suggested that there is a third type of fibroblast, called *proto-myofibroblast*. 'Normal' fibroblasts are more mobile than myofibroblasts. However, they are unable to exert significant forces on the granulation tissue and surrounding skin tissue, as opposed to the other types. All of the types can excrete collagen fibres. This is very important in wound healing, because collagen provides scars with the necessary tensile strength. Throughout this thesis we will not distinguish between the three types. Instead, we will use only one type of fibroblast that can exert forces and excrete collagen. We assume that this type is representative for the whole heterogenous fibroblast population.

During the proliferation phase, the fibroblasts will construct an ECM, by laying down collagen fibres. The ECM in uninjured skin is of higher quality than what is seen in granulation tissue. Around 80 to 90 percent of healthy skin consists of so-called *type I collagen*. *Type III collagen* comprises ten to 20

percent [1]. Type I collagen is stronger, while type III collagen can be produced at a faster rate. In granulation tissue the collagen composition is skewed towards type III, where it now accounts for 30%.

Another important process that starts is *angiogenesis*, which is the creation of new blood vessels from ones that exist close to the wound area. To this end, *endothelial cells*, which make up the inside of blood vessels, proliferate, and migrate into the wound. The new blood vessel network will be very important in the proliferation phase: it allows for transport of the debris that leukocytes are trying to remove, and it provides nutrients and oxygen to a variety of cells. Fibroblasts, for example, need oxygen to carry out their work. Additional leukocytes that are needed in the wound area will also start using the newly constructed network.

2.3.3. maturation

As soon as fibroblasts enter the wound, they start remodeling the ECM. In the early stages of the healing process, they break down fibrin and replace it by collagen. As the healing process progresses, they continue to modify the tissue by removing existing collagen fibres and laying down new ones. This remodeling of the tissue is called *maturation*. In this process, which lasts until a mature scar is formed, much of the type III collagen is turned into type I collagen. This will be reflected by the mechanical properties of the tissue.

In figure 2.3 we present a timeline that shows when the phases approximately commence and end. An indication is also given for the period in which the wound experiences contraction.

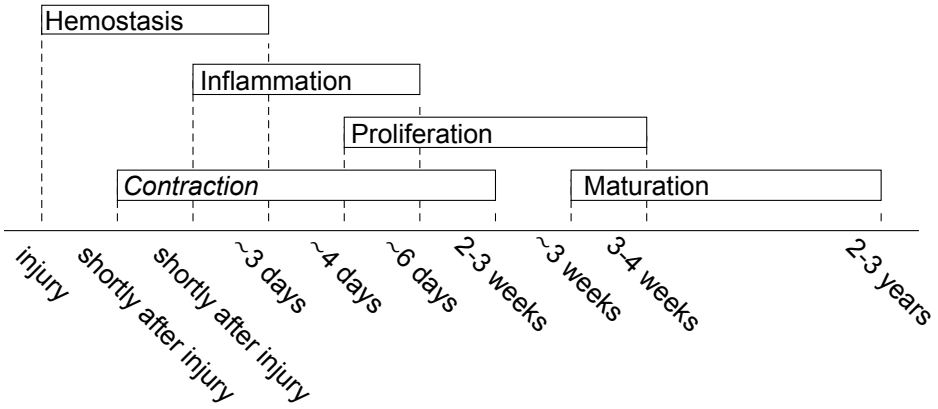

Figure 2.3: A non-linear timeline including the four phases of wound healing, based on [1]. We also included contraction, because of the important role in this thesis. It must be noted that the time values are approximate and may vary from case to case.

2.4. Contraction, mechanical properties and contractures

In view of the change in the composition of the ECM described in subsection **??**, it stands to reason that a scar will have different mechanical properties than uninjured skin. It is not just the type of collagen that plays a role though, the orientation is also essential. It is known that fibroblasts lay down collagen fibres predominantly along the axis subject to the highest normal stress. In scar tissue, the resulting disposition will show a lot of fibres that are roughly parallel to the skin. There is some discord as to how this compares to collagen arrangement in healthy skin. For example, [12] speaks of a random alignment, whereas [1] presumes a “basket weave-like pattern”.

Figures 2.1, 2.2, 2.4 and 2.5 are in chronological order. Together, they visualize the process leading to residual stress and altered mechanical properties of the wounded area.

In terms of strength, it is known that a wound has three percent of its final strength after a week, and 20 percent after three weeks. After three months the strength will be 80 percent of that of uninjured skin, and it will stay at this level.

It can also be seen that after the wound healing process, uninjured skin is spanning a larger area than before. This means that there will be residual stress. This stress defines a contracture. Symptoms are restriction of movement, a feeling of tightness, and pain. Especially contractures resulting from

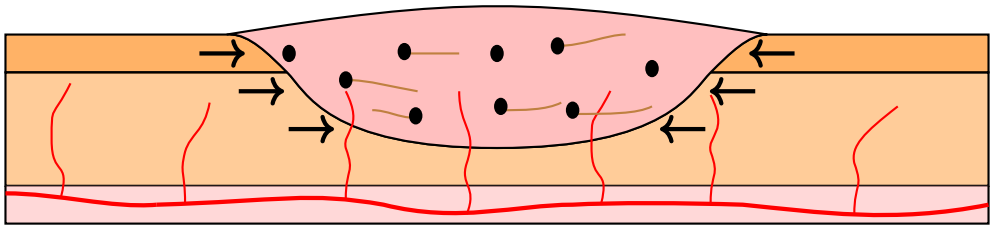

Figure 2.4: Injured skin with granulation tissue (pink). Fibroblasts (black dots) induce contraction, and secrete collagen fibres (brown), oriented along the axis with highest normal stress.

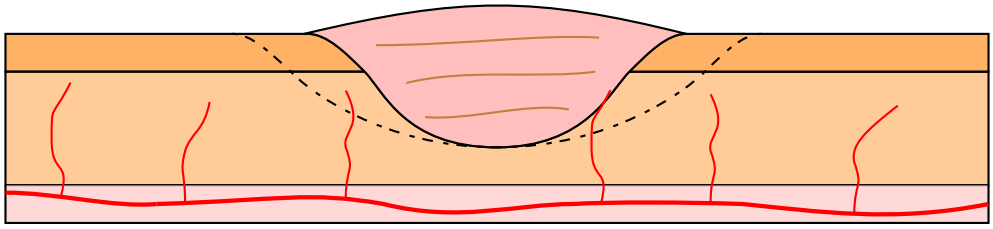

Figure 2.5: Wound in the final stages of the healing process. The uninjured skin is spanning a larger area than it did before contraction. Therefore there will be residual stress. Collagen fibres (brown) in the area that has been injured are now predominantly oriented parallel to the skin.

large burns can lead to serious complications.

In figure 2.6, we can see a contracture.

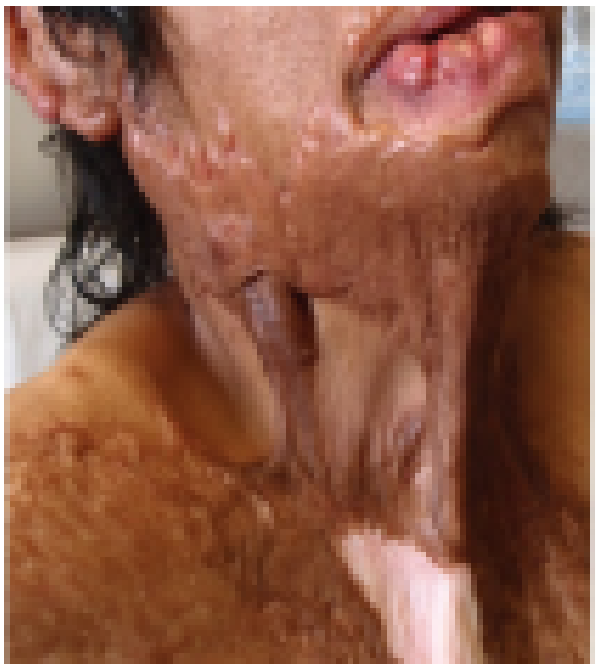

Figure 2.6: A debilitating case of a contracture. This photo was taken from [1].

3

Definitions of stress and strain

In this chapter we will give a brief introduction to stress and strain. We will also discuss some other important topics that would be distracting if we introduced them in other chapters.

3.1. Definition of stress

In physics, stress is a quantity that measures forces that adjacent particles in a material exert on each other. Stress resulting from a force applied perpendicular to an area is called *normal stress*. If the force is applied parallel to the area we call it *shear stress*. In both cases, stress is defined as the force divided by the area over which it is exerted, i.e.:

$$\sigma := \frac{F}{A}. \tag{3.1}$$

In three dimensions, there is a total of three normal stresses, and six shear stresses to be considered. See figure 3.1.

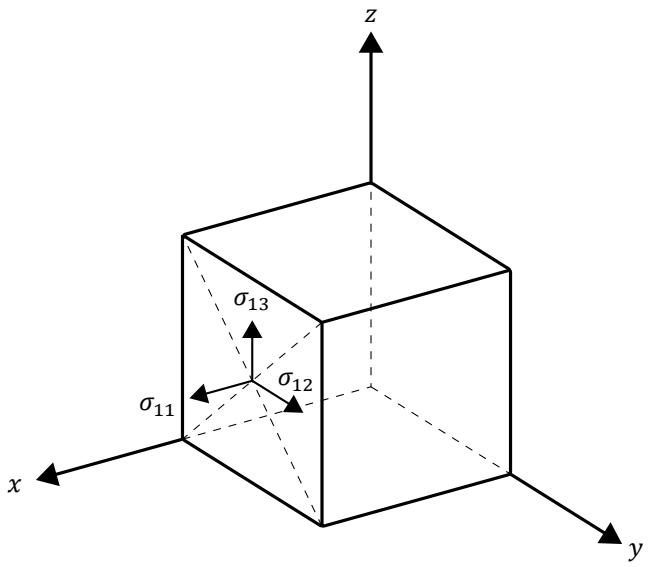

Figure 3.1: A cube subject to stresses.

The stress tensor is then given by:

$$\overline{\overline{\sigma}} := \begin{bmatrix} \sigma_{11} & \sigma_{12} & \sigma_{13} \\ \sigma_{21} & \sigma_{22} & \sigma_{23} \\ \sigma_{31} & \sigma_{32} & \sigma_{33} \end{bmatrix}. \tag{3.2}$$

3.1.1. Symmetry of the stress tensor

Assume that the cube in figure 3.1 is subject to forces, but it *does not rotate*. Then the sum of the momenta must be zero. If the forces are distributed uniformly along the surfaces, we find that:

$$\sigma_{12} - \sigma_{21} = 0, \tag{3.3}$$

$$\sigma_{13} - \sigma_{31} = 0, \tag{3.4}$$

$$\sigma_{23} - \sigma_{32} = 0. \tag{3.5}$$

This shows that $\overline{\overline{\sigma}}$ must be symmetric.

3.2. Eulerian vs. Lagrangian and the material derivative

Let $x := x(X,t)$ be a flow, where X is the initial position of a particle, and x is the position of the particle with initial coordinates X, at time t. Consider a physical quantity c that depends on space and time. There are two common ways of looking at the quantity. Firstly, we can look at a specific point, and see how c evolves over time. In this case, we usually write $c := c(x,t)$. We call this the *Eulerian specification* of c.

Secondly, we can follow a particle, and see how c evolves as the particle moves through the fluid. It is common to label the particle using its initial position. We can write $c := c(X,t) := c(x(X,t),t)$, where $x(X,t)$ is the position at time of the particle with initial position X. This is called the *Lagrangian specification* of c, and in this thesis we will call X the *Lagrangian coordinates* or *initial position* of the particle. Similarly, we will call x the *Eulerian coordinates* or *current position* of the particle.

In this setting, derivatives depend on the specification we use. If we want to know the rate of change of c with respect to time at a fixed position x, we simply regard $\partial c/\partial t$. However, if we are interested in the rate of change of c experienced by a particle as it moves through fluid, we have to consider:

$$\frac{\mathrm{d}(c(x,t))}{\mathrm{d}t} = \frac{\partial c}{\partial t} + \frac{\mathrm{d}x}{\mathrm{d}t} \cdot \nabla^E c = \frac{\partial c}{\partial t} + v \cdot \nabla^E c, \tag{3.6}$$

where $\nabla^E = (\partial/\partial x, \partial/\partial y, \partial/\partial z)^T$ is the so-called *Eulerian gradient operator*, and $v := v(X,t) := v(x(X,t),t)$ is the velocity at time t of the particle with initial position X. Here we used the chain rule for differentiation.

Because the distinction between the two types of derivatives is so important, the latter has its own notation in most texts; the *material derivative* is defined by:

$$\frac{\mathrm{D}c}{\mathrm{D}t} = \frac{\partial c}{\partial t} + v \cdot \nabla^E c. \tag{3.7}$$

3.3. Definition of strain

Displacement is defined as the difference between a particle's current and initial position. The distinction between Eulerian and Lagrangian coordinates comes in handy now. We have, in one dimension:

$$u(x) = x - X, \tag{3.8}$$

where u is the displacement of a particle with current position x and initial position X. In three dimensions we have:

$$u(x) = x - X, \tag{3.9}$$

where u is the displacement of a particle with current position $x = (x,y,z)^T$ and initial position $X = (X,Y,Z)^T$. *Strain* is a measure of deformation. One can define strain for a body as a whole. In one dimension, if a body with initial length l undergoes a stress such that it has current length l', then a possible definition is:

$$\epsilon := \frac{l' - l}{l}. \tag{3.10}$$

Often more useful is a *local* definition of strain. The local analagon of (3.10) is:

$$\epsilon := \frac{\partial u}{\partial X}. \tag{3.11}$$

As the derivative is taken with respect to X, we call this the *Lagrangian strain*. Similarly, the *Eulerian strain* is given by:

$$\epsilon := \frac{\partial u}{\partial x}. \tag{3.12}$$

In three dimensions we have for the Lagrangian strain:

$$\bar{\bar{\epsilon}} = \begin{pmatrix} \epsilon_{11} & \epsilon_{12} & \epsilon_{13} \\ \epsilon_{21} & \epsilon_{22} & \epsilon_{23} \\ \epsilon_{31} & \epsilon_{32} & \epsilon_{33} \end{pmatrix} := \frac{1}{2}(\nabla^L u + (\nabla^L u)^T), \tag{3.13}$$

where $\nabla^L = (\partial/\partial X, \partial/\partial Y, \partial/\partial Z)^T$ is the Lagrangian gradient operator. The three-dimensional Eulerian strain is defined as:

$$\bar{\bar{\epsilon}} := \frac{1}{2}(\nabla^E u + (\nabla^E u)^T). \tag{3.14}$$

There are plenty of other definitions of strain. In [14], for example, the following is considered:

$$\bar{\bar{\epsilon}} := (\nabla^L x)^2 - \nabla^E X. \tag{3.15}$$

It can be seen that the latter suggestion is non-linear, as opposed to the ones listed before.

3.3.1. Symmetry of the strain tensor

The stress tensor is always guaranteed to be symmetric. The same cannot be said for the strain tensor, where this depends on the definition used. For definitions (3.13) and (3.14) taking the transpose easily shows that symmetry holds. If we use another definition, symmetry may either be hard to prove, or not true at all. We will later see that this is an important caveat to keep in mind, and once we have established the morphoelasticity model we will show that the strain tensor that is involved is indeed symmetric.

4

Mathematical models

In this chapter we will consider some models that are well-known in elasticity theory. We will start with the simplest, and build from there. Because we desire to gain qualitative insight in the morphoelastic models that will follow later in this chapter, a solid foundation is necessary. Therefore, we will give derivations for most of the one-dimensional models. The three-dimensional derivations can be tedious whilst not providing a lot more insight, so we will omit them most of the time.

4.1. Pure elasticity in one dimension

4.1.1. Hooke's law

If we assume that there is a function mapping ϵ to σ, we can write

$$\sigma = f(\epsilon). \tag{4.1}$$

For small values of ϵ it is justified to linearize this equation. Since we expect zero stress to correspond to zero strain we have:

$$\sigma = E\epsilon, \tag{4.2}$$

where $E := f'(0)$ is called the *Young's modulus*. This constant is material-dependent. The above equation is known as *Hooke's law*. Although quadratic and higher order approximations are also used in the literature, Hooke's law is most popular. For small deformations it is accurate, while being simpler than higher order approximations. This is particularly helpful when we build upon it to construct more advanced models.

Consider figure 4.1. An example of a stress-strain curve is presented that could be observed in reality. Note that away from $\epsilon = 0$, the relationship is non-linear. However, closer to the origin, Hooke's law is accurate. We assume that all the materials that we will consider in this thesis obey Hooke's law, if we consider small enough strain values.

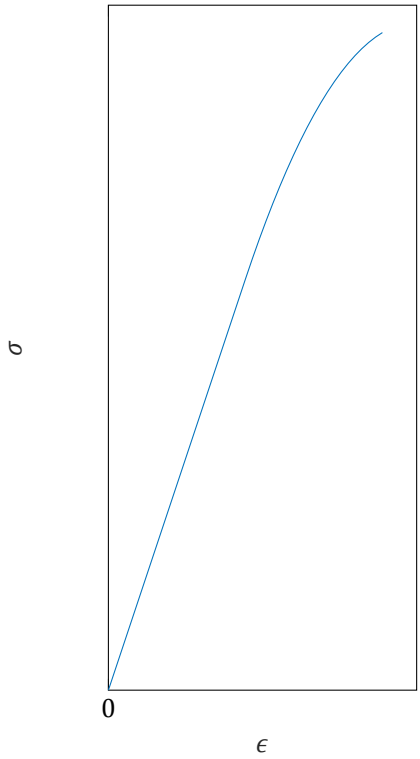

Figure 4.1: An example of a stress-strain curve.

4.2. Pure elasticity in three dimensions

As we have seen in chapter 3, in three dimensions there are six distinct stresses to be considered. For the normal stresses, we have already established (4.2). For shear stresses a similar linearization can be stated:

$$\sigma_{\text{shear}} = G\epsilon_{\text{shear}}. \tag{4.3}$$

As it turns out, the so-called *shear modulus* G can be expressed in terms of E, and another parameter, ν. We will define ν first, and then we will derive the expression for G. After that we will be ready to establish Hooke's law in three dimensions.

4.2.1. The Poisson effect

Consider *Poisson's effect*, depicted in figure 4.2. The figure illustrates what happens if a beam is

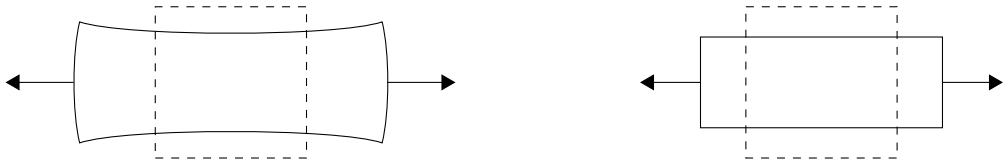

(a) A beam in two dimensions, subject to expansion in the horizontal direction. Contraction occurs in the vertical direction.

(b) A simplification that is justified when looking at a small piece of the beam, making the definition of Poisson's ratio intuitive.

Figure 4.2: Figures illustrating Poisson's effect. In dashed we have the stress-free shape of a beam. The solid lines show the shapes that result when stresses are imposed.

elongated in a certain direction: compression will happen in the two other directions. Conversely, compression in one direction will induce elongation in the other two. This effect can be quantified using

Poisson's ratio:

$$\nu := -\frac{\mathrm{d}\epsilon_y}{\mathrm{d}\epsilon_x} = -\frac{\mathrm{d}\epsilon_z}{\mathrm{d}\epsilon_x}. \tag{4.4}$$

In figure 4.3a we present a simulation of Poisson's effect, performed using model 4.42. The Poisson's ratio used is $\nu = 0.48$. In figure 4.3b the body forces are presented that give rise to the deformation.

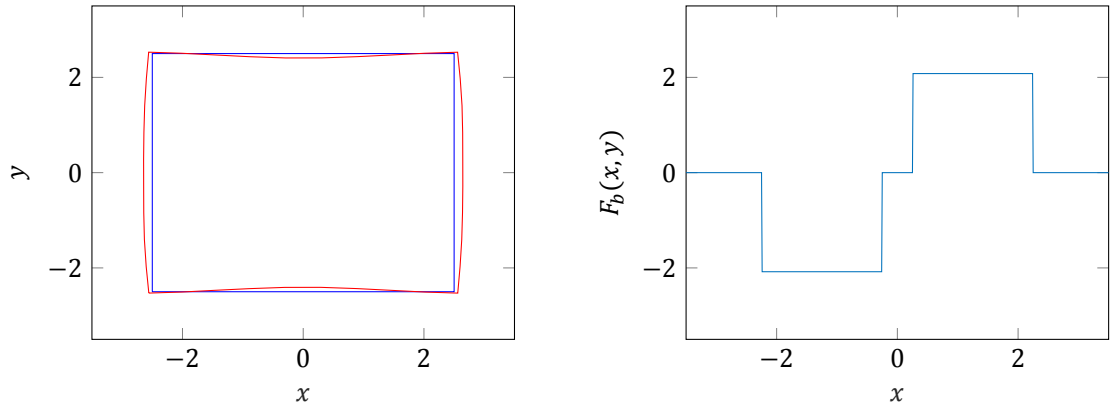

(a) An unstrained square (blue) gets deformed to the red shape, displaying Poisson's effect.

(b) Body force $F_b(\cdot, y)$ for $-3.5 \leq y \leq 3.5$.

Figure 4.3: A simulation illustrating Poisson's effect.

4.2.2. Relationship between elastic constants

The so-called *shear modulus* G can be expressed in terms of E and ν. We will loosely follow a derivation from [16].

We consider figure 4.4a, which shows a side view of a cube with side length a. The lengths of the diagonals (of the face of the cube) are $d_1 = d_2 = \sqrt{2} \cdot a$. In figure 4.4b we see the shape that results

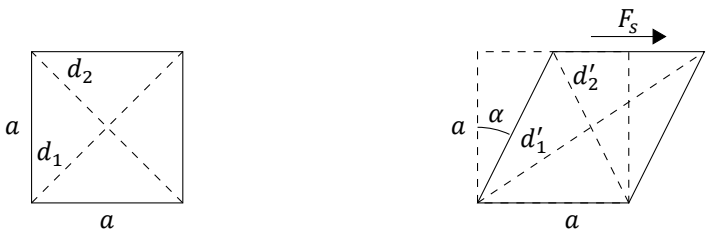

(a) A side view of an unstrained cube

(b) A side view of the cube after shear force F_s has induced strain α

Figure 4.4

when shear force F_s is exerted. We assume that the force is uniformly distributed. The shear strain is usually defined by the angle between the strained shape and the unstrained shape. In our case we have $\epsilon_s = \alpha$. The lengths of the diagonals are now denoted by d_1' and d_2'.

Let us consider the change that d_1 experiences through the straining of the cube. In figure 4.4b we see that the top right corner has moved a distance of $a \tan \alpha$ to the right . For small deformations we have that $a \tan \alpha \approx a\alpha$. This means that:

$$d_1' = \sqrt{a^2 + (a + a\alpha)^2} = \sqrt{2a^2 + 2a^2\alpha + a^2\alpha^2} \approx \sqrt{2a^2 + 2a^2\alpha}. \tag{4.5}$$

Now d_1' can be linearized around $\alpha = 0$ using Taylor's theorem:

$$\begin{aligned} d_1' &\approx \left[\sqrt{2}a\sqrt{1+\alpha}\right]_{\alpha=0} + \left[\frac{1}{2}\sqrt{2}\frac{a}{\sqrt{1+\alpha}}\right]_{\alpha=0} \cdot \alpha \\ &= \sqrt{2}a\left(1+\frac{\alpha}{2}\right). \end{aligned} \tag{4.6}$$

Let us denote $\Delta d_1 := d_1' - d_1$ and $\Delta d_2 = d_2' - d_2$. It follows that the following linearization holds:

$$\frac{\Delta d_1}{d_1} = \frac{d_1' - d_1}{d_1} = \frac{a\alpha}{\sqrt{2}\sqrt{2}a} = \frac{\alpha}{2}. \tag{4.7}$$

We can write the shear strain in terms of the shear stress σ_s, so that:

$$\frac{\Delta d_1}{d_1} = \frac{1}{2}\epsilon_s = \frac{1}{2}\frac{\sigma_s}{G} = \frac{1}{2}\frac{F_s}{Ga^2}. \tag{4.8}$$

Analogously we can show that $\Delta d_2/d_2$ has the same magnitude, but opposite sign.

Now we will consider four of these shear forces, that will add up in such a way that they can be viewed as normal forces. This will allow us to compare normal strain to shear strain. So, consider figure 4.5a. In both the x and the y-direction the strained shape will make an angle of 2α with the

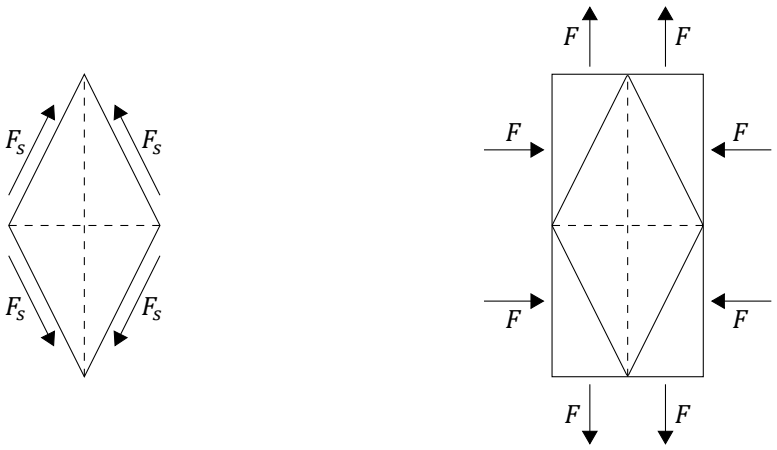

(a) Side view of a strained cube subject to four shear forces

(b) Side view of the strained cube with the shear forces decomposed into forces that can be perceived as normal if we imagine them working on the faces of an imaginary embedding cuboid

Figure 4.5: Side views of an unstrained and a strained cube.

original cube, since there are two shear forces working in each direction. The total shear strain is the sum of these angles, hence we have $\epsilon_s = 2\alpha + 2\alpha = 4\alpha$. The shear stress is also four times as big now, we have $\sigma_s = 4F_s/a^2$. It is easy to show that in this case the deformations of d_1 and d_2 are respectively equal to 2α and -2α.

Each of the shear forces can be decomposed into an x- and y-component. The magnitude of these components must be $F = \frac{1}{2}\sqrt{2}F_s$, because only then we have $\sqrt{F^2 + F^2} = F_s$.

Now imagine the cube embedded in a bigger cuboid, see figure 4.5b in which we show a side view. We will apply the forces with magnitude F to the faces of the cuboid. This gives the same strain as applying them to the cube. To see why, observe that the normal forces F are distributed uniformly, since the shear forces are, and recall that Lagrangian strain is defined relative to original length.

Now both in the x- and y-direction we have a stress with magnitude:

$$\sigma = 4\frac{F}{\frac{1}{2}\sqrt{2}a} = 4\frac{\frac{1}{2}\sqrt{2}F_s}{\frac{1}{2}\sqrt{2}a} = \frac{4F_s}{a}. \tag{4.9}$$

The signs of these stresses are opposite. Now, taking into account the Poisson effect, the deformation in the y-direction is:

$$\epsilon = \frac{4F_s/a}{E} - \nu \cdot \Big(- \frac{4F_s/a}{E} \Big) = \frac{1+\nu}{E} \frac{4F_s}{a}. \tag{4.10}$$

So now we have two expressions for the deformation of d_1. We can equate them, and see that:

$$\frac{1+\nu}{E} \frac{4F_s}{a} = 2\alpha = \frac{1}{2}(4\alpha) = \frac{1}{2}(\epsilon_s) = \frac{1}{2}(4\frac{F_s}{Ga^2}) = 2\frac{F_s}{Ga^2}. \tag{4.11}$$

From this it follows that:

$$G = \frac{E}{2(1+\nu)}. \tag{4.12}$$

N.B.: Assume that an unstrained cube has a vertex that is located in the origin, and three of its edges are on the x-, y- and z-axes. Then here we defined strain as the sum of the angles that the strained cube makes with the axes. This is quite common in the literature. However, some texts use strain α for a strained cube that makes angle α in all three directions. Consequently, they find $E/(1+\nu)$ as an alternative expression for the shear modulus.

4.2.3. Hooke's law in three dimensions

We have now established that:

$$\begin{bmatrix} \epsilon_{11} \\ \epsilon_{22} \\ \epsilon_{23} \end{bmatrix} = \begin{bmatrix} 1/E & -\nu/E & -\nu/E \\ -\nu/E & 1/E & -\nu/E \\ -\nu/E & -\nu/E & 1/E \end{bmatrix} \begin{bmatrix} \sigma_{11} \\ \sigma_{22} \\ \sigma_{33} \end{bmatrix} \tag{4.13}$$

Inverting the matrix gives:

$$\begin{bmatrix} \sigma_{11} \\ \sigma_{22} \\ \sigma_{33} \end{bmatrix} = \frac{E}{1+\nu} \begin{bmatrix} \nu/(1-2\nu)+1 & \nu/(1-2\nu) & \nu/(1-2\nu) \\ \nu/(1-2\nu) & \nu/(1-2\nu)+1 & \nu/(1-2\nu) \\ \nu/(1-2\nu) & \nu/(1-2\nu) & \nu/(1-2\nu)+1 \end{bmatrix} \begin{bmatrix} \epsilon_{11} \\ \epsilon_{22} \\ \epsilon_{33} \end{bmatrix} \tag{4.14}$$

For the shear stresses we have, with our derived expression for G:

$$\begin{bmatrix} \sigma_{12} \\ \sigma_{13} \\ \sigma_{23} \end{bmatrix} = \frac{E}{2(1+\nu)} \begin{bmatrix} \epsilon_{12} \\ \epsilon_{13} \\ \epsilon_{23} \end{bmatrix} \tag{4.15}$$

Assuming the strain tensor is symmetric, it now follows that:

$$\bar{\bar{\sigma}} = \bar{\bar{\epsilon}} + \frac{\nu}{1-2\nu} \mathrm{Tr}(\bar{\bar{\epsilon}}) I, \tag{4.16}$$

where $\mathrm{Tr}(\bar{\bar{\epsilon}}) := \epsilon_{11} + \epsilon_{22} + \epsilon_{33}$ is the *trace* of $\bar{\bar{\epsilon}}$. This is the three-dimensional analogon of Hooke's law.

4.3. Viscous stress

A highly simplified one-dimensional sketch of a *dashpot* is presented in figure 4.6. A rod is connected to a piston, which is immersed in some fluid. The piston is almost as wide as the outer cilinder, so it leaves little space for fluid to flow through. As we try to move the piston by pushing or pulling on the rod, it is hindered by the fluid. Stress results, which in turn slows down. It may be clear that now stress and strain are not related via Hooke's law, because if the rectangle is not moving there should not be any stress. Also, it seems intuitive that moving faster will induce higher stress values. Indeed, it turns out that the stress is proportional to the *rate of change* of strain, i.e.:

$$\sigma = \mu \frac{\partial \epsilon}{\partial t}, \tag{4.17}$$

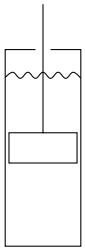

Figure 4.6: A highly simplified sketch of a dashpot

where μ is the dynamic viscosity. The occurrence of this parameter reflects that moving the rectangle through a viscous fluid like honey would induce much larger stresses than moving it through something like water.

If we use $\epsilon = \partial u/\partial x$, then if follows that:

$$\frac{\partial \epsilon}{\partial t} = \frac{\partial}{\partial t}\left(\frac{\partial u}{\partial x}\right) = \frac{\partial}{\partial x}\left(\frac{\partial u}{\partial t}\right) = \frac{\partial v}{\partial x}. \tag{4.18}$$

4.4. Viscoelasticity

4.4.1. One-dimensional

Although the purely elastic and the viscous laws can both be very useful, a lot of materials do not obey them. Rather, they behave like something in between a solid and a fluid, and a so-called *viscoelastic* law is appropriate:

$$\sigma = \mu \frac{\partial v}{\partial x} + E\epsilon. \tag{4.19}$$

This is commonly refered to as the Kelvin-Voigt law. In [14] it is argued that a viscoelastic law will be most appropriate in the development of the morphoelastic model. They base this statement upon experimental findings showing that skin re-expansion in the later stages of wound healing is not instantaneous. Therefore, viscosity should not be ignored.

4.4.2. Three-dimensional

The viscoelastic stress-strain law can be extended to three dimensions. In [11] the following is used:

$$\overline{\overline{\sigma}} = \mu_1 \mathrm{sym}(\nabla v) + (\mu_2 \nabla \cdot v)I + \frac{E\sqrt{\rho}}{1+\nu}\Big(\overline{\overline{\epsilon}} + \frac{\nu}{1-2\nu}\mathrm{Tr}(\overline{\overline{\epsilon}})I\Big). \tag{4.20}$$

Here $v = (u, v, w)^T$, where u, v and w are the velocities in the x-,y- and z-direction respectively. We will not further derive or substantiate this expression. Note however, that compared to the usual elasticity model, here $E\sqrt{\rho}$ is used, by means of which a density-dependent Young's modulus is incorporated.

4.5. The Cauchy momentum equation

The Cauchy momentum equation can be viewed as a transcription of Newton's second law to the framework of stresses. It provides a relationship between accelleration, stress, and body forces. In this section we will derive this equation in three dimensions.

Consider a small cube $\Omega := [x, x+\Delta x] \times [y, y+\Delta y] \times [z, z+\Delta z] \subseteq \mathbb{R}^3$. The impulse in the x-direction is given by:

$$\int_\Omega \rho u \, \mathrm{d}V. \tag{4.21}$$

The forces on Ω can be subdivided into external and internal forces. The external ones can be ex-

pressed in terms of normal and shear stresses:

$$\int_z^{z+\Delta z}\int_y^{y+\Delta y}\big(\sigma_{11}(x+\Delta x)-\sigma_{11}(x)\big)\,\mathrm{d}A \approx \int_\Omega \frac{\partial\,\sigma_{11}}{\partial x}\mathrm{d}V \tag{4.22}$$

$$\int_z^{z+\Delta z}\int_x^{x+\Delta x}\big(\sigma_{21}(y+\Delta y)-\sigma_{21}(y)\big)\,\mathrm{d}A \approx \int_\Omega \frac{\partial\,\sigma_{21}}{\partial y}\mathrm{d}V \tag{4.23}$$

$$\int_y^{y+\Delta y}\int_x^{x+\Delta x}\big(\sigma_{21}(z+\Delta z)-\sigma_{21}(z)\big)\,\mathrm{d}A \approx \int_\Omega \frac{\partial\,\sigma_{31}}{\partial z}\mathrm{d}V. \tag{4.24}$$

For the internal forces we can write:

$$\int_\Omega f\,\mathrm{d}V, \tag{4.25}$$

where f represents force per unit volume, also known as *body force*. Now, by Newton's second law, the rate of change of the impulse with respect to time should be equal to the sum of all forces. So:

$$\frac{\mathrm{d}}{\mathrm{d}t}\int_\Omega \rho u\,\mathrm{d}V = \int_\Omega \big(\nabla\cdot\sigma_{\cdot 1}+f\big)\,\mathrm{d}V. \tag{4.26}$$

For the left-hand side we have, using Reynolds' theorem:

$$\frac{\mathrm{d}}{\mathrm{d}t}\int_\Omega \rho u\,\mathrm{d}V = \int_\Omega \frac{\partial\,(\rho u)}{\partial t}\mathrm{d}V + \int_{\partial\Omega}\big((u\rho u)|_{x+\Delta x}-(u\rho u)|_x\big)\,\mathrm{d}A \tag{4.27}$$

$$= \int_\Omega \frac{\partial(\rho u)}{\partial t}\,\mathrm{d}V + \int_\Omega \frac{\partial(u\rho u)}{\partial x}\,\mathrm{d}V \tag{4.28}$$

$$= \int_\Omega \big(\rho\frac{\partial u}{\partial t}+u\frac{\partial \rho}{\partial t}+u\frac{\partial(\rho u)}{\partial x}+\rho u\frac{\partial u}{\partial x}\big)\,\mathrm{d}V \tag{4.29}$$

$$= \int_\Omega \rho\big(\frac{\partial u}{\partial t}+u\frac{\partial u}{\partial x}\big)\,\mathrm{d}V \tag{4.30}$$

$$= \int_\Omega \rho\frac{\mathrm{D}u}{\mathrm{D}t}\,\mathrm{d}V. \tag{4.31}$$

Here we used that $\frac{\partial\rho}{\partial t}+\frac{\partial(\rho u)}{\partial x}=0$. This equality is known as the *continuity equation*. It now follows that:

$$\int_\Omega \big(\rho\frac{\mathrm{D}u}{\mathrm{D}t}-\nabla\cdot\sigma_{\cdot 1}-f\big)\,\mathrm{d}V = 0. \tag{4.32}$$

Since the choice for Ω was arbitrary, the integrand must be zero. Doing the work for all three dimensions now gives the *convective form* of the *Cauchy momentum equation*:

$$\rho\frac{\mathrm{D}v}{\mathrm{D}t} = \nabla\cdot\overline{\overline{\sigma}}+f. \tag{4.33}$$

The continuity equation in three dimensions reads $\frac{\partial\rho}{\partial t}+\nabla\cdot(\rho v)=0$. We can use this to rewrite the left-handside of (4.33):

$$\rho\frac{\mathrm{D}v}{\mathrm{D}t} = \rho\frac{\mathrm{D}v}{\mathrm{D}t}+\Big(\frac{\partial\rho}{\partial t}+\nabla\cdot(\rho v)\Big)v \tag{4.34}$$

$$= \rho\frac{\partial v}{\partial t}+\rho v\cdot\nabla v+\Big(\frac{\partial\rho}{\partial t}+\rho(\nabla\cdot v)+(v\cdot\nabla\rho)\Big)v \tag{4.35}$$

$$= \frac{\partial(\rho v)}{\partial t}+\rho v\cdot\nabla v+(v\cdot\nabla\rho)v+\rho v(\nabla\cdot v) \tag{4.36}$$

$$= \frac{\partial(\rho v)}{\partial t}+v\cdot\nabla(\rho v)+\rho v(\nabla\cdot v) \tag{4.37}$$

$$= \frac{\mathrm{D}(\rho v)}{\mathrm{D}t}+\rho v(\nabla\cdot v). \tag{4.38}$$

This gives us the *conservation form* of the Cauchy momentum equation:

$$\frac{\mathrm{D}(\rho v)}{\mathrm{D}t} + \rho v(\nabla \cdot v) = \nabla \cdot \overline{\overline{\sigma}} + f. \tag{4.39}$$

4.6. A purely elastic model

Here we consider a simple static model based on pure elasticity, in one dimension. We have:

$$\begin{cases} -\frac{\partial \sigma}{\partial x} = F_b, \\ \sigma = E\epsilon, \\ \epsilon = \frac{\partial u}{\partial x}, \ 0 < x < L \\ u(0) = 0, \\ \sigma(L) = 0. \end{cases} \tag{4.40}$$

This model describes a tissue (or other material) in one dimension, with length L. The second equation can be obtained by taking (4.39) and setting $\mathrm{D}v/\mathrm{D}t = 0$. The solution of this model therefore corresponds to the equilibrium state reached due to the exertion of body force F_b. The fourth equation is a boundary condition corresponding to the tissue being tethered to say a petridish on its left end. The fifth equation is also a boundary condition and indicates that the tissue can move freely on its right end. With these conditions, we have a tissue that can contract and expand, while at the same being fixed in place on one end. This way we do not have to worry about the tissue drifting away because of numerical inaccuracies.

4.7. A one-dimensional dynamical viscoelastic model

Here we consider a dynamical model incorporating viscoelasticity, in one dimension. We have:

$$\begin{cases} \sigma = \mu\frac{\partial v}{\partial x} + E\epsilon, \\ \frac{\mathrm{D}(\rho v)}{\mathrm{D}t} + \rho v\frac{\partial v}{\partial x} = \frac{\partial \sigma}{\partial x} + F_b, \\ \epsilon = \frac{\partial u}{\partial x}, \\ v = \frac{\mathrm{D}u}{\mathrm{D}t}, \ 0 < x < L, \\ u(0) = 0, \\ \sigma(L) = 0. \end{cases} \tag{4.41}$$

We see that the second equation is the one-dimensional analagon of (4.39). We also use the viscoelastic law (4.19) now. This model is dynamical, and this allows us to investigate more closely the interaction between elastic and viscous stresses.

We will vary μ in the simulations. For now, we will use constant density, $\rho = ...$ For the other parameters we use the same values as for (4.40).

4.8. A two-dimensional dynamical viscoelastic model

Here we consider basically the same model as (4.41), but in two dimensions. In order to get the most accurate results, a three-dimensional model would probably be desirable. However, when we get to morphoelasticity, the models will start to get quite computationally expensive. Therefore we choose to work in two dimensions.

Consider (**??**). We set $\epsilon_{13} = \epsilon_{31} = \epsilon_{23} = \epsilon_{32} = \epsilon_{33} = 0$. Furthermore we take (4.39), and set $v_3 = 0$. Let $\Omega := \{(x, y) \in \mathbb{R}^2 : -L/2 < x < L/2, -H/2 < y < H/2\}$. Then we can establish the

following model:

$$\begin{cases} \frac{\mathrm{D}(\rho v_1)}{\mathrm{D}t} + \rho v_1 \nabla \cdot v = \nabla \cdot \sigma_{\cdot 1} + (F_b)_1, \\ \frac{\mathrm{D}(\rho v_2)}{\mathrm{D}t} + \rho v_2 \nabla \cdot v = \nabla \cdot \sigma_{\cdot 2} + (F_b)_2, \\ \sigma_{11} = \mu_1 \frac{\partial v_1}{\partial x} + \mu_2 \nabla \cdot v + \frac{E\sqrt{\rho}}{1+\nu}\left(\epsilon_{11} + \frac{\nu}{1-2\nu}(\epsilon_{11} + \epsilon_{22})\right), \\ \sigma_{12} = \frac{1}{2}\mu_1\left(\frac{\partial v_1}{\partial y} + \frac{\partial v_2}{\partial x}\right) + \frac{E\sqrt{\rho}}{1+\nu}\epsilon_{12}, \\ \sigma_{21} = \frac{1}{2}\mu_1\left(\frac{\partial v_2}{\partial x} + \frac{\partial v_1}{\partial y}\right) + \frac{E\sqrt{\rho}}{1+\nu}\epsilon_{21}, \\ \sigma_{22} = \mu_1 \frac{\partial v_2}{\partial y} + \mu_2 \nabla \cdot v + \frac{E\sqrt{\rho}}{1+\nu}\left(\epsilon_{22} + \frac{\nu}{1-2\nu}(\epsilon_{11} + \epsilon_{22})\right), \\ \epsilon_{11} = \frac{\partial u_1}{\partial x}, \\ \epsilon_{12} = \epsilon_{21} = \frac{1}{2}\left(\frac{\partial u_1}{\partial y} + \frac{\partial u_2}{\partial x}\right), \\ \epsilon_{22} = \frac{\partial u_2}{\partial y},\ x \in \Omega, \\ v_1 = v_2 = 0,\ x \in \partial\Omega, \\ \sigma_{11} = \sigma_{12} = \sigma_{21} = \sigma_{21} = v_1 = v_2 = 0,\ t = 0. \end{cases} \tag{4.42}$$

This model does not contain boundary conditions analogous to the zero-stress conditions imposed on the one-dimensional models presented so far. However, we can emulate the stress-free boundary condition simply by using this model, and considering deformations that happen far away from the boundary.

4.9. One-dimensional morphoelasticity

Here we will introduce *morphoelasticity*. The fundamental idea is to decompose deformations into an elastic and a plastic part. This idea was first presented in [5]. In [12], it was cast into a bio-mathematical framework. In this section we will walk through the derivation of a one-dimensional morphoelasticity equation.

We will loosely follow the construction of the model in [14].

Imagine a tissue that undergoes both plastic and elastic deformations. We denote the initial coordinates of a point in the tissue by X, using Lagrangian coordinates (see section 3.2). Similarly, we denote the current coordinates of a point by x, using Eulerian coordinates. We assume that initially no stresses are imposed on the tissue.

The deformation gradient F that maps X to x is now given by:

$$F = \frac{\partial x}{\partial X}. \tag{4.43}$$

This mapping captures both plastic and elastic deformations. We now decompose F as

$$F = \alpha\gamma, \tag{4.44}$$

where elastic effects should be described by α, and growth effects by γ. Since initially the tissue is stress-free, we infer that the image of γ contains the coordinates of the so-called *zero-stress state* of the tissue. This is an imaginary state in which the tissue has experienced growth, but no stresses are imposed. The coordinates of the tissue in the zero-stress state will be denoted by z.

Using the chain rule for differentiation we see that:

$$F = \frac{\partial x}{\partial X} = \frac{\partial z}{\partial X}\frac{\partial x}{\partial z} = \alpha\gamma, \tag{4.45}$$

where $\alpha = \partial x/\partial z$ is the local size ratio between the current state and the zero-stress state, and $\gamma = \partial z/\partial X$ is the local size ratio between the zero stress state and the initial state.

Figure 4.7 summarizes the above.

In ([14]) it is argued that γ should be of the form:

$$\frac{\mathrm{D}\gamma}{\mathrm{D}t} = Fg(x,t), \tag{4.46}$$

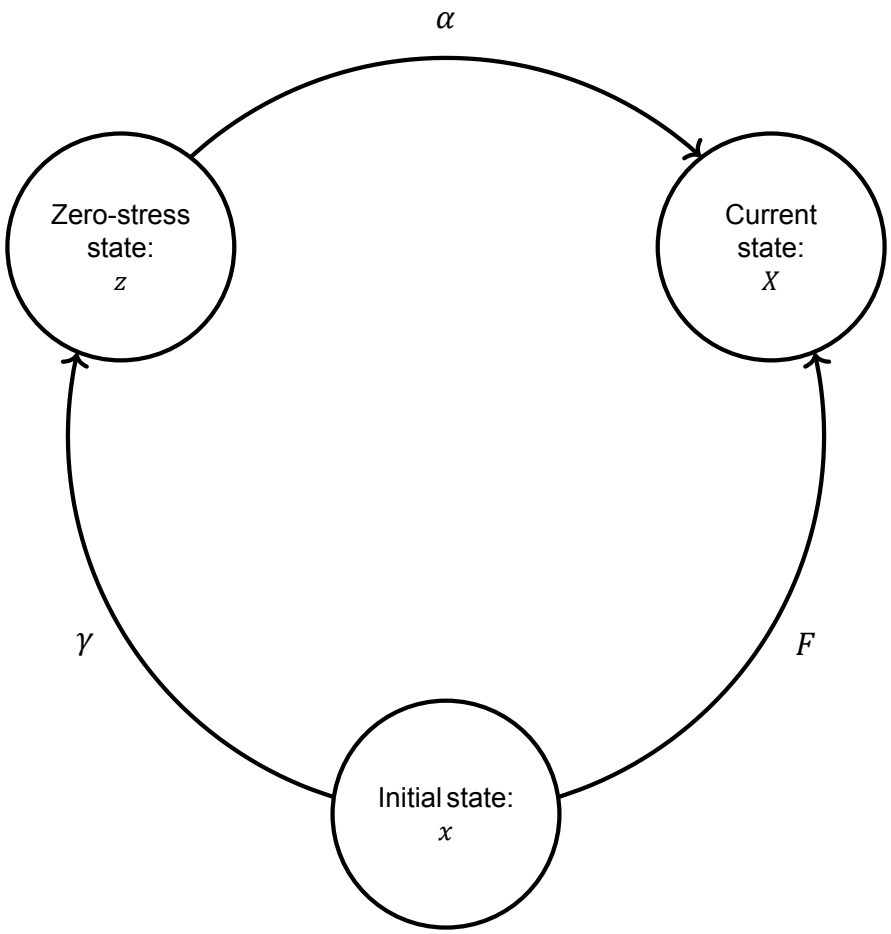

Figure 4.7: The three states underlying the fundamental morphoelasticity assumption, the corresponding coordinates, and the mappings connecting them.

where $g(x,t)$ represents the growth rate of the tissue at position x and time t.

The strain is chosen according to definition (3.12). The main reason for this is that this will result in an elegant equation. Substitution of (4.44) into (4.46) gives:

$$F\frac{\mathrm{D}\alpha^{-1}}{\mathrm{D}t} + \alpha^{-1}\frac{\mathrm{D}F}{\mathrm{D}t} = Fg. \tag{4.47}$$

This means that:

$$\frac{\mathrm{D}\alpha^{-1}}{\mathrm{D}t} + \alpha^{-1}F^{-1}\frac{\mathrm{D}F}{\mathrm{D}t} = g. \tag{4.48}$$

It holds that:

$$F^{-1}\frac{\mathrm{D}F}{\mathrm{D}t} = \frac{\mathrm{D}}{\mathrm{D}t}\left(\frac{\partial x}{\partial X}\right)\frac{\partial X}{\partial x} \tag{4.49}$$

$$= \frac{\partial}{\partial X}\left(\frac{\mathrm{D}x}{\mathrm{D}t}\right)\frac{\partial X}{\partial x} \tag{4.50}$$

$$= \frac{\partial v}{\partial X}\frac{\partial X}{\partial x} \tag{4.51}$$

$$= \frac{\partial v}{\partial x}. \tag{4.52}$$

Substituting this we can write our equation as:

$$\frac{\mathrm{D}(1-\alpha^{-1})}{\mathrm{D}t} + (1-\alpha^{-1}-1)\frac{\partial v}{\partial x} = -g. \tag{4.53}$$

For the Eulerian strain we have:

$$\epsilon = \frac{\partial u}{\partial x} = \frac{\partial x - X}{\partial x} = 1 - \frac{\partial X}{\partial x} = 1 - \alpha^{-1}, \tag{4.54}$$

from which it now follows that:

$$\frac{\mathrm{D}\epsilon}{\mathrm{D}t} + (\epsilon - 1)\frac{\partial v}{\partial x} = -g. \tag{4.55}$$

This equation can be viewed as an evolution equation for the elastic strain. In the remainder of this thesis we will refer to equation (4.55) as the strain evolution equation.

4.10. Three-dimensional morphoelasticity

Every matrix A can be written in terms of a *symmetric part* and a *skew part*:

$$A = \mathrm{sym}(A) + \mathrm{skw}(A), \tag{4.56}$$

where

$$\mathrm{sym}(A) = \frac{1}{2}(A + A^T), \quad \text{and} \tag{4.57}$$

$$\mathrm{skw}(A) = \frac{1}{2}(A - A^T). \tag{4.58}$$

Note that $\mathrm{sym}(A)$ and $\mathrm{skw}(A)$ are respectively symmetric and skew-symmetric, i.e. $[\mathrm{sym}(A)]^T = \mathrm{sym}(A)$ and $[\mathrm{skw}(A)]^T = -\mathrm{skw}(A)$. In [12] the morphoelasticity equation is extended to a three-dimensional one. It reads:

$$\frac{\mathrm{D}\bar{\bar{\epsilon}}}{\mathrm{D}t} + \bar{\bar{\epsilon}}\mathrm{skw}(\nabla v) - \mathrm{skw}(\nabla v)\bar{\bar{\epsilon}} + \big(\mathrm{Tr}(\bar{\bar{\epsilon}}) - 1\big)\mathrm{sym}(\nabla v) = -\bar{\bar{g}} \tag{4.59}$$

Here $\bar{\bar{\epsilon}}$ is the three-dimensional strain tensor, and $\bar{\bar{g}}$ is the three-dimensional growth tensor, analogous to g. The derivation of this equation is very technical, and therefore we will omit it here.

4.10.1. Symmetry of the strain tensor

In section 3.3.1 we noted that symmetry of the strain tensor is not always guaranteed. Having derived a model in $\bar{\epsilon}$ and v, we observe that symmetry would be a convenient property. Indeed, it would reduce the number of variables we have to solve for. As we will see in 5, finding a numerical approximation for the solution of the model is quite a tedious task. We can state the following:

Theorem 1. *Let $\bar{\epsilon}$ be defined by* (4.65)*. Suppose that $\bar{\bar{g}}$ is symmetric for all $t \geq 0$, and $\bar{\epsilon}$ is symmetric at $t = 0$. Then $\bar{\epsilon}$ is symmetric for all $t \geq 0$.*

Proof. By definition $\bar{\epsilon}$ satisfies:

$$\frac{\mathrm{D}\bar{\bar{\epsilon}}}{\mathrm{D}t} + \bar{\bar{\epsilon}}\mathrm{skw}(\nabla v) - \mathrm{skw}(\nabla v)\bar{\bar{\epsilon}} + (\mathrm{Tr}(\bar{\bar{\epsilon}}) - 1)\mathrm{sym}(\nabla v) = -\bar{\bar{g}}. \tag{4.60}$$

We can take the transpose on both sides, to obtain:

$$\frac{\mathrm{D}\bar{\bar{\epsilon}}^T}{\mathrm{D}t} + \mathrm{skw}(\nabla v)^T\bar{\bar{\epsilon}}^T - \bar{\bar{\epsilon}}^T\mathrm{skw}(\nabla v)^T + (\mathrm{Tr}(\bar{\bar{\epsilon}}^T) - 1)\mathrm{sym}(\nabla v)^T = -\bar{\bar{g}}^T. \tag{4.61}$$

Now, because $\text{skw}(\nabla v)^T = -\text{swk}(\nabla v)$, and $\text{sym}(\nabla v)^T = \text{sym}(\nabla v)$, we have:

$$\frac{\mathrm{D}\bar{\bar{\epsilon}}^T}{\mathrm{D}t} - \text{skw}(\nabla v)\bar{\bar{\epsilon}}^T + \bar{\bar{\epsilon}}^T\text{skw}(\nabla v) + (\text{Tr}(\bar{\bar{\epsilon}}) - 1)\text{sym}(\nabla v) = -\bar{\bar{g}}. \tag{4.62}$$

Here we also used the symmetry of $\bar{\bar{g}}$. Subtracting (4.62) from (4.60) gives:

$$\frac{\mathrm{D}(\bar{\bar{\epsilon}} - \bar{\bar{\epsilon}}^T)}{\mathrm{D}t} + (\bar{\bar{\epsilon}} - \bar{\bar{\epsilon}}^T)\text{skw}(\nabla v) - \text{skw}(\nabla v)(\bar{\bar{\epsilon}} - \bar{\bar{\epsilon}}^T) = 0. \tag{4.63}$$

We see that, if $\bar{\bar{\epsilon}} = \bar{\bar{\epsilon}}^T$, then $\mathrm{D}\bar{\bar{\epsilon}}/\mathrm{D}t = 0$. Since $\bar{\bar{\epsilon}}$ is symmetric at $t = 0$, symmetry holds for all $t \geq 0$. □

4.11. A one-dimensional morphoelastic model

By replacing the third equation of (**??**) by our newly established strain evolution equation (4.55), we can obtain the following morpholelastic model:

$$\begin{cases} \sigma = \mu\frac{\partial v}{\partial x} + E\epsilon, \\ \frac{\mathrm{D}(\rho v)}{\mathrm{D}t} + \rho v\frac{\partial v}{\partial x} = \frac{\partial \sigma}{\partial x} + F_b, \\ \frac{\mathrm{D}\epsilon}{\mathrm{D}t} + (\epsilon - 1)\frac{\partial v}{\partial x} = -g, \\ v = \frac{\mathrm{D}u}{\mathrm{D}t},\ 0 < x < L, \\ v(0) = 0, \\ \sigma(L) = 0. \end{cases} \tag{4.64}$$

Note that now ϵ is defined as the second element of the solution pair (v, ϵ) of model (4.64). This model describes the morphoelastic behavior of a one-dimensional tissue, with one edge fixed in place, and one edge moving freely.

4.12. A three-dimensional morphoelastic model

Similarly to the one-dimensional case, we can state a three-dimensional morphoelastic model, by combining mechanics and strain evolution. We have:

$$\begin{cases} \frac{\mathrm{D}(\rho v)}{\mathrm{D}t} + \rho v(\nabla \cdot v) = \nabla \cdot \bar{\bar{\sigma}} + f, \\ \frac{\mathrm{D}\bar{\bar{\epsilon}}}{\mathrm{D}t} + \bar{\bar{\epsilon}}\text{skw}(\nabla v) - \text{skw}(\nabla v)\bar{\bar{\epsilon}} + (\text{Tr}(\bar{\bar{\epsilon}}) - 1)\text{sym}(\nabla v) = -\bar{\bar{g}}, \\ \bar{\bar{\sigma}} = \mu_1\text{sym}(\nabla v) + (\mu_2\nabla \cdot v)I + \frac{E\sqrt{\rho}}{1+\nu}\left(\bar{\bar{\epsilon}} + \frac{\nu}{1-2\nu}\text{Tr}(\bar{\bar{\epsilon}})I\right),\ x \in \Omega, \\ v = 0,\ x \in \partial\Omega, \end{cases} \tag{4.65}$$

where $\Omega := \{(x, y) \in \mathbb{R}^2 : -L/2 < x < L/2, -H/2 < y < H/2, -W/2 < z < W/2\}$. This model describes the morphoelastic behavior of a three-dimensional tissue, fixed in place on its edges.

4.13. A two-dimensional morphoelastic model

We will be working a lot with a two-dimensional model, and for that reason we explicitly state it here. It can be derived from (4.65). Note that we use $\epsilon_{21} = \epsilon_{12}$, which is allowed because we have proven that $\bar{\bar{\epsilon}}$ is symmetric.

We have:

$$\begin{cases} \frac{\mathrm{D}(\rho v_1)}{\mathrm{D}t} + \rho v_1 \nabla \cdot v = \nabla \cdot \sigma_{\cdot 1} + (F_b)_1, \\ \frac{\mathrm{D}(\rho v_2)}{\mathrm{D}t} + \rho v_2 \nabla \cdot v = \nabla \cdot \sigma_{\cdot 2} + (F_b)_2, \\ \frac{\mathrm{D}\epsilon_{11}}{\mathrm{D}t} + \epsilon_{11} \nabla \cdot v = (1-\epsilon_{22}) \frac{\partial v_1}{\partial x} + \epsilon_{11} \frac{\partial v_2}{\partial y} + \frac{1}{2}\left(\frac{\partial v_1}{\partial y} - \frac{\partial v_2}{\partial x}\right)(\epsilon_{21} + \epsilon_{12}) - g_{11}, \\ \frac{\mathrm{D}\epsilon_{12}}{\mathrm{D}t} + \epsilon_{12} \nabla \cdot v = \epsilon_{12}\left(\frac{\partial v_1}{\partial x} + \frac{\partial v_2}{\partial y}\right) + \frac{1}{2}\left((1-2\epsilon_{11}) \frac{\partial v_1}{\partial y} + (1-2\epsilon_{22}) \frac{\partial v_2}{\partial x}\right) - g_{12}, \\ \frac{\mathrm{D}\epsilon_{22}}{\mathrm{D}t} + \epsilon_{22} \nabla \cdot v = (1-\epsilon_{11}) \frac{\partial v_2}{\partial y} + \epsilon_{22} \frac{\partial v_1}{\partial x} - \frac{1}{2}\left(\frac{\partial v_1}{\partial y} - \frac{\partial v_2}{\partial x}\right)(\epsilon_{12} + \epsilon_{21}) - g_{22}, \\ \epsilon_{21} = \epsilon_{12}, \\ \epsilon_{13} = \epsilon_{31} = \epsilon_{23} = \epsilon_{32} = \epsilon_{33} = 0, \\ \sigma_{11} = \mu_1 \frac{\partial v_1}{\partial x} + \mu_2 \nabla \cdot v + \frac{E\sqrt{\rho}}{1+\nu}\left(\epsilon_{11} + \frac{\nu}{1-2\nu}(\epsilon_{11} + \epsilon_{22})\right), \\ \sigma_{12} = \frac{1}{2}\mu_1\left(\frac{\partial v_1}{\partial y} + \frac{\partial v_2}{\partial x}\right) + \frac{E\sqrt{\rho}}{1+\nu}\epsilon_{12}, \\ \sigma_{21} = \frac{1}{2}\mu_1\left(\frac{\partial v_2}{\partial x} + \frac{\partial v_1}{\partial y}\right) + \frac{E\sqrt{\rho}}{1+\nu}\epsilon_{21}, \\ \sigma_{22} = \mu_1 \frac{\partial v_2}{\partial y} + \mu_2 \nabla \cdot v + \frac{E\sqrt{\rho}}{1+\nu}\left(\epsilon_{22} + \frac{\nu}{1-2\nu}(\epsilon_{11} + \epsilon_{22})\right), \ x \in \Omega, \\ v_1 = v_2 = 0, \ x \in \partial\Omega, \end{cases} \tag{4.66}$$

where $\Omega := \{(x, y) \in \mathbb{R}^2 : -L/2 < x < L/2, -H/2 < y < H/2\}$. This model describes the morphoelastic behavior of a two-dimensional tissue, the edges of which are fixed in place.

5

Numerical methods

In this chapter we will derive Finite Element Method (FEM) approximations for some of the models presented in chapter 4. From there it should be clear how FEM approximations for the other models can be derived. If the reader is not familiar with the Finite Element Method, [7] can be consulted for an elaborate description.

5.1. Finite Element Approximations in one dimension

Consider model (4.64). We work through the Finite Element Method (FEM) applied to this model. From there, it should be clear how the same can be done for more rudimentary models.

5.1.1. Weak forms

First we will derive two weak forms: one for the mechanical equation, and one for the strain evolution equation. First we consider:

$$\frac{\mathrm{D}(\rho v)}{\mathrm{D}t} + \rho v \frac{\partial v}{\partial x} = \frac{\partial \sigma}{\partial x} + F_b. \tag{5.1}$$

We will assume that ρ is constant. We multiply the above equation by a test function $\chi \in \Sigma' := \{v \text{ smooth } : v(0) = 0\}$ and integrate over Ω_t. We get:

$$\int_0^{l(t)} \left\{ \rho \frac{\mathrm{D}v}{\mathrm{D}t} + \rho v \frac{\partial v}{\partial x} - \frac{\partial \sigma}{\partial x} - F_b \right\} \chi \, \mathrm{d}x = 0 \tag{5.2}$$

It can be proven that $\mathrm{D}\chi/\mathrm{t} = 0$, if χ is a basis function (see [6]). This means that we can pull χ through the material derivative. If we then work out the material derivative, we get:

$$\int_0^{l(t)} \left\{ \rho \left(\frac{\partial (v\chi)}{\partial t} + v \frac{\partial (v\chi)}{\partial x} + v\chi \frac{\partial v}{\partial x} \right) - \frac{\partial \sigma}{\partial x} \chi - F_b \chi \right\} \mathrm{d}x = 0 \tag{5.3}$$

This can be written as:

$$\int_0^{l(t)} \left\{ \rho \frac{\partial (v\chi)}{\partial t} + \rho \frac{\partial (v^2 \chi)}{\partial x} - \frac{\partial (\sigma \chi)}{\partial x} + \sigma \frac{\partial \chi}{\partial x} - F_b \chi \right\} \mathrm{d}x = 0 \tag{5.4}$$

Now we apply Leibniz' theorem to the first term, and Gauss' theorem to the second and third term. We get:

$$\left(\frac{\mathrm{d}}{\mathrm{d}t} \int_0^{l(t)} \rho v \chi \, \mathrm{d}x - [\rho v^2 \chi]_{x=0}^{x=l(t)} \right) + [\rho v^2 \chi]_{x=0}^{x=l(t)} + [\sigma \chi]_{x=0}^{x=l(t)} + \int_0^{l(t)} \left\{ \sigma \frac{\partial \chi}{\partial x} - F_b \chi \right\} \mathrm{d}x = 0 \tag{5.5}$$

Now we use the boundary conditions. Since $\sigma(l(t)) = 0$ and $\chi(0) = 0$ since $\chi \in \Sigma'$, we get, after tidying up:

$$\frac{\mathrm{d}}{\mathrm{d}t} \int_0^{l(t)} \rho v \chi \, \mathrm{d}x + \int_0^{l(t)} \left\{ \sigma \frac{\partial \chi}{\partial x} - F_b \chi \right\} \mathrm{d}x = 0. \tag{5.6}$$

Recalling that $\sigma = E\epsilon + \mu\frac{\partial v}{\partial x}$, we find as our weak form:

$$\frac{\mathrm{d}}{\mathrm{d}t}\int_0^{l(t)} \rho v\chi \,\mathrm{d}x + \int_0^{l(t)} \Big(E\epsilon + \mu\frac{\partial v}{\partial x}\Big)\frac{\partial \chi}{\partial x}\,\mathrm{d}x = \int_0^{l(t)} F_b\chi \,\mathrm{d}x. \tag{5.7}$$

Secondly we will work towards the weak form of:

$$\frac{\mathrm{D}\epsilon}{\mathrm{D}t} + (\epsilon - 1)\frac{\partial v}{\partial x} = -\zeta\epsilon. \tag{5.8}$$

We multiply by a test function $\eta \in \Sigma := \{\epsilon \text{ smooth}\}$ and integrate over Ω_t. We get:

$$\int_0^{l(t)} \left\{\frac{\mathrm{D}\epsilon}{\mathrm{D}t} + (\epsilon - 1)\frac{\partial v}{\partial x} + \zeta\epsilon\right\}\eta \,\mathrm{d}x = 0. \tag{5.9}$$

As we will later pick η to be a basis function, we can again pull it through the material derivative. We get:

$$\int_0^{l(t)} \left\{\frac{\mathrm{D}(\epsilon\eta)}{\mathrm{D}t} + \eta(\epsilon - 1)\frac{\partial v}{\partial x} + \zeta\eta\epsilon\right\}\mathrm{d}x = 0. \tag{5.10}$$

Working out the material derivative, we get:

$$\int_0^{l(t)} \left\{\frac{\partial(\epsilon\eta)}{\partial t} + v\frac{\partial(\epsilon\eta)}{\partial x} + \eta(\epsilon - 1)\frac{\partial v}{\partial x} + \zeta\eta\epsilon\right\}\mathrm{d}x = 0 \tag{5.11}$$

This is equal to

$$\int_0^{l(t)} \left\{\frac{\partial\epsilon\eta}{\partial t} + \frac{\partial(v\epsilon\eta)}{\partial x} - \eta\frac{\partial v}{\partial x} + \zeta\eta\epsilon\right\}\mathrm{d}x = 0 \tag{5.12}$$

To the first term within the integral we can apply Leibniz' theorem, and to the second term Gauss' theorem (which is the same as the Fundamental Theorem of Calculus in this one-dimensional case). We obtain:

$$\frac{\mathrm{d}}{\mathrm{d}t}\int_0^{l(t)} \epsilon\eta \,\mathrm{d}x - \Big[\frac{\mathrm{d}x}{\mathrm{d}t}\epsilon\eta\Big]_{x=0}^{x=l(t)} + [v\epsilon\eta]_{x=0}^{x=l(t)} + \int_0^{l(t)} \Big\{-\eta\frac{\partial v}{\partial x} + \zeta\eta\epsilon\Big\}\mathrm{d}x = 0. \tag{5.13}$$

Since $v := \mathrm{d}x/\mathrm{d}t$, this simply reduces to:

$$\frac{\mathrm{d}}{\mathrm{d}t}\int_0^{l(t)} \epsilon\eta \,\mathrm{d}x + \int_0^{l(t)} \Big\{-\eta\frac{\partial v}{\partial x} + \zeta\eta\epsilon\Big\}\mathrm{d}x = 0. \tag{5.14}$$

Note: although the original equations are nonlinear, we have established linear weak forms.

5.1.2. Discretization

Now the weak forms that have been established are going to be discretized. Three methods to go about this are:

1. A segregated approach, i.e. we do something like:
   for $t = 0, \Delta t, \ldots, T - \Delta t$, **do**
   determine ϵ at time $t + \Delta t$
   determine v at time $t + \Delta t$
   end for
2. The same segregated approach, but at every timestep we first find v, and then ϵ.
3. A monolithic approach: instead of working segregatedly, we construct a single system from which we can derive both ϵ and v at $t + \Delta t$.

We will work through all three methods, and explore which one will be most suitable.

For both segregated approaches, we will use a forward-in-time method for one of the variables, and a backward-in-time for the other.

To avoid akwardly long equations, we will agree on the following: if an integral is evaluated over Ω_s, then the whole integrand should be evaluated at time s. For example, instead of $\int_{\Omega_{t+\Delta t}} \epsilon_{22}(x(t+\Delta t), t+\Delta t)\eta(x(t+\Delta t), t+\Delta t)\,\mathrm{d}\Omega$ we will simply write $\int_{\Omega_{t+\Delta t}} \epsilon_{22}\eta\,\mathrm{d}\Omega$.

Method 1

Subdivide $[0, l(t)]$ into n elements, denoted by $e_1, \dots, e_n$, so that we have $n+1$ gridpoints: $0 = x_1, \dots, x_{n+1} = l(t)$. Let $v_j(t)$ be the approximation for v in $x = x_j$ at time t, so $v_j(t) \approx v(x_j(t), t)$, for $j = 0, \dots, n$. Now we will approximate v by:

$$v(x,t) \approx \sum_{j=0}^{n} v_j(t)\phi_j(x,t). \tag{5.15}$$

where the ϕ_j are basis functions. Note that they depend on time because x does (we have $\mathrm{D}\phi_j/\mathrm{D}t = 0$, but $\partial\phi_j/\partial t \neq 0$). Because of the boundary condition $v(0) = 0$, it makes sense to impose that $v_0(t) = 0$. So:

$$\sum_{j=0}^{n} v_j(t)\phi_j(x,t) = v_0(t)\phi_0(x,t) + \sum_{j=1}^{n} v_j(t)\phi_j(x,t) = \sum_{j=1}^{n} v_j(t)\phi_j(x,t). \tag{5.16}$$

We will implement Euler Forward, so that (5.7) results in:

$$\int_0^{l(t+\Delta t)} \rho v\chi\,\mathrm{d}x = \int_0^{l(t)} \rho v\chi\,\mathrm{d}x - \Delta t\int_0^{l(t)} \Big(E\epsilon + \mu\frac{\partial v}{\partial x}\Big)\frac{\partial \chi}{\partial x}\,\mathrm{d}x + \Delta t\int_0^{l(t)} F_b\chi\,\mathrm{d}x. \tag{5.17}$$

Now we will choose $\chi = \phi_i$, $i = 1, \dots, n$, and fill in the discretization for v. The resulting system is:

$$\begin{aligned}\rho\sum_{j=1}^{n} v_j(t+\Delta t)\int_0^{l(t+\Delta t)} \phi_j\phi_i\,\mathrm{d}x = \rho\sum_{j=2}^{n+1} v_j(t)\int_0^{l(t)} \rho\phi_j\phi_i\,\mathrm{d}x - \Delta tE\sum_{j=1}^{n+1}\epsilon_j(t)\int_0^{l(t)} \phi_j\frac{\partial\phi_i}{\partial x}\,\mathrm{d}x \\ -\Delta t\mu\sum_{j=2}^{n+1} v_j(t)\int_0^{l(t)} \frac{\partial\phi_j}{\partial x}\frac{\partial\phi_i}{\partial x}\,\mathrm{d}x + \Delta t\int_0^{l(t)} F_b\phi_i\,\mathrm{d}x, \quad i = 2, \dots, n+1.\end{aligned} \tag{5.18}$$

We simplify this a bit, and get:

$$\begin{aligned}\rho\sum_{j=2}^{n+1} v_j(t+\Delta t)\int_0^{l(t+\Delta t)} \phi_j\phi_i\,\mathrm{d}x = \sum_{j=2}^{n+1} v_j(t)\left[\rho\int_0^{l(t)} \phi_j\phi_i\,\mathrm{d}x - \Delta t\mu\int_0^{l(t)} \frac{\partial\phi_j}{\partial x}\frac{\partial\phi_i}{\partial x}\,\mathrm{d}x\right] \\ -\Delta tE\sum_{j=1}^{n+1}\epsilon_j(t)\int_0^{l(t)} \phi_j\frac{\partial\phi_i}{\partial x}\,\mathrm{d}x + \Delta t\int_0^{l(t)} F_b\phi_i\,\mathrm{d}x, \quad i = 2, \dots, n+1.\end{aligned} \tag{5.19}$$

We can now do the same for the strain evolution equation. We will approximate ϵ by:

$$\epsilon(x,t) \approx \sum_{j=0}^{n} \epsilon_j(t)\phi_j(x,t). \tag{5.20}$$

We will use Euler Backward for the strain evolution equation. This way, (5.14) can be expressed as:

$$\int_0^{l(t+\Delta t)} \epsilon\eta\,\mathrm{d}x = \int_0^{l(t)} \epsilon\eta\,\mathrm{d}x + \Delta t\int_0^{l(t+\Delta t)} \Big\{\eta\frac{\partial v}{\partial x} - \zeta\eta\epsilon\Big\}\,\mathrm{d}x. \tag{5.21}$$

This is equivalent to:

$$(1+\Delta t\zeta)\int_0^{l(t+\Delta t)}\epsilon\eta\,\mathrm{d}x=\int_0^{l(t)}\epsilon\eta\,\mathrm{d}x+\Delta t\int_0^{l(t+\Delta t)}\frac{\partial v}{\partial x}\eta\,\mathrm{d}x. \tag{5.22}$$

Now we will choose $\eta=\phi_i,\ i=0,\dots n$, and fill in the discretization for ϵ. This results in the following system:

$$\begin{aligned}(1+\Delta t\zeta)\sum_{j=0}^{n}\epsilon_j(t+\Delta t)\int_0^{l(t+\Delta t)}\phi_j\phi_i\,\mathrm{d}x=\sum_{j=0}^{n}\epsilon_j(t)\int_0^{l(t)}\phi_j\phi_i\,\mathrm{d}x\\ +\Delta t\int_0^{l(t+\Delta t)}\frac{\partial v}{\partial x}\phi_i\,\mathrm{d}x,\quad i=0,\dots,n.\end{aligned} \tag{5.23}$$

Because the integral with the $\partial v/\partial x$-term appears by itself, i.e. it does not have ϵ in it, we could leave it as it is for now. If v is known, we can decide how we compute the corresponding integral in the above equation. For example, we could use forward differences to compute $\partial v/\partial x$ in $x_0,\dots,x_n$ and then use, for example, the trapezium rule to find the value of the integral. However, in order to respect the element-based character of the Finite Element Method, it makes more sense to substitute the approximation for v in terms of basis functions, see (5.16). This gives:

$$\begin{aligned}(1+\Delta t\zeta)\sum_{j=0}^{n}\epsilon_j(t+\Delta t)\int_0^{l(t+\Delta t)}\phi_j\phi_i\,\mathrm{d}x=\sum_{j=0}^{n}\epsilon_j(t)\int_0^{l(t)}\phi_j\phi_i\,\mathrm{d}x\\ +\Delta t\sum_{j=1}^{n}v_j(t+\Delta t)\int_0^{l(t+\Delta t)}\frac{\partial\phi_j}{\partial x}\phi_i\,\mathrm{d}x,\quad i=0,\dots,n.\end{aligned} \tag{5.24}$$

We will write (5.19) in matrix-vector form as

$$\rho M_1^{k+1}v^{k+1}=(\rho M_1^k-\tau\mu M_2^k)v^k-\tau EM_3^k\epsilon^k+\tau F_b^k, \tag{5.25}$$

where $v^k=(v_0((k-1)\Delta t),\dots,v_n((k-1)\Delta t))$, $\epsilon^k=(\epsilon_0((k-1)\Delta t),\dots,\epsilon_n((k-1)\Delta t))$, M_1,M_2,M_3 and M_4 are $(n+1)\times(n+1)$-matrices, and F_b is a vector of length $n+1$. They are defined by the following element matrices and element vector:

$$(M_1^k)_{\text{el}}=\frac{h}{6}\begin{bmatrix}2&1\\1&2\end{bmatrix} \tag{5.26}$$

$$(M_2^k)_{\text{el}}=\frac{1}{h}\begin{bmatrix}1&-1\\-1&1\end{bmatrix} \tag{5.27}$$

$$(M_3^k)_{\text{el}}=\frac{1}{2}\begin{bmatrix}-1&-1\\1&1\end{bmatrix} \tag{5.28}$$

$$(F_b^k)_{\text{el}}=\frac{h}{2}\begin{bmatrix}F_b(x_m^k)\\F_b(x_{m+1}^k)\end{bmatrix} \tag{5.29}$$

where $h:=h_m^k$ is the length of element el with vertices x_m^k and x_{m+1}^k. Note that h_m^{k+1} needs to be determined for all elements before we can compute v^{k+1}. This means that we have to use a forward-in-time method to compute $x_1^{k+1},\dots,x_n^{k+1}$ at every timestep. We use $x_j^{k+1}=x_j^k+\Delta t v_j^k$, which we can use to compute the spacing, $h_m^{k+1}=x_{m+1}^k-x_m^k$.

The full matrices can be found by summing all the element contributions, and then including the boundary condition $v(0)=0$. To do this, observe that if we set $v_0^1=0$, we can just take $v_0^{k+1}=v_1^k$. This amounts to replacing the first row of M_1^k by $[1,0,\dots,0]$, and the first rows of M_2^k and M_3^k by zeros, and then replacing the remainders of the first columns of all three matrices by zeros.

Similarly, we will write (5.24) in matrix-vector form as

$$(1+\Delta t\zeta)N_1^{k+1}\epsilon^{k+1}=N_1^k\epsilon^k+\tau N_2^k v^{k+1}, \tag{5.30}$$

where N_1, N_2 and N_3 are $(n+1)\times(n+1)$-matrices. For the element matrices we get:

$$(N_1^k)_{\text{el}}: \quad \frac{h_m^k}{6}\begin{bmatrix}2 & 1\\ 1 & 2\end{bmatrix}, \tag{5.31}$$

$$(N_2^k)_{\text{el}}: \quad \frac{1}{2}\begin{bmatrix}-1 & 1\\ -1 & 1\end{bmatrix}, \tag{5.32}$$

The full matrices can be found by summing all the element contributions. Notice that there is no boundary condition to be implemented. This is because there is no direct boundary condition imposed on the strain evolution equation. In fact, this equation can be viewed as an ordinary differential equation as it only involves derivatives with respect to t.

Method 2
We will implement Euler Backward, so that (5.7) results in:

$$\int_0^{l(t+\Delta t)} \rho v\chi \,\mathrm{d}x = \int_0^{l(t)} \rho v\chi \,\mathrm{d}x - \Delta t \int_0^{l(t+\Delta t)} \Big(E\epsilon + \mu\frac{\partial v}{\partial x}\Big)\frac{\partial \chi}{\partial x}\,\mathrm{d}x - \Delta t\int_0^{l(t+\Delta t)} F_b\chi\,\mathrm{d}x \tag{5.33}$$

Now we will choose $\eta = \phi_i$, $i = 1, \dots, n$, and fill in the discretization for v. We then obtain:

$$\begin{aligned}\rho\sum_{j=1}^{n} v_j(t+\Delta t)\int_0^{l(t+\Delta t)} \phi_j\phi_i\,\mathrm{d}x = \rho\sum_{j=1}^{n} v_j(t)\int_0^{l(t)}\phi_j\phi_i\,\mathrm{d}x\\ -\Delta tE\sum_{j=0}^{n}\epsilon_j(t+\Delta t)\int_0^{l(t+\Delta t)}\phi_j\frac{\partial\phi_i}{\partial x}\,\mathrm{d}x - \Delta t\mu\sum_{j=2}^{n+1} v_j(t+\Delta t)\int_0^{l(t+\Delta t)}\frac{\partial\phi_j}{\partial x}\frac{\partial\phi_i}{\partial x}\,\mathrm{d}x\\ +\Delta t\int_0^{l(t+\Delta t)} F_b\phi_i\,\mathrm{d}x, \quad i = 1,\dots,n,\end{aligned} \tag{5.34}$$

or equivalently:

$$\begin{aligned}\rho\sum_{j=1}^{n} v_j(t+\Delta t)\left[\int_0^{l(t+\Delta t)}\phi_j\phi_i\,\mathrm{d}x + \Delta t\mu\int_0^{l(t+\Delta t)}\frac{\partial\phi_j}{\partial x}\frac{\partial\phi_i}{\partial x}\,\mathrm{d}x\right] =\\ \sum_{j=1}^{n} v_j(t)\left[\rho\int_0^{l(t)}\phi_j\phi_i\,\mathrm{d}x\right] - \Delta tE\sum_{j=0}^{n}\epsilon_j\int_0^{l(t+\Delta t)}\phi_j\frac{\partial\phi_i}{\partial x}\,\mathrm{d}x + \tau\int_0^{l(t+\Delta t)}F_b\phi_i\,\mathrm{d}x,\\ i = 1,\dots,n.\end{aligned} \tag{5.35}$$

If we use Euler forward, (5.14) can be expressed as:

$$\int_0^{l(t+\Delta t)}\epsilon\eta\,\mathrm{d}x = \int_0^{l(t)}\epsilon\eta\,\mathrm{d}x + \Delta t\int_0^{l(t)}\left\{\eta\frac{\partial v}{\partial x} - \zeta\eta\epsilon\right\}\mathrm{d}x, \tag{5.36}$$

or, equivalently:

$$\int_0^{l(t+\Delta t)}\epsilon\eta\,\mathrm{d}x = (1-\Delta t\zeta)\int_0^{l(t)}\epsilon\eta\,\mathrm{d}x + \Delta t\int_0^{l(t)}\frac{\partial v}{\partial x}\eta\,\mathrm{d}x \tag{5.37}$$

Now we will choose $\eta = \phi_i, i = 1, \dots n+1$, and fill in the discretizations for ϵ and v. This results in the following system:

$$\begin{aligned}\sum_{j=0}^{n}\epsilon_j(t+\Delta t)\int_0^{l(t+\Delta t)}\phi_j\phi_i\,\mathrm{d}x = (1-\Delta t\zeta)\sum_{j=0}^{n}\epsilon_j(t)\int_0^{l(t)}\phi_j\phi_i\,\mathrm{d}x\\ +\tau\sum_{j=1}^{n} v_j(t)\int_0^{l(t)}\frac{\partial\phi_j}{\partial x}\phi_i\,\mathrm{d}x, \quad i = 1,\dots,n+1.\end{aligned} \tag{5.38}$$

We write (5.35) in matrix-vector form as:

$$N_1^{k+1}\epsilon^{k+1} = (1 - \Delta t\zeta)N_1^k\epsilon^k + \Delta t N_2^k v^k, \tag{5.39}$$

and (5.38) as:

$$(\rho M_1^{k+1} + \Delta t\mu M_2^{k+1})v^{k+1} = \rho M_1^k v^k - \Delta t E M_3^{k+1}\epsilon^k + \Delta t\mathbf{F}_b^{k+1}, \tag{5.40}$$

where all the vectors and matrices have the same definition as in 5.1.2.

Method 3
For method 3 we combine the backward-in-time approximations from methods 1 and 2, (5.35) and (5.24). We write this as a matrix-vector system:

$$N^{k+1}w^{k+1} = M^k w^k + \Delta t\hat{F_b}^{k+1}, \tag{5.41}$$

where $w^k = [\epsilon_0^k, \dots, \epsilon_n^k, v_0^k, \dots, v_n^k]^T$, and N^k and M^k are $2(n+1)\times 2(n+1)$-matrices that can be composed by matrices defined earlier as follows:

$$N^k = \begin{bmatrix} (1 + \Delta t\zeta)N_1^k & -\Delta t N_2^k \\ \Delta t E M_3^k & \rho M_1^k + \Delta t\mu M_2^k \end{bmatrix}, \tag{5.42}$$

$$M^k = \begin{bmatrix} N_1^k & 0 \\ 0 & \rho M_1^k \end{bmatrix}, \tag{5.43}$$

where 0 is in this case the $(n+1)\times(n+1)$-matrix consisting of only zeros. Similarly, we define $\hat{F_b}^k := [0, \dots, 0, (F_b^k)^T]^T$.

5.1.3. Choice for the method

The plots in figures were obtained using method 1. Clearly, there is something wrong. It turns out that Euler Forward applied to the mechanical equation is very unstable.

Methods 2 and 3 both give good results. In this thesis we will follow [11], and use a monolithic approach. Hence we choose method 3.

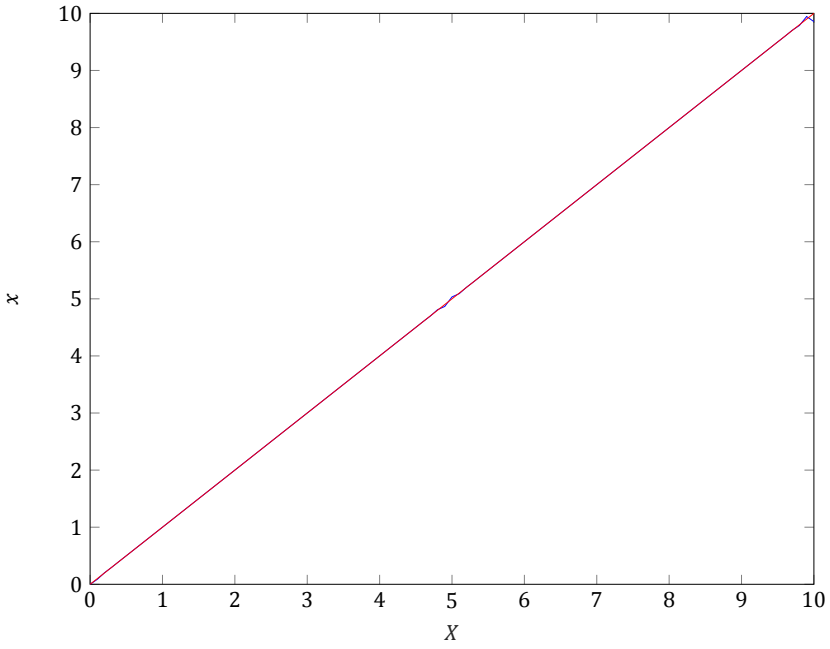

Figure 5.1: Plots of $(X, x(X,t))$ (blue) at $t = 0.25$, using method 1, and (X, X) (red) as a reference.

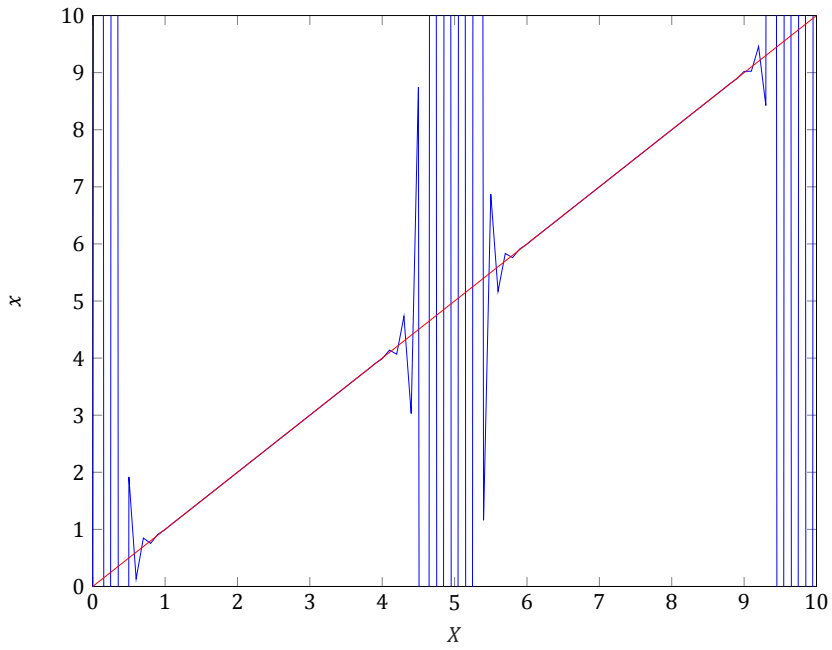

Figure 5.2: Plots of $(X, x(X,t))$ (blue) at $t = 0.3$, using method 1, and (X, X) (red) as a reference.

5.2. Finite Element Approximations in two dimensions

In the one-dimensional case we have compared three methods to discretize a morphoelastic model. We chose the monolithic approach. For the two-dimensional case, we will not walk through different methods again. We will use the monolithic approach straight away. In this section we will walk through the Finite Element Method applied to model (4.66), using a monolithic approach.

5.2.1. Weak forms

We multiply each of the v-equations by the test function η and we integrate over Ω_t. We get:

$$\begin{cases} \int_{\Omega_t} \left\{ \rho \left(\frac{\mathrm{D}v_1}{\mathrm{D}t} + v_1 \nabla \cdot v \right) - \nabla \cdot \sigma_{\cdot 1} \right\} \eta \, \mathrm{d}\Omega = \int_{\Omega_t} (F_b)_1 \eta \, \mathrm{d}\Omega, \\ \int_{\Omega_t} \left\{ \rho \left(\frac{\mathrm{D}v_2}{\mathrm{D}t} + v_2 \nabla \cdot v \right) - \nabla \cdot \sigma_{\cdot 2} \right\} \eta \, \mathrm{d}\Omega = \int_{\Omega_t} (F_b)_2 \eta \, \mathrm{d}\Omega. \end{cases} \tag{5.44}$$

To the stress terms in each equation we can apply the product rule. This gives:

$$\begin{cases} \int_{\Omega_t} \left\{ \rho\eta \left(\frac{\mathrm{D}v_1}{\mathrm{D}t} + v_1 \nabla \cdot v \right) - \nabla \cdot (\sigma_{\cdot 1}\eta) + \sigma_{\cdot 1} \cdot (\nabla \eta) \right\} \mathrm{d}\Omega = \int_{\Omega_t} (F_b)_1 \eta \, \mathrm{d}\Omega, \\ \int_{\Omega_t} \left\{ \rho\eta \left(\frac{\mathrm{D}v_2}{\mathrm{D}t} + v_2 \nabla \cdot v \right) - \nabla \cdot (\sigma_{\cdot 2}\eta) + \sigma_{\cdot 2} \cdot (\nabla \eta) \right\} \mathrm{d}\Omega = \int_{\Omega_t} (F_b)_2 \eta \, \mathrm{d}\Omega. \end{cases} \tag{5.45}$$

Now we can apply Gauss' theorem, to obtain:

$$\begin{cases} \int_{\Omega_t} \left\{ \rho\eta \left(\frac{\mathrm{D}v_1}{\mathrm{D}t} + v_1 \nabla \cdot v \right) + \sigma_{\cdot 1} \cdot (\nabla \eta) \right\} \mathrm{d}\Omega - \int_{\partial\Omega_t} n \cdot (\sigma_{\cdot 1}\eta) \, \mathrm{d}\Gamma = \int_{\Omega_t} (F_b)_1 \eta \, \mathrm{d}\Omega, \\ \int_{\Omega_t} \left\{ \rho\eta \left(\frac{\mathrm{D}v_2}{\mathrm{D}t} + v_2 \nabla \cdot v \right) + \sigma_{\cdot 2} \cdot (\nabla \eta) \right\} \mathrm{d}\Omega - \int_{\partial\Omega_t} n \cdot (\sigma_{\cdot 2}\eta) \, \mathrm{d}\Gamma = \int_{\Omega_t} (F_b)_2 \eta \, \mathrm{d}\Omega, \end{cases} \tag{5.46}$$

where $n = (n_1, n_2, n_3)^T$ is the unit vector pointing away from the surface. Now we will proceed by performing some manipulations that we have seen many times before: pull η through the material derivative, expand the material derivative, apply Reynolds' theorem and tidy up. Some terms cancel out nicely, like in the one-dimensional case, so that we obtain:

$$\begin{cases} \frac{\mathrm{d}}{\mathrm{d}t} \int_{\Omega_t} v_1 \eta \, \mathrm{d}\Omega + \int_{\Omega_t} \sigma_{\cdot 1} \cdot (\nabla \eta) \, \mathrm{d}\Omega - \int_{\partial\Omega_t} n \cdot (\sigma_{\cdot 1}\eta) \, \mathrm{d}\Gamma = \int_{\Omega_t} (F_b)_1 \eta \, \mathrm{d}\Omega, \\ \frac{\mathrm{d}}{\mathrm{d}t} \int_{\Omega_t} v_2 \eta \, \mathrm{d}\Omega + \int_{\Omega_t} \sigma_{\cdot 2} \cdot (\nabla \eta) \, \mathrm{d}\Omega - \int_{\partial\Omega_t} n \cdot (\sigma_{\cdot 2}\eta) \, \mathrm{d}\Gamma = \int_{\Omega_t} (F_b)_2 \eta \, \mathrm{d}\Omega. \end{cases} \tag{5.47}$$

Now we will derive the weak form for the strain evolution equations. We multiply each of the ϵ-equations by a test function ξ and integrate over Ω_t. We get:

$$\begin{cases} \int_{\Omega_t} \left\{ \frac{\mathrm{D}\epsilon_{11}}{\mathrm{D}t} + \epsilon_{11} \nabla \cdot v \right\} \xi \, \mathrm{d}\Omega = \\ \quad \int_{\Omega_t} \left\{ (1-\epsilon_{22}) \frac{\partial v_1}{\partial x} + \epsilon_{11} \frac{\partial v_2}{\partial y} + \frac{1}{2} \left(\frac{\partial v_1}{\partial y} - \frac{\partial v_2}{\partial x} \right) (\epsilon_{21} + \epsilon_{12}) - g_{22} \right\} \xi \, \mathrm{d}\Omega, \\ \int_{\Omega_t} \left\{ \frac{\mathrm{D}\epsilon_{12}}{\mathrm{D}t} + \epsilon_{12} \nabla \cdot v \right\} \xi \, \mathrm{d}\Omega = \\ \quad \int_{\Omega_t} \left\{ \epsilon_{12} \left(\frac{\partial v_1}{\partial x} + \frac{\partial v_2}{\partial y} \right) + \frac{1}{2} \left((1-2\epsilon_{11}) \frac{\partial v_1}{\partial y} + (1-2\epsilon_{22}) \frac{\partial v_2}{\partial x} \right) - g_{12} \right\} \xi \, \mathrm{d}\Omega, \\ \int_{\Omega_t} \left\{ \frac{\mathrm{D}\epsilon_{22}}{\mathrm{D}t} + \epsilon_{22} \nabla \cdot v \right\} \xi \, \mathrm{d}\Omega = \\ \quad \int_{\Omega_t} \left\{ (1-\epsilon_{11}) \frac{\partial v_2}{\partial y} + \epsilon_{22} \frac{\partial v_1}{\partial x} - \frac{1}{2} \left(\frac{\partial v_1}{\partial y} - \frac{\partial v_2}{\partial x} \right) (\epsilon_{21} + \epsilon_{12}) - g_{22} \right\} \xi \, \mathrm{d}\Omega. \end{cases} \tag{5.48}$$

We will do some manipulations to the left-hand sides of the equations. First observe that we can pull ξ through the material derivative. This is because, similar to the one-dimensional case, we have that $\mathrm{D}\xi/\mathrm{D}t = 0$. Working out the material derivative the left-hand sides become:

$$\begin{cases} \int_{\Omega_t} \left\{ \frac{\partial \epsilon_{11} \xi}{\partial t} + v \cdot \nabla(\epsilon_{11}\xi) + \epsilon_{11} \xi \nabla \cdot v \right\} \mathrm{d}\Omega, \\ \int_{\Omega_t} \left\{ \frac{\partial \epsilon_{12} \xi}{\partial t} + v \cdot \nabla(\epsilon_{12}\xi) + \epsilon_{12} \xi \nabla \cdot v \right\} \mathrm{d}\Omega, \\ \int_{\Omega_t} \left\{ \frac{\partial \epsilon_{22} \xi}{\partial t} + v \cdot \nabla(\epsilon_{22}\xi) + \epsilon_{22} \xi \nabla \cdot v \right\} \mathrm{d}\Omega. \end{cases} \tag{5.49}$$

This is, by means of the product rule, equal to

$$\begin{cases} \int_{\Omega_t} \left\{ \frac{\partial \epsilon_{11} \xi}{\partial t} + \nabla \cdot (v \epsilon_{11} \xi) \right\} \mathrm{d}\Omega \\ \int_{\Omega_t} \left\{ \frac{\partial \epsilon_{12} \xi}{\partial t} + \nabla \cdot (v \epsilon_{12} \xi) \right\} \mathrm{d}\Omega \\ \int_{\Omega_t} \left\{ \frac{\partial \epsilon_{22} \xi}{\partial t} + \nabla \cdot (v \epsilon_{22} \xi) \right\} \mathrm{d}\Omega. \end{cases} \tag{5.50}$$

Now we will apply Reynolds' transport theorem, which is the three-dimensional analogon of Leibniz' theorem. We get:

$$\begin{cases} \frac{\mathrm{d}}{\mathrm{d}t} \int_{\Omega_t} \epsilon_{11} \xi \, \mathrm{d}\Omega - \int_{\partial\Omega_t} (v \cdot n) \epsilon_{11} \xi \, \mathrm{d}\Gamma + \int_{\Omega_t} \{ \nabla \cdot (v \epsilon_{11} \xi) \} \, \mathrm{d}\Omega \\ \frac{\mathrm{d}}{\mathrm{d}t} \int_{\Omega_t} \epsilon_{12} \xi \, \mathrm{d}\Omega - \int_{\partial\Omega_t} (v \cdot n) \epsilon_{12} \eta \, \mathrm{d}\Gamma + \int_{\Omega_t} \{ \nabla \cdot (v \epsilon_{12} \xi) \} \, \mathrm{d}\Omega \\ \frac{\mathrm{d}}{\mathrm{d}t} \int_{\Omega_t} \epsilon_{22} \xi \, \mathrm{d}\Omega - \int_{\partial\Omega_t} (v \cdot n) \epsilon_{22} \xi \, \mathrm{d}\Gamma + \int_{\Omega_t} \{ \nabla \cdot (v \epsilon_{22} \xi) \} \, \mathrm{d}\Omega. \end{cases} \tag{5.51}$$

By Gauss' theorem the last two terms of each left-hand side now cancel out, so that we find:

$$\begin{cases} \frac{\mathrm{d}}{\mathrm{d}t} \int_{\Omega_t} \epsilon_{11} \xi \, \mathrm{d}\Omega = \int_{\Omega_t} \left\{ (1-\epsilon_{22}) \frac{\partial v_1}{\partial x} + \epsilon_{11} \frac{\partial v_2}{\partial y} + \frac{1}{2} \left(\frac{\partial v_1}{\partial y} - \frac{\partial v_2}{\partial x} \right) (\epsilon_{21} + \epsilon_{12}) - g_{22} \right\} \xi \, \mathrm{d}\Omega \\ \frac{\mathrm{d}}{\mathrm{d}t} \int_{\Omega_t} \epsilon_{12} \xi \, \mathrm{d}\Omega = \int_{\Omega_t} \left\{ \epsilon_{12} \left(\frac{\partial v_1}{\partial x} + \frac{\partial v_2}{\partial y} \right) + \frac{1}{2} \left((1-2\epsilon_{11}) \frac{\partial v_1}{\partial y} + (1-2\epsilon_{22}) \frac{\partial v_2}{\partial x} \right) - g_{12} \right\} \xi \, \mathrm{d}\Omega \\ \frac{\mathrm{d}}{\mathrm{d}t} \int_{\Omega_t} \epsilon_{22} \xi \, \mathrm{d}\Omega = \int_{\Omega_t} \left\{ (1-\epsilon_{11}) \frac{\partial v_2}{\partial y} + \epsilon_{22} \frac{\partial v_1}{\partial x} - \frac{1}{2} \left(\frac{\partial v_1}{\partial y} - \frac{\partial v_2}{\partial x} \right) (\epsilon_{21} + \epsilon_{12}) - g_{22} \right\} \xi \, \mathrm{d}\Omega \end{cases} \tag{5.52}$$

Finally the weak form for model (4.66) is given by:

$$\begin{cases} \begin{cases} \frac{\mathrm{d}}{\mathrm{d}t} \int_{\Omega_t} \epsilon_{11} \xi \, \mathrm{d}\Omega = \\ \quad \int_{\Omega_t} \left\{ (1-\epsilon_{22}) \frac{\partial v_1}{\partial x} + \epsilon_{11} \frac{\partial v_2}{\partial y} + \frac{1}{2} \left(\frac{\partial v_1}{\partial y} - \frac{\partial v_2}{\partial x} \right) (\epsilon_{21} + \epsilon_{12}) - g_{11} \right\} \xi \, \mathrm{d}\Omega, \\ \frac{\mathrm{d}}{\mathrm{d}t} \int_{\Omega_t} \epsilon_{12} \xi \, \mathrm{d}\Omega = \\ \quad \int_{\Omega_t} \left\{ \epsilon_{12} \left(\frac{\partial v_1}{\partial x} + \frac{\partial v_2}{\partial y} \right) + \frac{1}{2} \left((1-2\epsilon_{11}) \frac{\partial v_1}{\partial y} + (1-2\epsilon_{22}) \frac{\partial v_2}{\partial x} \right) - g_{12} \right\} \xi \, \mathrm{d}\Omega, \\ \frac{\mathrm{d}}{\mathrm{d}t} \int_{\Omega_t} \epsilon_{22} \xi \, \mathrm{d}\Omega = \\ \quad \int_{\Omega_t} \left\{ (1-\epsilon_{11}) \frac{\partial v_2}{\partial y} + \epsilon_{22} \frac{\partial v_1}{\partial x} - \frac{1}{2} \left(\frac{\partial v_1}{\partial y} - \frac{\partial v_2}{\partial x} \right) (\epsilon_{21} + \epsilon_{12}) - g_{22} \right\} \xi \, \mathrm{d}\Omega, \\ \epsilon_{21} = \epsilon_{12}, \end{cases} \\ \begin{cases} \frac{\mathrm{d}}{\mathrm{d}t} \int_{\Omega_t} v_1 \xi \, \mathrm{d}\Omega + \int_{\Omega_t} \sigma_{\cdot 1} \cdot (\nabla \xi) \, \mathrm{d}\Omega - \int_{\partial\Omega_t} n \cdot (\sigma_{\cdot 1} \xi) \, \mathrm{d}\Gamma = \int_{\Omega_t} f_1 \xi \, \mathrm{d}\Omega, \\ \frac{\mathrm{d}}{\mathrm{d}t} \int_{\Omega_t} v_2 \xi \, \mathrm{d}\Omega + \int_{\Omega_t} \sigma_{\cdot 2} \cdot (\nabla \xi) \, \mathrm{d}\Omega - \int_{\partial\Omega_t} n \cdot (\sigma_{\cdot 2} \xi) \, \mathrm{d}\Gamma = \int_{\Omega_t} f_2 \xi \, \mathrm{d}\Omega. \end{cases} \end{cases} \tag{5.53}$$

5.2.2. Discretization

Again we will agree on the following: if an integral is evaluated over Ω_s or $\partial\Omega_s$, then the integrand is evaluated at time s. We will also omit the spatial variable x. For example, instead of $\int_{\Omega_{t+\Delta t}} \epsilon_{11}(x(t+\Delta t), t+\Delta t)\phi_i(x(t+\Delta t), t+\Delta t)\,\mathrm{d}\Omega$ we will simply write $\int_{\Omega_{t+\Delta t}} \epsilon_{11}\phi_i\,\mathrm{d}\Omega$.

Implementing Euler Backwards we now get the following equations:

$$\begin{cases} \int_{\Omega_{t+\Delta t}} v_1\eta\,\mathrm{d}\Omega = \int_{\Omega_t} v_1\eta\,\mathrm{d}\Omega + \Delta t\Big[-\int_{\Omega_{t+\Delta t}} \sigma_{\cdot 2}\cdot(\nabla\eta)\,\mathrm{d}\Omega + \int_{\partial\Omega_{t+\Delta t}} n\cdot(\sigma_{\cdot 1}\eta)\,\mathrm{d}\Gamma \\ \quad + \int_{\Omega_{t+\Delta t}} (F_b)_1\eta\,\mathrm{d}\Omega\Big] \\ \int_{\Omega_{t+\Delta t}} v_2\eta\,\mathrm{d}\Omega = \int_{\Omega_t} v_2\eta\,\mathrm{d}\Omega + \Delta t\Big[-\int_{\Omega_{t+\Delta t}} \sigma_{\cdot 2}\cdot(\nabla\eta)\,\mathrm{d}\Omega + \int_{\partial\Omega_{t+\Delta t}} n\cdot(\sigma_{\cdot 2}\eta)\,\mathrm{d}\Gamma \\ \quad + \int_{\Omega_{t+\Delta t}} (F_b)_2\eta\,\mathrm{d}\Omega\Big] \end{cases} \tag{5.54a}$$

$$\begin{cases} \int_{\Omega_{t+\Delta t}} \epsilon_{11}\chi\,\mathrm{d}\Omega = \int_{\Omega_t} \epsilon_{11}\chi\,\mathrm{d}\Omega + \\ \qquad \Delta t\int_{\Omega_{t+\Delta t}} \Big[(1-\epsilon_{22})\frac{\partial v_1}{\partial x} + \epsilon_{11}\frac{\partial v_2}{\partial y} + \Big(\frac{\partial v_1}{\partial y} - \frac{\partial v_2}{\partial x}\Big)\epsilon_{12} - g_{11}\Big]\chi\,\mathrm{d}\Omega \\ \int_{\Omega_{t+\Delta t}} \epsilon_{12}\chi\,\mathrm{d}\Omega = \int_{\Omega_t} \epsilon_{12}\chi\,\mathrm{d}\Omega + \\ \qquad \Delta t\int_{\Omega_{t+\Delta t}} \Big[\epsilon_{12}\Big(\frac{\partial v_1}{\partial x} + \frac{\partial v_2}{\partial y}\Big) + \frac{1}{2}\Big((1-2\epsilon_{11})\frac{\partial v_1}{\partial y} + (1-2\epsilon_{22})\frac{\partial v_2}{\partial x}\Big) - G_{12}\Big]\chi\,\mathrm{d}\Omega \\ \int_{\Omega_{t+\Delta t}} \epsilon_{22}\chi\,\mathrm{d}\Omega = \int_{\Omega_t} \epsilon_{22}\chi\,\mathrm{d}\Omega + \\ \qquad \Delta t\int_{\Omega_{t+\Delta t}} \Big[(1-\epsilon_{11})\frac{\partial v_2}{\partial y} + \epsilon_{22}\frac{\partial v_1}{\partial x} - \Big(\frac{\partial v_1}{\partial y} - \frac{\partial v_2}{\partial x}\Big)\epsilon_{12} - g_{22}\Big]\chi\,\mathrm{d}\Omega \end{cases} \tag{5.54b}$$

5.2.3. Matrix-vector system for mechanics with pure elasticity

To keep things organized we will present a matrix-vector systems for the mechanical part of (4.66) here, omitting viscous stress. After that we will add viscous stress, and finally we will include the strain evolution equations

We fill in

$$v_1(x,y,t) \approx \sum_{j=1}^{n} (v_1)_j^t \phi_j(x,y,t), \tag{5.55}$$

and $\eta = \phi_i(x,y,t)$, and get:

$$\sum_{j=1,2,3} (v_1)_j^{t+\Delta t} \int_{\mathrm{el}^{t+\Delta t}} \phi_j\phi_i\,\mathrm{d}\Omega = \sum_{j=1,2,3} (v_1)_j^t \int_{\mathrm{el}^t} \phi_j\phi_i\,\mathrm{d}\Omega + \Delta t\Big[-\int_{\mathrm{el}^{t+\Delta t}} \sigma_{11}\frac{\partial\phi_i}{\partial x}\,\mathrm{d}\Omega - \int_{\mathrm{el}^{t+\Delta t}} \sigma_{21}\frac{\partial\phi_i}{\partial y}\,\mathrm{d}\Omega + \int_{\partial\mathrm{el}^{t+\Delta t}} n_1\sigma_{11}\phi_i\,\mathrm{d}\Gamma + \int_{\partial\mathrm{el}^{t+\Delta t}} n_2\sigma_{22}\phi_i\,\mathrm{d}\Gamma + \int_{\partial\mathrm{el}^{t+\Delta t}} (F_b)_1\phi_i\,\mathrm{d}\Omega\Big]. \tag{5.56}$$

Here we denoted by el_t the element with vertices $1, 2$ and 3 at time t, and by $\partial\mathrm{el}_t$ we denoted its boundary. Filling in

$$\sigma_{11} = \frac{E\sqrt{\rho}}{1+\nu}\Big(\epsilon_{11} + \frac{\nu}{1-2\nu}(\epsilon_{11}+\epsilon_{22})\Big), \tag{5.57}$$

$$\sigma_{21} = \frac{E\sqrt{\rho}}{1+\nu}\epsilon_{21}, \tag{5.58}$$

we have:

$$\sum_{j=1,2,3} (v_1)_j^{t+\Delta t} \int_{\mathrm{el}^{t+\Delta t}} \phi_j\phi_i\,\mathrm{d}V = \sum_{j=1,2,3} (v_1)_j^{t+\Delta t} \int_{\mathrm{el}^t} \phi_j\phi_i\,\mathrm{d}V + \Delta t\frac{E\sqrt{\rho}}{1+\nu}\Big[\Big(\frac{1-\nu}{1-2\nu}\sum_{j=1,2,3}(\epsilon_{11})_j^{t+\Delta t} + \frac{\nu}{1-2\nu}\sum_{j=1,2,3}(\epsilon_{22})_j^{t+\Delta t}\Big)\Big\{ -\int_{\mathrm{el}^{t+\Delta t}} \phi_j\frac{\partial\phi_i}{\partial y}\,\mathrm{d}V + n_1\int_{\partial\mathrm{el}^{t+\Delta t}} \phi_j\phi_i\,\mathrm{d}V\Big\} + \sum_{j=1,2,3}(\epsilon_{12})_j^{t+\Delta t}\Big\{ -\int_{\mathrm{el}^{t+\Delta t}} \phi_j\frac{\partial\phi_i}{\partial y}\,\mathrm{d}V + n_2\int_{\partial\mathrm{el}^{t+\Delta t}} \phi_j\phi_i\,\mathrm{d}\Gamma\Big\}\Big] + \Delta t\int_{\mathrm{el}^{t+\Delta t}} (F_b)_1\phi_i\,\mathrm{d}V. \tag{5.59}$$

We denote $v_1^t := [(v_1)_1^t, \dots, (v_1)_n^t]^T$ and $v_2^t := [(v_2)_1^t, \dots, (v_2)_n^t]^T$, where $(v_1)_i^t$ and $(v_2)_i^t$ are the Finite Element Approximations for v_1 and v_2 respectively, at gridpoint i at time t. Also, we denote by $|\Delta| := |\Delta|^t$ the doubled area of an element. We will use the subscripts $1, 2$ and 3 to indicate a symbol belongs to vertex $1, 2$ or 3 of an element. If ϕ_1, ϕ_2 and ϕ_3 are the basis functions corresponding to the three vertices of an element, we can write:

$$\phi_1 := \phi_1(x, y, t) = \alpha_1 + \beta_1 x + \gamma_1 y, \tag{5.60}$$

$$\phi_2 := \phi_2(x, y, t) = \alpha_2 + \beta_2 x + \gamma_2 y, \tag{5.61}$$

$$\phi_3 := \phi_3(x, y, t) = \alpha_3 + \beta_3 x + \gamma_3 y, \tag{5.62}$$

where $\alpha_i := \alpha_i(t)$, $\beta_i := \beta_i(t)$ and $\gamma_i := \gamma_i(t)$ are constant with respect to x and y, $i = 1, 2, 3$. It must hold that:

$$\begin{bmatrix} \alpha_1 & \beta_1 & \gamma_1 \\ \alpha_2 & \beta_2 & \gamma_2 \\ \alpha_3 & \beta_3 & \gamma_3 \end{bmatrix} \begin{bmatrix} 1 & 1 & 1 \\ x_1 & x_2 & x_3 \\ y_1 & y_2 & y_3 \end{bmatrix} = \begin{bmatrix} 1 & 0 & 0 \\ 0 & 1 & 0 \\ 0 & 0 & 1 \end{bmatrix} \tag{5.63}$$

This means that:

$$\begin{bmatrix} \alpha_1 & \beta_1 & \gamma_1 \\ \alpha_2 & \beta_2 & \gamma_2 \\ \alpha_3 & \beta_3 & \gamma_3 \end{bmatrix} = \begin{bmatrix} 1 & 1 & 1 \\ x_1 & x_2 & x_3 \\ y_1 & y_2 & y_3 \end{bmatrix}^{-1}, \tag{5.64}$$

which gives:

$$\begin{bmatrix} \beta_1 & \gamma_1 \\ \beta_2 & \gamma_2 \\ \beta_3 & \gamma_3 \end{bmatrix} = \frac{1}{|\Delta|} \begin{bmatrix} y_2 - y_3 & x_3 - x_2 \\ y_3 - y_1 & x_1 - x_3 \\ y_1 - y_2 & x_2 - x_1 \end{bmatrix}, \tag{5.65}$$

$$\alpha_1 = 1 - \beta_1 x_1 - \gamma_1 y_1, \tag{5.66}$$

$$\alpha_2 = 1 - \beta_2 x_2 - \gamma_2 y_2, \tag{5.67}$$

$$\alpha_3 = 1 - \beta_3 x_3 - \gamma_3 y_3. \tag{5.68}$$

Now we can write (5.59) as a system

$$\begin{aligned} &M^{t+\Delta t} v_1^{t+\Delta t} = M^t v_1^t \\ &+ \Delta t \frac{E\sqrt{\rho}}{1+\nu} \left[(P_1^{t+\Delta t} + P_3^{t+\Delta t}) \left\{ \frac{1-\nu}{1-2\nu} \epsilon_{11}^{t+\Delta t} + \frac{\nu}{1-2\nu} \epsilon_{22}^{t+\Delta t} \right\} + (P_2^{t+\Delta t} + P_4^{t+\Delta t}) \epsilon_{12}^{t+\Delta t} \right] + \Delta t f_{v_1}^{t+\Delta t}, \end{aligned} \tag{5.69}$$

defined by the following element matrices and vector:

$$(M_{\epsilon_{11}}^t)_{\text{el}} = \frac{1}{24} |\Delta| \begin{bmatrix} 2 & 1 & 1 \\ 1 & 2 & 1 \\ 1 & 1 & 2 \end{bmatrix}, \tag{5.70}$$

$$(P_1^t)_{\text{el}} = -\frac{|\Delta|}{6} \begin{bmatrix} \beta_1 & \beta_1 & \beta_1 \\ \beta_2 & \beta_2 & \beta_2 \\ \beta_3 & \beta_3 & \beta_3 \end{bmatrix}, \tag{5.71}$$

$$(P_2^t)_{\text{el}} = -\frac{|\Delta|}{6} \begin{bmatrix} \gamma_1 & \gamma_1 & \gamma_1 \\ \gamma_2 & \gamma_2 & \gamma_2 \\ \gamma_3 & \gamma_3 & \gamma_3 \end{bmatrix}, \tag{5.72}$$

$$(P_3)_{\text{el}}^t = n_1 \frac{|\partial|}{6} I_b \begin{bmatrix} 2 & 1 & 1 \\ 1 & 2 & 1 \\ 1 & 1 & 2 \end{bmatrix}, \tag{5.73}$$

$$(P_4)_{\text{el}}^t = n_2 \frac{|\partial|}{6} I_b \begin{bmatrix} 2 & 1 & 1 \\ 1 & 2 & 1 \\ 1 & 1 & 2 \end{bmatrix}, \tag{5.74}$$

$$(f_{v_1})_{\text{el}}^t = \frac{|\Delta|}{6} \begin{bmatrix} ((F_b)_1)_1 \\ ((F_b)_1)_2 \\ ((F_b)_1)_3 \end{bmatrix}. \tag{5.75}$$

Here, $(n_1, n_2)^T$ is the unit vector pointing outward of a boundary element. For an internal element we impose $n_1 = n_2 = 0$. The length of the boundary segment part of an element is denoted by $|\partial|$. The matrix I_b will consist of only zeros, except for the rows j that correspond to a boundary point. Here we will have a 1 at the j-th position. Worded differently, I_b is the identity matrix where the j-th diagonal entry is set to zero if j corresponds to an internal vertex.

For the equation for v_2 we get, analoguously:

$$\sum_{j=1,2,3}(v_2)_j^{t+\Delta t}\int_{\text{el}^{t+\Delta t}}\phi_j\phi_i\,\mathrm{d}V = \sum_{j=1,2,3}(v_2)_j^{t+\Delta t}\int_{\text{el}^{t}}\phi_j\phi_i\,\mathrm{d}V + \Delta t\frac{E\sqrt{\rho}}{1+\nu}\Bigg[\Bigg(\frac{\nu}{1-2\nu}\sum_{j=1,2,3}(\epsilon_{11})_j^{t+\Delta t} + \frac{1-\nu}{1-2\nu}\sum_{j=1,2,3}(\epsilon_{22})_j^{t+\Delta t}\Bigg)\Bigg\{-\int_{\text{el}^{t+\Delta t}}\phi_j\frac{\partial\phi_i}{\partial y}\,\mathrm{d}V + n_3\int_{\partial\text{el}^{t+\Delta t}}\phi_j\phi_i\,\mathrm{d}V\Bigg\} + \sum_{j=1,2,3}(\epsilon_{12})_j^{t+\Delta t}\Bigg\{-\int_{\text{el}^{t+\Delta t}}\phi_j\frac{\partial\phi_i}{\partial x}\,\mathrm{d}V + n_2\int_{\partial\text{el}^{t+\Delta t}}\phi_j\phi_i\,\mathrm{d}\Gamma\Bigg\}\Bigg] + \Delta t\int_{\text{el}^{t+\Delta t}}(F_b)_2\phi_i\,\mathrm{d}V, \quad (5.76)$$

which results in the following system:

$$M^{t+\Delta t}v_2^{t+\Delta t} = M^t v_2^t + \Delta t\frac{E\sqrt{\rho}}{1+\nu}\Bigg[(P_2^{t+\Delta t}+P_4^{t+\Delta t})\Bigg\{\frac{\nu}{1-2\nu}\epsilon_{11}^{t+\Delta t} + \frac{1-\nu}{1-2\nu}\epsilon_{22}^{t+\Delta t}\Bigg\} + (P_1^{t+\Delta t}+P_3^{t+\Delta t})\epsilon_{12}^{t+\Delta t}\Bigg]. + \Delta t f_{v_2}^{t+\Delta t}. \quad (5.77)$$

Now our full elastic system reads:

$$\begin{bmatrix}M^{t+\Delta t} & \emptyset\\ \emptyset & M^{t+\Delta t}\end{bmatrix}\begin{bmatrix}v_1^{t+\Delta t}\\ v_2^{t+\Delta t}\end{bmatrix} = \begin{bmatrix}M^t & \emptyset\\ \emptyset & M^t\end{bmatrix}\begin{bmatrix}v_1^t\\ v_2^t\end{bmatrix} + \Delta t\frac{E\sqrt{\rho}}{1+\nu}\begin{bmatrix}\frac{1-\nu}{1-2\nu}(P_1^{t+\Delta t}+P_3^{t+\Delta t}) & (P_2^{t+\Delta t}+P_4^{t+\Delta t}) & \frac{\nu}{1-2\nu}(P_1^{t+\Delta t}+P_3^{t+\Delta t})\\ \frac{\nu}{1-2\nu}(P_2^{t+\Delta t}+P_4^{t+\Delta t}) & (P_1^{t+\Delta t}+P_3^{t+\Delta t}) & \frac{1-\nu}{1-2\nu}(P_2^{t+\Delta t}+P_4^{t+\Delta t})\end{bmatrix}\begin{bmatrix}\epsilon_{11}^{t+\Delta t}\\ \epsilon_{12}^{t+\Delta t}\\ \epsilon_{22}^{t+\Delta t}\end{bmatrix} + \Delta t\begin{bmatrix}f_{v_1}^{t+\Delta t}\\ f_{v_2}^{t+\Delta t}\end{bmatrix}. \quad (5.78)$$

5.2.4. Matrix-vector system for mechanics with viscoelasticity

To include viscosity, we must now use the full viscoelastic law (4.20). This amounts to adding the following to the right-hand side of (5.59):

$$\Delta t\Bigg[\sum_{j=1,2,3}(v_1)_j^{t+\Delta t}\Bigg\{(\mu_1+\mu_2)\Bigg(-\int_{\text{el}^{t+\Delta t}}\frac{\partial\phi_j}{\partial x}\frac{\partial\phi_i}{\partial x}\,\mathrm{d}V + \int_{\partial\text{el}^{t+\Delta t}}n_x\frac{\partial\phi_j}{\partial x}\phi_i\,\mathrm{d}\Gamma\Bigg) - \mu_1\int_{\text{el}^{t+\Delta t}}\frac{\partial\phi_j}{\partial z}\frac{\partial\phi_i}{\partial y}\,\mathrm{d}V + \frac{\mu_1}{2}\int_{\partial\text{el}^{t+\Delta t}}n_y\frac{\partial\phi_j}{\partial y}\phi_i\,\mathrm{d}\Gamma\Bigg\} + \sum_{j=1,2,3}(v_2)_j^{t+\Delta t}\Bigg\{-\mu_2\int_{\text{el}^{t+\Delta t}}\frac{\partial\phi_j}{\partial y}\frac{\partial\phi_i}{\partial x}\,\mathrm{d}V - \frac{\mu_1}{2}\int_{\text{el}^{t+\Delta t}}\frac{\partial\phi_j}{\partial x}\frac{\partial\phi_i}{\partial y}\,\mathrm{d}V + \mu_2\int_{\partial\text{el}^{t+\Delta t}}n_x\frac{\partial\phi_j}{\partial y}\phi_i\,\mathrm{d}\Gamma + \frac{\mu_1}{2}\int_{\partial\text{el}^{t+\Delta t}}n_y\frac{\partial\phi_j}{\partial x}\phi_i\,\mathrm{d}\Gamma\Bigg\}\Bigg]. \quad (5.79)$$

We then get the following viscoelastic system:

$$M^{t+\Delta t}v_1^{t+\Delta t} = M^t v_1^t + \Delta t\frac{E\sqrt{\rho}}{1+\nu}\Bigg[(P_1^{t+\Delta t}+P_3^{t+\Delta t})\Bigg\{\frac{1-\nu}{1-2\nu}\epsilon_{11}^{t+\Delta t} + \frac{\nu}{1-2\nu}\epsilon_{22}^{t+\Delta t}\Bigg\} + (P_2^{t+\Delta t}+P_4^{t+\Delta t})\epsilon_{12}^{t+\Delta t}\Bigg] + \Delta t\Bigg[\Bigg\{(\mu_1+\mu_2)(V_1^{t+\Delta t}+V_4^{t+\Delta t}) + \frac{\mu_1}{2}(V_2^{t+\Delta t}+V_7^{t+\Delta t})\Bigg\}v_1 + \Bigg\{\mu_2(V_3^{t+\Delta t}+V_6^{t+\Delta t}) + \frac{\mu_1}{2}((V_3^{t+\Delta t})^T+V_5^{t+\Delta t})\Bigg\}v_2 + f_{v_1}^{t+\Delta t}\Bigg], \quad (5.80)$$

where the $V_1, \dots, V_7$ are defined by the following element matrices:

$$(V_1)_{\text{el}} = -\frac{|\Delta|}{2}\begin{bmatrix}\beta_1\beta_1 & \beta_1\beta_2 & \beta_1\beta_3\\ \beta_2\beta_1 & \beta_2\beta_2 & \beta_2\beta_3\\ \beta_3\beta_1 & \beta_3\beta_2 & \beta_3\beta_3\end{bmatrix}, \tag{5.81}$$

$$(V_2)_{\text{el}} = -\frac{|\Delta|}{2}\begin{bmatrix}\gamma_1\gamma_1 & \gamma_1\gamma_2 & \gamma_1\gamma_3\\ \gamma_2\gamma_1 & \gamma_2\gamma_2 & \gamma_2\gamma_3\\ \gamma_3\gamma_1 & \gamma_3\gamma_2 & \gamma_3\gamma_3\end{bmatrix}, \tag{5.82}$$

$$(V_3)_{\text{el}} = -\frac{|\Delta|}{2}\begin{bmatrix}\beta_1\gamma_1 & \beta_1\gamma_2 & \beta_1\gamma_3\\ \beta_2\gamma_1 & \beta_2\gamma_2 & \beta_2\gamma_3\\ \beta_3\gamma_1 & \beta_3\gamma_2 & \beta_3\gamma_3\end{bmatrix}, \tag{5.83}$$

$$(V_4)_{\text{el}} = n_2\frac{|\partial|}{2}I_b\begin{bmatrix}\beta_1 & \beta_2 & \beta_3\\ \beta_1 & \beta_2 & \beta_3\\ \beta_1 & \beta_2 & \beta_3\end{bmatrix}, \tag{5.84}$$

$$(V_5)_{\text{el}} = n_2\frac{|\partial|}{2}I_b\begin{bmatrix}\gamma_1 & \gamma_2 & \gamma_3\\ \gamma_1 & \gamma_2 & \gamma_3\\ \gamma_1 & \gamma_2 & \gamma_3\end{bmatrix}, \tag{5.85}$$

$$(V_6)_{\text{el}} = n_3\frac{|\partial|}{2}I_b\begin{bmatrix}\beta_1 & \beta_2 & \beta_3\\ \beta_1 & \beta_2 & \beta_3\\ \beta_1 & \beta_2 & \beta_3\end{bmatrix}, \tag{5.86}$$

$$(V_7)_{\text{el}} = n_3\frac{|\partial|}{2}I_b\begin{bmatrix}\gamma_1 & \gamma_2 & \gamma_3\\ \gamma_1 & \gamma_2 & \gamma_3\\ \gamma_1 & \gamma_2 & \gamma_3\end{bmatrix}. \tag{5.87}$$

Analoguously, we can find a system for v_2:

$$\begin{aligned}M^{t+\Delta t}v_2^{t+\Delta t} = M^t v_2^t + \Delta t\frac{E\sqrt{\rho}}{1+\nu}\Bigg[&(P_1^{t+\Delta t}+P_3^{t+\Delta t})\left\{\frac{1-\nu}{1-2\nu}\epsilon_{11}^{t+\Delta t}+\frac{\nu}{1-2\nu}\epsilon_{22}^{t+\Delta t}\right\}\\ &+(P_2^{t+\Delta t}+P_4^{t+\Delta t})\epsilon_{12}^{t+\Delta t}\Bigg] + \Delta t\Bigg[\left\{\mu_2(V_3^{t+\Delta t}+V_6^{t+\Delta t})+\frac{\mu_1}{2}((V_3^{t+\Delta t})^T+V_5^{t+\Delta t})\right\}v_1\\ &+\left\{(\mu_1+\mu_2)(V_1^{t+\Delta t}+V_4^{t+\Delta t})+\frac{\mu_1}{2}(V_2^{t+\Delta t}+V_7^{t+\Delta t})\right\}v_2 + f_{v_2}^{t+\Delta t}\Bigg].\end{aligned} \tag{5.88}$$

This now leads to the full viscoelastic mechanical system:

$$\begin{aligned}\begin{bmatrix}M^{t+\Delta t} & \emptyset\\ \emptyset & M^{t+\Delta t}\end{bmatrix}\begin{bmatrix}v_1^{t+\Delta t}\\ v_2^{t+\Delta t}\end{bmatrix} &= \begin{bmatrix}M^t & \emptyset\\ \emptyset & M^t\end{bmatrix}\begin{bmatrix}v_1^t\\ v_2^t\end{bmatrix}\\ &+\Delta t\frac{E\sqrt{\rho}}{1+\nu}\begin{bmatrix}\frac{1-\nu}{1-2\nu}(P_1+P_3) & (P_2+P_4) & \frac{\nu}{1-2\nu}(P_1+P_3)\\ \frac{\nu}{1-2\nu}(P_2+P_4) & (P_1+P_3) & \frac{1-\nu}{1-2\nu}(P_2+P_4)\end{bmatrix}\begin{bmatrix}\epsilon_{11}^{t+\Delta t}\\ \epsilon_{12}^{t+\Delta t}\\ \epsilon_{22}^{t+\Delta t}\end{bmatrix}\\ &+\Delta t\begin{bmatrix}(\mu_1+\mu_2)(V_1+V_4)+\frac{\mu_1}{2}(V_2+V_7) & \mu_2(V_3+V_6)+\frac{\mu_1}{2}(V_3^T+V_5)\\ \mu_2(V_3+V_6)+\frac{\mu_1}{2}(V_3^T+V_5) & (\mu_1+\mu_2)(V_1+V_4)+\frac{\mu_1}{2}(V_2+V_7)\end{bmatrix}\begin{bmatrix}v_1^{t+\Delta t}\\ v_2^{t+\Delta t}\end{bmatrix}\\ &+\Delta t\begin{bmatrix}f_{v_1}^{t+\Delta t}\\ f_{v_2}^{t+\Delta t}\end{bmatrix},\end{aligned} \tag{5.89}$$

where the matrices $P1, \dots, P_4, V1 \dots, V_7$ should be evaluated at $t + \Delta t$.

5.2.5. Matrix-vector system for morphoelasticity

System (5.54b) already reveals that we will be dealing with a nonlinear discretization for each of the strain evolution equations. We will therefore split the matrix-vector system up in a linear part and a non-linear part.

For the equation for ϵ_{11} we have:

$$\sum_{j=1,2,3}(\epsilon_{11})_j^{t+\Delta t}\int_{\text{el}^{t+\Delta t}}\phi_j\phi_i\,\mathrm{d}\Omega=\sum_{j=1,2,3}(\epsilon_{11})_j^{t}\int_{\text{el}^{t}}\phi_j\phi_i\,\mathrm{d}\Omega$$
$$+\Delta t\Bigg[\sum_{j=1,2,3}(v_1)_j^{t+\Delta t}\int_{\text{el}^{t+\Delta t}}\frac{\partial\phi_j}{\partial x}\phi_i\,\mathrm{d}\Omega-$$
$$\sum_{j=1,2,3}(\epsilon_{22})_j^{t+\Delta t}\Bigg(\sum_{j'=1,2,3}(v_1)_{j'}^{t+\Delta t}\int_{\text{el}^{t+\Delta t}}\phi_j\frac{\partial\phi_{j'}}{\partial x}\phi_i\,\mathrm{d}\Omega\Bigg)$$
$$+\sum_{j=1,2,3}(\epsilon_{11})_j^{t+\Delta t}\Bigg(\sum_{j'=1,2,3}(v_2)_{j'}^{t+\Delta t}\int_{\text{el}^{t+\Delta t}}\phi_j\frac{\partial\phi_{j'}}{\partial y}\phi_i\,\mathrm{d}\Omega\Bigg)+$$
$$\sum_{j=1,2,3}(\epsilon_{12})_j^{t+\Delta t}\Bigg(\sum_{j'=1,2,3}(v_1)_{j'}^{t+\Delta t}\int_{\text{el}^{t+\Delta t}}\phi_j\frac{\partial\phi_{j'}}{\partial y}\phi_i\,\mathrm{d}\Omega\Bigg)$$
$$-\sum_{j=1,2,3}(\epsilon_{12})_j^{t+\Delta t}\Bigg(\sum_{j'=1,2,3}(v_2)_{j'}^{t+\Delta t}\int_{\text{el}^{t+\Delta t}}\phi_j\frac{\partial\phi_{j'}}{\partial x}\phi_i\,\mathrm{d}\Omega\Bigg)-\int_{e_m^{t+\Delta t}}g_{11}\phi_i\,\mathrm{d}\Omega\Bigg]. \quad (5.90)$$

We will set

$$\epsilon_{11}^t:=((\epsilon_{11})_1^t,\dots,(\epsilon_{11})_n^t)^T, \quad (5.91)$$
$$\epsilon_{12}^t:=((\epsilon_{12})_1^t,\dots,(\epsilon_{12})_n^t)^T, \quad (5.92)$$
$$\epsilon_{22}^t:=((\epsilon_{22})_1^t,\dots,(\epsilon_{22})_n^t)^T, \quad (5.93)$$
$$w^t:=\begin{bmatrix}\epsilon_{11}^t\\ \epsilon_{12}^t\\ \epsilon_{22}^t\\ v_1^t\\ v_2^t\end{bmatrix}. \quad (5.94)$$

Now (5.90) gives rise to the following system:

$$M^{t+\Delta t}\epsilon_{11}^{t+\Delta t}=M^t\epsilon_{11}^t+\Delta t\cdot\left[L_1^{t+\Delta t}v_1^{t+\Delta t}+N_{\epsilon_{11}}^{t+\Delta t}(w^{t+\Delta t})+f_{\epsilon_{11}}^{t+\Delta t}\right]. \quad (5.95)$$

Here, M^t is defined by (5.70), and:

$$(L_1^t)_{\text{el}}=\frac{1}{6}|\Delta|\begin{bmatrix}\beta_1&\beta_2&\beta_3\\ \beta_1&\beta_2&\beta_3\\ \beta_1&\beta_2&\beta_3\end{bmatrix}, \quad (5.96)$$

$$(N_{\epsilon_{11}}^t(w^t))_{\text{el}}=\frac{1}{24}|\Delta|\begin{bmatrix}\gamma^T(v_2^1)_{\text{el}}(\bar\epsilon_{11})-\beta^T(v_1^1)_{\text{el}}(\bar\epsilon_{22})+\{\gamma^T(v_1^1)_{\text{el}}-\beta^T(v_2^1)_{\text{el}}\}(\bar\epsilon_{12})\\ \gamma^T(v_2^2)_{\text{el}}(\bar\epsilon_{11})-\beta^T(v_1^2)_{\text{el}}(\bar\epsilon_{22})+\{\gamma^T(v_1^2)_{\text{el}}-\beta^T(v_2^2)_{\text{el}}\}(\bar\epsilon_{12})\\ \gamma^T(v_2^3)_{\text{el}}(\bar\epsilon_{11})-\beta^T(v_1^3)_{\text{el}}(\bar\epsilon_{22})+\{\gamma^T(v_1^3)_{\text{el}}-\beta^T(v_2^3)_{\text{el}}\}(\bar\epsilon_{12})\end{bmatrix}, \quad (5.97)$$

$$(f_{\epsilon_{11}}^t)_{\text{el}}=-\frac{1}{6}|\Delta|\begin{bmatrix}(g_{11})_1^t\\ (g_{11})_2^t\\ (g_{11})_3^t\end{bmatrix}, \quad (5.98)$$

and:

$$(v_k^i)_{\text{el}}^T:=((v_k^i)^t)_{\text{el}}^T=\begin{bmatrix}(1+\delta_{1i})(v_k)_1^t\\ (1+\delta_{2i})(v_k)_2^t\\ (1+\delta_{3i})(v_k)_3^t\end{bmatrix},\ i=1,2,3,\ k=1,2, \quad (5.99)$$
$$(\bar\epsilon_k):=(\bar\epsilon_k)^t=(\epsilon_k)_1^t+(\epsilon_k)_2^t+(\epsilon_k)_3^t,\ k=\{11\},\{12\},\{22\}, \quad (5.100)$$

δ_{ij} is the Kronecker delta, and the elements of the last two vectors are Finite Element Approximations for $v_2, v_3, \epsilon_{11}, \epsilon_{12}$ and ϵ_{22} at the three vertices of the element.

For the second of the ϵ-equations filling in the discretization gives:

$$\begin{aligned}\sum_{j=1,2,3}(\epsilon_{12})_j^{t+\Delta t}\int_{\text{el}^{t+\Delta t}}\phi_j\phi_i\,\mathrm{d}\Omega = \sum_{j=1,2,3}(\epsilon_{12})_j^{t}\int_{\text{el}^{t}}\phi_j\phi_i\,\mathrm{d}\Omega \\ +\Delta t\Bigg[\frac{1}{2}\sum_{j=1,2,3}(v_1)_j^{t+\Delta t}\int_{\text{el}^{t+\Delta t}}\frac{\partial\phi_j}{\partial y}\phi_i\,\mathrm{d}\Omega+\frac{1}{2}\sum_{j=1,2,3}(v_2)_j^{t+\Delta t}\int_{e_m^{t+\Delta t}}\frac{\partial\phi_j}{\partial x}\phi_i\,\mathrm{d}\Omega \\ +\sum_{j=1,2,3}(\epsilon_{12})_j^{t+\Delta t}\Bigg(\sum_{j'=1,2,3}(v_1)_{j'}^{t+\Delta t}\int_{\text{el}^{t+\Delta t}}\phi_j\frac{\partial\phi_{j'}}{\partial x}\phi_i\,\mathrm{d}\Omega\Bigg) \\ +\sum_{j=1,2,3}(\epsilon_{12})_j^{t+\Delta t}\Bigg(\sum_{j'=1,2,3}(v_2)_{j'}^{t+\Delta t}\int_{\text{el}^{t+\Delta t}}\phi_j\frac{\partial\phi_{j'}}{\partial y}\phi_i\,\mathrm{d}\Omega\Bigg) \\ -\sum_{j=1,2,3}(\epsilon_{11})_j^{t+\Delta t}\Bigg(\sum_{j'=1,2,3}(v_1)_{j'}^{t+\Delta t}\int_{\text{el}^{t+\Delta t}}\phi_j\frac{\partial\phi_{j'}}{\partial y}\phi_i\,\mathrm{d}\Omega\Bigg) \\ -\sum_{j=1,2,3}(\epsilon_{22})_j^{t+\Delta t}\Bigg(\sum_{j'=1,2,3}(v_2)_{j'}^{t+\Delta t}\int_{\text{el}^{t+\Delta t}}\phi_j\frac{\partial\phi_{j'}}{\partial x}\phi_i\,\mathrm{d}\Omega\Bigg) \\ -\int_{\text{el}^{t+\Delta t}}g_{12}\phi_i\,\mathrm{d}\Omega\Bigg].\end{aligned} \tag{5.101}$$

This results in a system

$$M^{t+\Delta t}\epsilon_{12}^{t+\Delta t}=M^t\epsilon_{12}^t+\Delta t\cdot\left[\frac{1}{2}(L_2^{t+\Delta t}v_1^{t+\Delta t}+L_1^{t+\Delta t}v_2^{t+\Delta t})+N_{\epsilon_{12}}^{t+\Delta t}(w^{t+\Delta t})+f_{\epsilon_{12}}^{t+\Delta t}\right], \tag{5.102}$$

where

$$(L_2^t)_{\text{el}}=\frac{1}{6}|\Delta|\begin{bmatrix}\gamma_1&\gamma_2&\gamma_3\\ \gamma_1&\gamma_2&\gamma_3\\ \gamma_1&\gamma_2&\gamma_3\end{bmatrix}, \tag{5.103}$$

$$(N_{\epsilon_{12}}^t(w^t))_{\text{el}}=\frac{1}{24}|\Delta|\begin{bmatrix}\{\beta^T(v_2^1)_{\text{el}}+\gamma^T(v_2^1)_{\text{el}}\}(\bar{\epsilon}_{12})_{\text{el}}-\gamma^T(v_1^1)_{\text{el}}(\bar{\epsilon}_{11})_{\text{el}}-\beta^T(v_2^1)_{\text{el}}(\bar{\epsilon}_{22})_{\text{el}}\\ \{\beta^T(v_2^1)_{\text{el}}+\gamma^T(v_2^2)_{\text{el}}\}(\bar{\epsilon}_{12})_{\text{el}}-\gamma^T(v_1^2)_{\text{el}}(\bar{\epsilon}_{11})_{\text{el}}-\beta^T(v_1^2)_{\text{el}}(\bar{\epsilon}_{22})_{\text{el}}\\ \{\beta^T(v_1^3)_{\text{el}}+\gamma^T(v_2^3)_{\text{el}}\}(\bar{\epsilon}_{23})_{\text{el}}-\gamma^T(v_1^3)_{\text{el}}(\bar{\epsilon}_{11})_{\text{el}}-\beta^T(v_2^3)_{\text{el}}(\bar{\epsilon}_{22})_{\text{el}}\end{bmatrix}, \tag{5.104}$$

$$(f_{\epsilon_{12}}^t)_{\text{el}}=-\frac{1}{6}|\Delta|\begin{bmatrix}(g_{12})_1\\ (g_{12})_2\\ (g_{12})_3\end{bmatrix}. \tag{5.105}$$

Finally, for the equation for ϵ_{22} we get:

$$\sum_{j=1,2,3}(\epsilon_{22})_j^{t+\Delta t}\int_{\text{el}^{t+\Delta t}}\phi_j\phi_i\,\mathrm{d}\Omega=\sum_{j=1,2,3}(\epsilon_{22})_j^{t}\int_{\text{el}^{t}}\phi_j\phi_i\,\mathrm{d}\Omega+$$
$$\Delta t\Bigg[\sum_{j=1,2,3}(v_2)_j^{t+\Delta t}\int_{\text{el}^{t+\Delta t}}\frac{\partial\phi_j}{\partial y}\phi_i\,\mathrm{d}\Omega$$
$$-\sum_{j=1,2,3}(\epsilon_{11})_j^{t+\Delta t}\Bigg(\sum_{j'=1,2,3}(v_2)_{j'}^{t+\Delta t}\int_{\text{el}^{t+\Delta t}}\phi_j\frac{\partial\phi_{j'}}{\partial y}\phi_i\,\mathrm{d}\Omega\Bigg)$$
$$+\sum_{j=1,2,3}(\epsilon_{22})_j^{t+\Delta t}\Bigg(\sum_{j'=1,2,3}(v_1)_{j'}^{t+\Delta t}\int_{\text{el}^{t+\Delta t}}\phi_j\frac{\partial\phi_{j'}}{\partial x}\phi_i\,\mathrm{d}\Omega\Bigg)$$
$$-\sum_{j=1,2,3}(\epsilon_{12})_j^{t+\Delta t}\Bigg(\sum_{j'=1,2,3}(v_1)_{j'}^{t+\Delta t}\int_{\text{el}^{t+\Delta t}}\phi_j\frac{\partial\phi_{j'}}{\partial y}\phi_i\,\mathrm{d}\Omega\Bigg)$$
$$+\sum_{j=1,2,3}(\epsilon_{12})_j\Bigg(\sum_{j'=1,2,3}(v_2)_{j'}^{t+\Delta t}\int_{\text{el}^{t+\Delta t}}\phi_j\frac{\partial\phi_{j'}}{\partial x}\phi_i\,\mathrm{d}\Omega\Bigg)$$
$$-\int_{\text{el}^{t+\Delta t}}g_{22}\phi_i\,\mathrm{d}\Omega\Bigg]. \quad (5.106)$$

This yields a system

$$M^{t+\Delta t}\epsilon_{22}^{t+\Delta t}=M^t\epsilon_{22}^t+\Delta t\cdot\left[L_2^{t+\Delta t}v_2^{t+\Delta t}+N_{\epsilon_{22}}^{t+\Delta t}(w^{t+\Delta t})+f_{\epsilon_{22}}^{t+\Delta t}\right], \quad (5.107)$$

where

$$(N_{\epsilon_{22}}(w))_{\text{el}}=\frac{1}{24}|\Delta|\begin{bmatrix}-\beta^T(v_1^1)_{\text{el}}(\bar{\epsilon}_{22})_{\text{el}}+\gamma^T(v_2^1)_{\text{el}}(\bar{\epsilon}_{33})_{\text{el}}+\{\beta^T(v_1^1)_{\text{el}}-\gamma^T(v_2^1)_{\text{el}}\}\cdot(\bar{\epsilon_{12}})_{\text{el}}\\-\beta^T(v_1^2)_{\text{el}}(\bar{\epsilon}_{22})_{\text{el}}+\gamma^T(v_2^2)_{\text{el}}(\bar{\epsilon}_{33})_{\text{el}}+\{\beta^T(v_1^1)_{\text{el}}-\gamma^T(v_2^1)_{\text{el}}\}\cdot(\bar{\epsilon_{12}})_{\text{el}}\\-\beta^T(v_1^3)_{\text{el}}(\bar{\epsilon}_{22})_{\text{el}}+\gamma^T(v_2^3)_{\text{el}}(\bar{\epsilon}_{33})_{\text{el}}+\{\beta^T(v_1^1)_{\text{el}}-\gamma^T(v_2^1)_{\text{el}}\}\cdot(\bar{\epsilon_{12}})_{\text{el}}\end{bmatrix}, \quad (5.108)$$

$$(f_{\epsilon_{22}}^t)_{\text{el}}=-\frac{1}{6}|\Delta|\begin{bmatrix}(g_{22})_1\\(g_{22})_2\\(g_{22})_3\end{bmatrix}. \quad (5.109)$$

Combining (5.95), (5.102) and (5.107) with (5.89) we obtain a full morphoelastic system:

$$\begin{bmatrix}\emptyset & M^{t+\Delta t} & & \\ & & M^{t+\Delta t} & \\ M^{t+\Delta t} & & & \\ & M^{t+\Delta t} & \emptyset & \\ & & M^{t+\Delta t} & \end{bmatrix}w^{t+\Delta t}=\begin{bmatrix}\emptyset & M^t & & \\ & & M^t & \\ M^t & & & \\ & M^t & \emptyset & \\ & & M^t & \end{bmatrix}w^t$$
$$+\Delta t\Bigg\{\begin{bmatrix}\bar{G}\frac{1-\nu}{1-2\nu}(P_1+P_3) & \bar{G}(P_2+P_4) & \bar{G}\frac{\nu}{1-2\nu}(P_1+P_3) & \tilde{\mu}(V_1+V_4)+\frac{\mu_1}{2}(V_2+V_7) & \mu_2(V_3+V_6)+\frac{\mu_1}{2}(V_3^T+V_5)\\ \bar{G}\frac{\nu}{1-2\nu}(P_2+P_4) & \bar{G}(P_1+P_3) & \bar{G}\frac{1-\nu}{1-2\nu}(P_2+P_4) & \mu_2(V_3+V_6)+\frac{\mu_1}{2}(V_3^T+V_5) & \tilde{\mu}(V_1+V_4)+\frac{\mu_1}{2}(V_2+V_7)\\ & & & L_1^{t+\Delta t} & \emptyset\\ & \emptyset & & \frac{1}{2}L_2^{t+\Delta t} & \frac{1}{2}L_3^{t+\Delta t}\\ & & & \emptyset & L_2^{t+\Delta t}\end{bmatrix}w^{t+\Delta t}$$
$$+\begin{bmatrix}\emptyset\\ \emptyset\\ N_{\epsilon_{11}}^{t+\Delta t}(w^{t+\Delta t})\\ N_{\epsilon_{12}}^{t+\Delta t}(w^{t+\Delta t})\\ N_{\epsilon_{22}}^{t+\Delta t}(w^{t+\Delta t})\end{bmatrix}+\begin{bmatrix}f_{v_1}^{t+\Delta t}\\ f_{v_2}^{t+\Delta t}\\ f_{\epsilon_{11}}^{t+\Delta t}\\ f_{\epsilon_{12}}^{t+\Delta t}\\ f_{\epsilon_{22}}^{t+\Delta t}\end{bmatrix}\Bigg\}, \quad (5.110)$$

where

$$\tilde{G} = \frac{E\sqrt{\rho}}{1+\nu}, \tag{5.111}$$

and

$$\tilde{\mu} = \mu_1 + \mu_2. \tag{5.112}$$

5.2.6. Fixed-point iterations

System (5.110) is non-linear, and therefore it has to be solved with an iterative method. We will use *Picard iterations*, see appendix A.

5.2.7. Remeshing to maintain accuracy

In order to do the FEM computations we have to construct a triangular mesh. By the nature of the problem we are considering, this mesh will be moving. Since we divide by $|\Delta|$ when we determine some of the matrices in (5.110), it is important that the triangles do not have very sharp angles. If they do, they will be close to singular, i.e. $|\Delta| \approx 0$, and this will lead to inaccuracies. Ideally every triangle has angles of around 60 degrees. However, for most choices of parameters, after enough time has passed, some triangles will become ill-shaped, i.e. some of their angles will become very small. We can mitigate the inaccuracies that will result, by generating a new mesh. After doing this, we will need to approximate the values of v and ϵ in the new mesh points. We do this using linear interpolation.

6

Results

In this chapter we will present results for some of the models we have constructed in chapter 4. Some of the results will be qualitative and aim at gaining even more understanding. Others will be more quantitative.

6.1. A purely elastic model

In this section we will derive the analytic solution to model (4.40), and present some plots.

6.1.1. Solution to model (4.40)

We have:

$$\frac{\partial \sigma}{\partial x} = -F_b. \tag{6.1}$$

We assume that the tissue will contract, and therefore we will use the following body force profile:

$$F_b(x) = \begin{cases} \bar{F}_b, & 0 \leq x \leq L/2, \\ -\bar{F}_b, & L/2 < x \leq L. \end{cases} \tag{6.2}$$

For now we take $\bar{F}_b = 0.36$. In section 6.2 we will elaborate on an appropriate choice for this value. The body force profile is depicted in figure 6.1. Integrating equation (6.1) now gives:

$$\sigma(x) = \begin{cases} -\bar{F}_b x + C_1, & 0 \leq x \leq L/2, \\ \bar{F}_b (x - L) + C_1, & L/2 < x \leq L, \end{cases} \tag{6.3}$$

where C_1 is a constant. The boundary condition $\sigma(L) = 0$ implies that $C_1 = 0$, so we have:

$$\sigma(x) = \begin{cases} -\bar{F}_b x, & 0 \leq x \leq L/2, \\ \bar{F}_b (x - L), & L/2 < x \leq L. \end{cases} \tag{6.4}$$

This stress profile is depicted in figure 6.6. It shows the stress magnitude becomes higher as we get closer to the center of the tissue. In [9] various models for cell distribution are presented. These models include diffusion and chemotaxis, i.e. movement in reaction to chemical stimuli. As stated in section 2.4, fibroblasts lay down collagen fibres predominantly along the axis subject to the highest normal stress. Therefore it seems reasonable to assume that high fibroblast concentrations are present in the wound area. As the models in [9] are diffusion-based, we presume a somewhat smooth transition from lower concentrations in healthy skin to higher ones in the wounded area. For this simple model, we consider (6.6) to be reasonable.

We have:

$$\frac{\partial u}{\partial x} = \frac{\sigma}{E}, \tag{6.5}$$

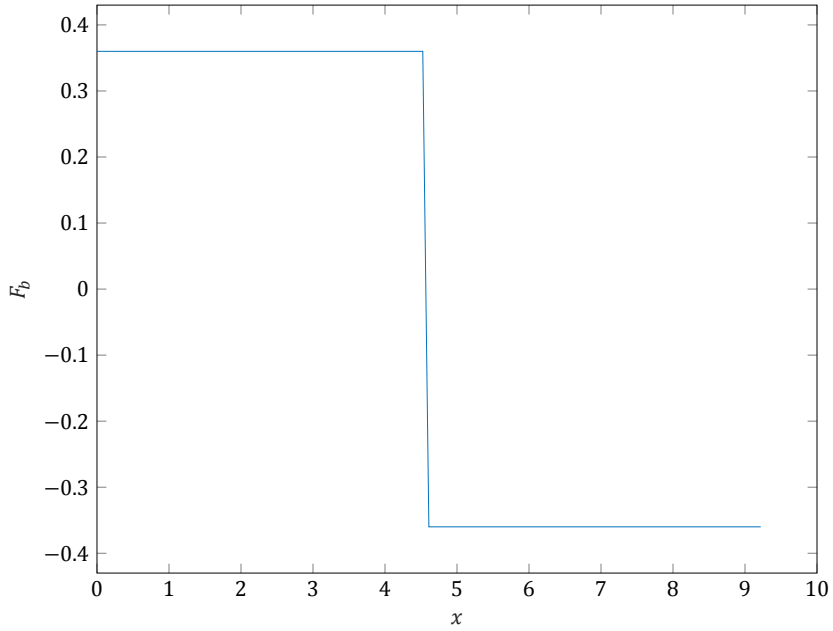

Figure 6.1: A plot of the body force profile $F_b(x)$.

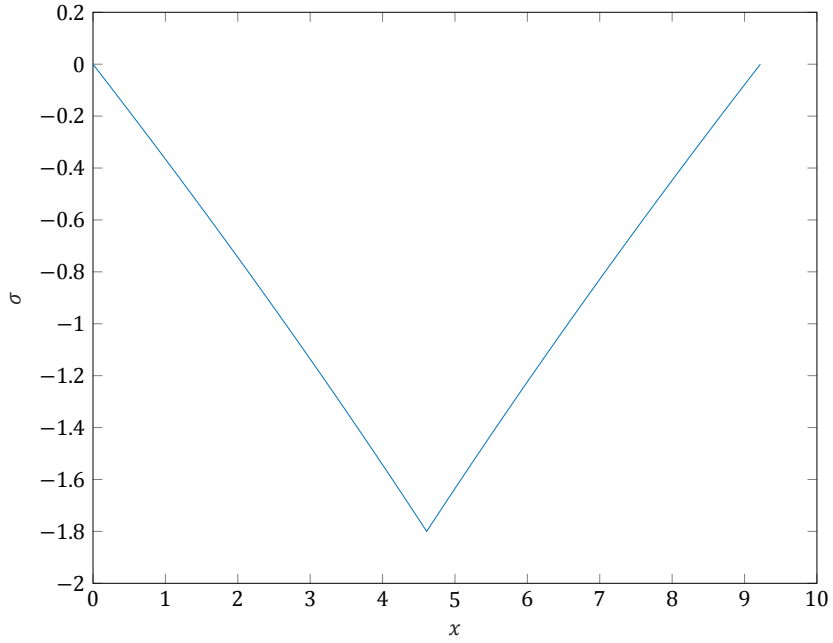

Figure 6.2: A plot of the stress profile $\sigma(x)$ induced by F_b.

from which it follows that:

$$u(x) = \begin{cases} -\frac{\bar{F}_b}{2E}x^2 + C_2, & 0 \le x \le L/2, \\ \frac{\bar{F}_b}{2E}\left[x - L\left(1 + \frac{1}{2}\sqrt{2}\right)\right]\left[\left(x - L\left(1 - \frac{1}{2}\sqrt{2}\right)\right] + C_2, & L/2 < x \le L. \end{cases} \tag{6.6}$$

The boundary condition $u(0) = 0$ implies that $C_2 = 0$, so that:

$$u(x) = \begin{cases} -\frac{\bar{F}_b}{2E}x^2, & 0 \le x \le L/2, \\ \frac{\bar{F}_b}{2E}\left[x - L\left(1 + \frac{1}{2}\sqrt{2}\right)\right]\left[\left(x - L\left(1 - \frac{1}{2}\sqrt{2}\right)\right], & L/2 < x \le L. \end{cases} \tag{6.7}$$

6.1.2. Results for time-invariant body forces

In figures 6.3 and 6.4 we see plots of u and $x = X + u$ versus X respectively. We see that the boundary condition on the left end is satisfied because $u(0) = 0$. The right boundary, however, can move freely, and has experienced the largest displacement out of all the points in the tissue.

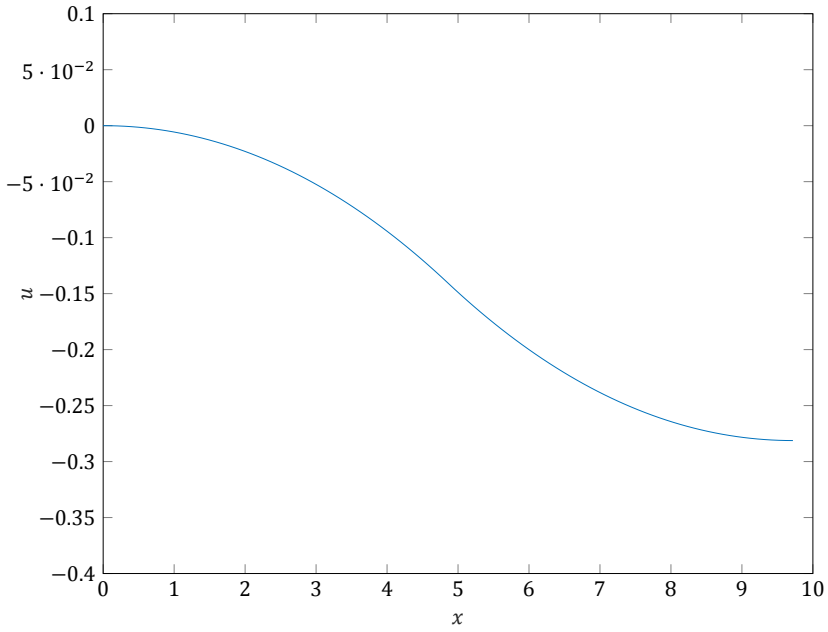

Figure 6.3: A plot of the displacement $u(x)$ induced by F_b.

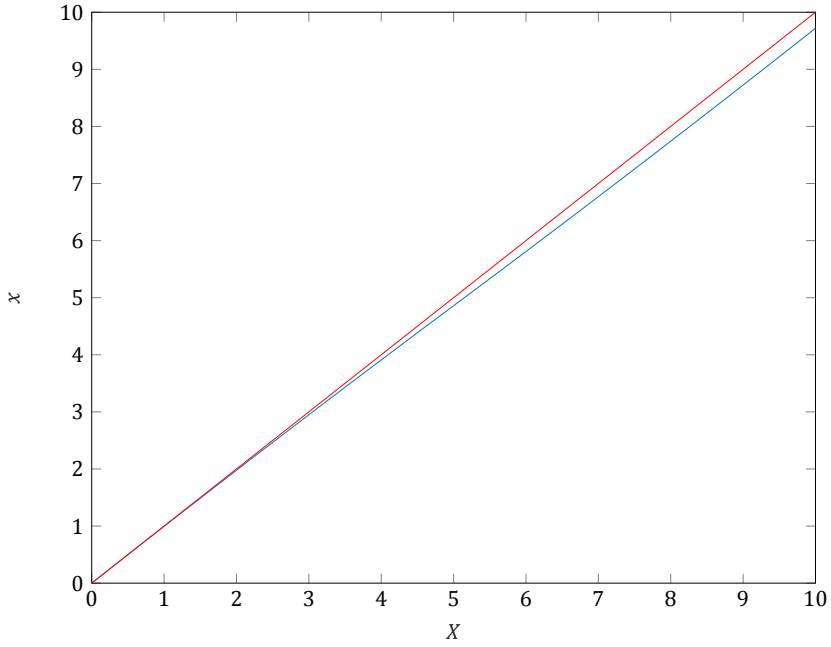

Figure 6.4: A plot of (X, x) induced by F_b (blue) along with (X, X) as a reference (red).

6.1.3. Results for time-dependent body forces

We will now construct a time-dependent body force term. To respect the diffusion-based distribution of the fibroblasts, we will use exponential functions for the increase and decay of the body forces:

$$\tilde{F}_b(x,t) = \begin{cases} 0, & t < t_{\text{f0}}, \\ F_b(x)\left(1 - \exp\left(-c_{\text{fd}}\frac{t-t_{\text{f0}}}{t_{\text{fm}}-t_{\text{f0}}}\right)\right), & t_{\text{f0}} \leq t < t_{\text{ap}}, \\ F_b(x)\left(1 - \exp\left(-c_{\text{fd}}\frac{t-t_{\text{f0}}}{t_{\text{fm}}-t_{\text{f0}}}\right)\right)\exp(-(t-t_{\text{ap}})), & t \geq t_{\text{ap}}. \end{cases} \tag{6.8}$$

where t_{f0} is the point in time at which fibroblasts first start entering the wound, t_{fm} is the time at which the fibroblast concentration is maximal, t_{ap} is the time at which the fibroblast concentration starts returning to 0. As argued in section 2.4, contraction starts shortly after injury, and lasts for 2-3 weeks. Therefore, we take $t_{\text{f0}=0.1}$, $t_{\text{fm}=20}$, and $t_{\text{ap}=20}$. By means of c_{fd} we include a factor to control the rate at which the fibroblast concentration increases. If we set $c_{\text{fd}=4}$, the body forces reach about 98% of the value of $\bar{F}_b$, while they do not increase too quickly. The purely elastic model with time-dependent body forces is given by:

$$\begin{cases} -\frac{\partial \sigma}{\partial x} = \tilde{F}_b, \\ \sigma = E\epsilon, \\ \epsilon = \frac{\partial u}{\partial x}, \ 0 < x < L, \\ u(0) = 0, \\ \sigma(L) = 0. \end{cases} \tag{6.9}$$

In figure 6.5 the time-dependent body force profile is visualized at four different values of t.

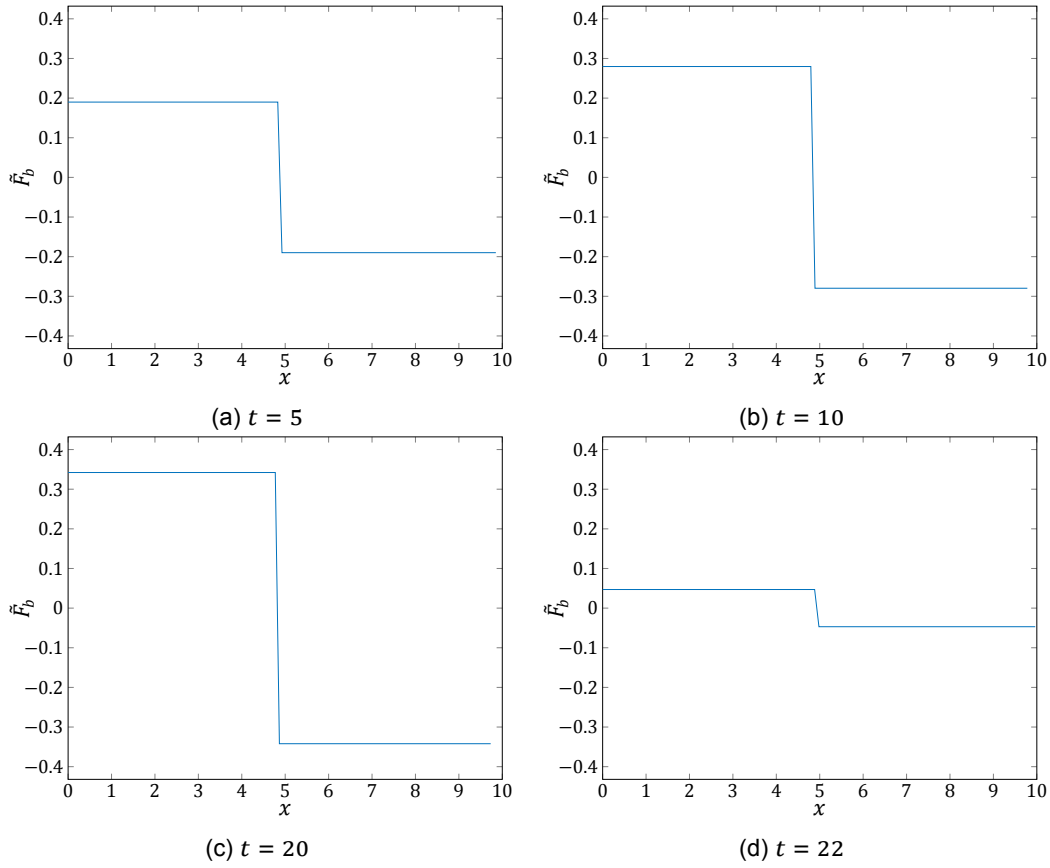

(a) $t = 5$ (b) $t = 10$

(c) $t = 20$ (d) $t = 22$

Figure 6.5: Plots of the body force profile $\tilde{F}_b$ for various values of t.

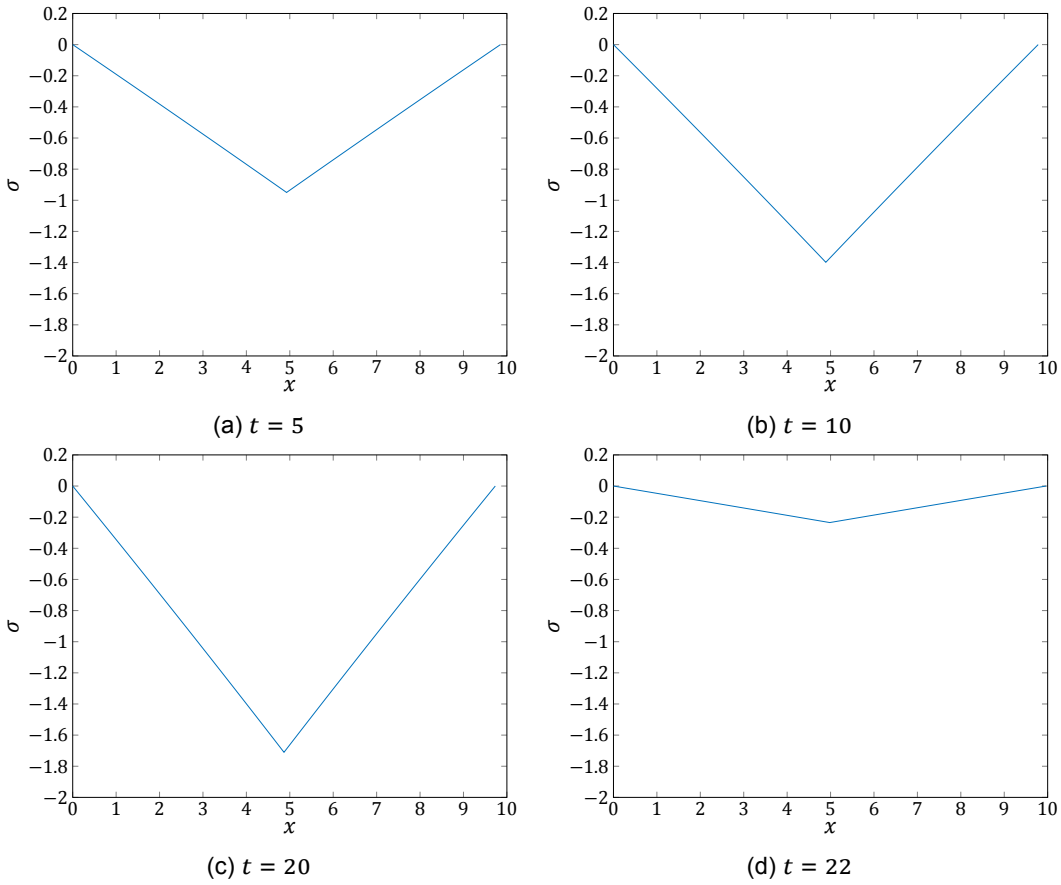

(a) $t = 5$ (b) $t = 10$

(c) $t = 20$ (d) $t = 22$

Figure 6.6: Plots of the stress profiles σ induced by $\tilde{F}_b$ for various values of t.

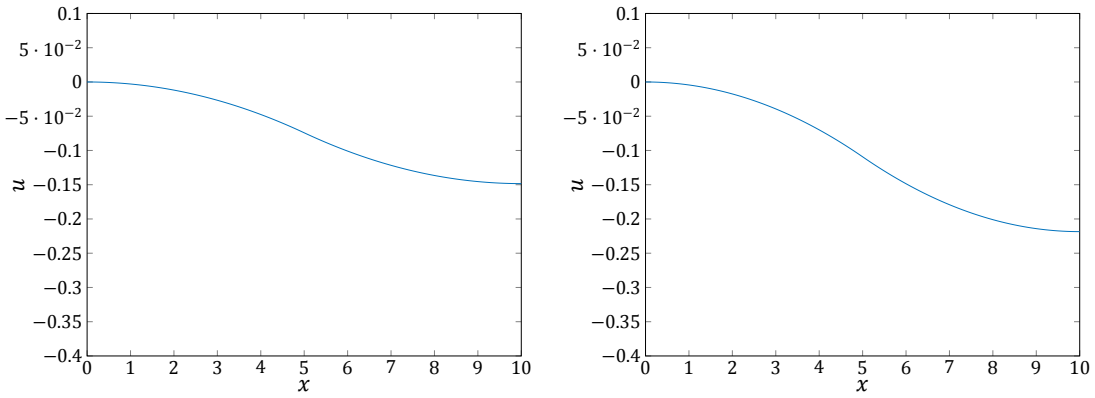

(a) $t = 5$ (b) $t = 10$

(c) $t = 20$ (d) $t = 22$

Figure 6.7: Plots of the displacement profiles u induced by $\tilde{F}_b$ for various values of t.

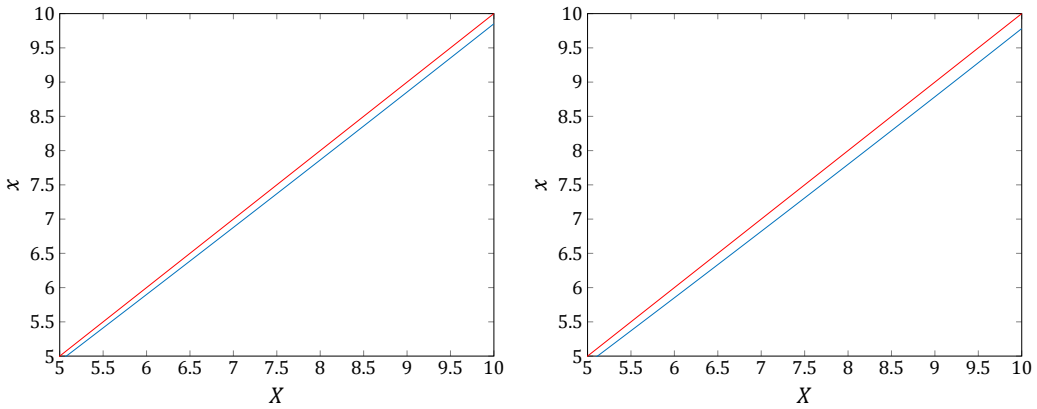

(a) $t = 5$

(b) $t = 10$

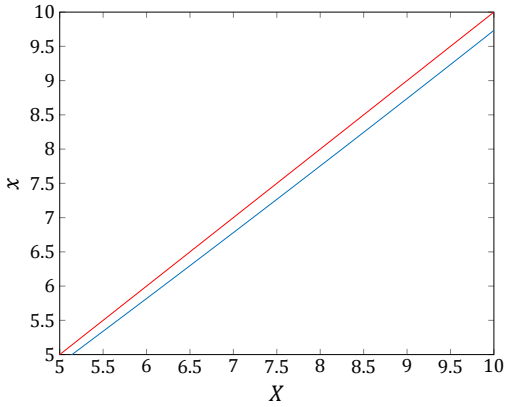

(c) $t = 20$

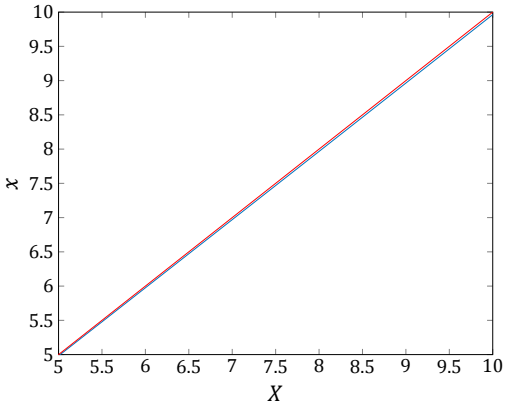

(d) $t = 22$

Figure 6.8: Plots of (X, x) induced by $\tilde{F}_b$ (blue) and (X, X) as a reference (red) for various values of t. Because differences are small, X-values range between 5 and 10.

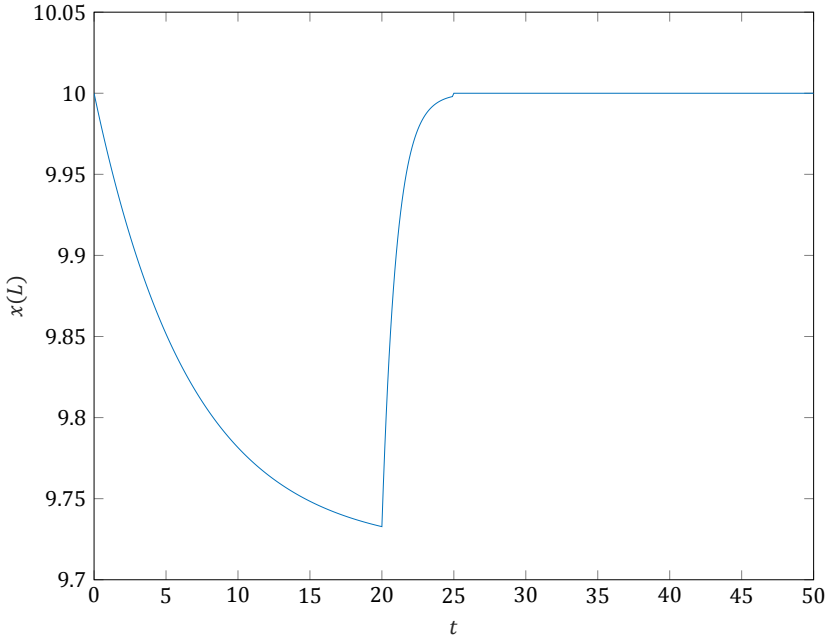

Figure 6.9: A plot of $x(L)$ versus t.

6.2. A one-dimensional dynamical viscoelastic model

In this section we will qualitatively analyze solutions to model (4.41). This model incorporates viscoelasticity. In [14] it is stated that re-expansion of skin tissue after fibroblast concentrations have returned to normal levels, is far from instantaneous. This indicates that viscosity plays an important role. Furthermore, this model is dynamical. To the purely elastic model considered in section 6.1 we did add time-dependence, but this was a rather artificial act. The inherent dynamics of model (4.41) will constitute a more realistic model and provide more insight in the contraction process.

6.2.1. Parameters

The parameters used for the results presented in this section can be found in table 6.1. The value for E was taken from [10]. The values of μ and ρ are taken from [11]. The time values t_{f0}, t_{fm} and t_{ap} are based on the timeline presented in section 2.3.3. For the body forces we use (6.8). The value of $\bar{F}_b$ has been chosen such that we obtain a reasonable contraction: in this simulation the tissue contracts to 74% of its original length. This percentage is deemed realistic ([8]).

6.2.2. Analysis of the results

Firstly, we will look at the interaction between viscous and elastic stress. Consider figures 6.14 and 6.11. At $t = 0$ the tissue is stress-free. Therefore, upon exertion of the body forces, the tissue will start contracting at a relatively high rate. This will cause viscous stress to be high. As the tissue contracts, elastic stresses will get higher, impeding the contraction rate. This will in turn cause viscous stresses to get smaller again. Close to $t = f_{\text{fm}}$, the contraction rate approaches 0, and in turn will the viscous stress. Once the body forces drop, re-expansion of the tissue occurs. Again viscous stress is initially large, but this time with opposite sign. Viscous stress converges to 0 as the tissue approaches a stable configuration. As viscous stress is proportional to the strain rate, it provides a means of *damping*. It does this not only realistically, but also numerically. For this study a dynamical model with only elastic stresses has also been investigated. However, no meaningful results could be obtained because of the inherent instability of such a model. The difference between the current dynamical model and the static model (4.40) can be seen nicely when figures 6.9 and 6.14 are compared. The dynamical model smoothens out the changes that the tissue undergoes.

Parameter	Value	Unit
E	31	$\text{N}/(\text{g cm})^{1/2}$
μ	10^2	(N day)/cm
ρ	1.02	g/cm
$\bar{F}_b$	5	(N g)/(cells cm)
t_{f0}	0.1	days
t_{fm}	20	days
t_{ap}	20	days

Table 6.1: The parameters used for the results in section 6.2.

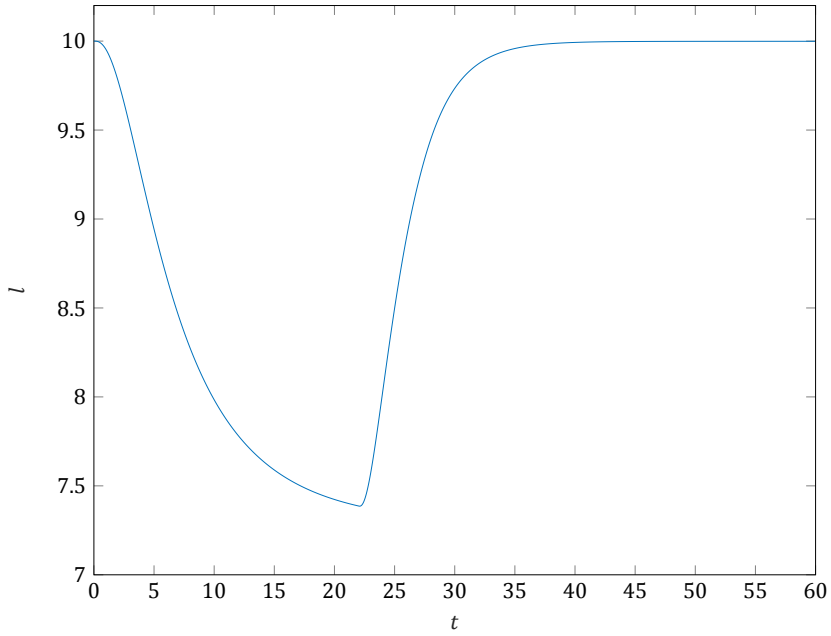

Figure 6.10: Plot of l versus t.

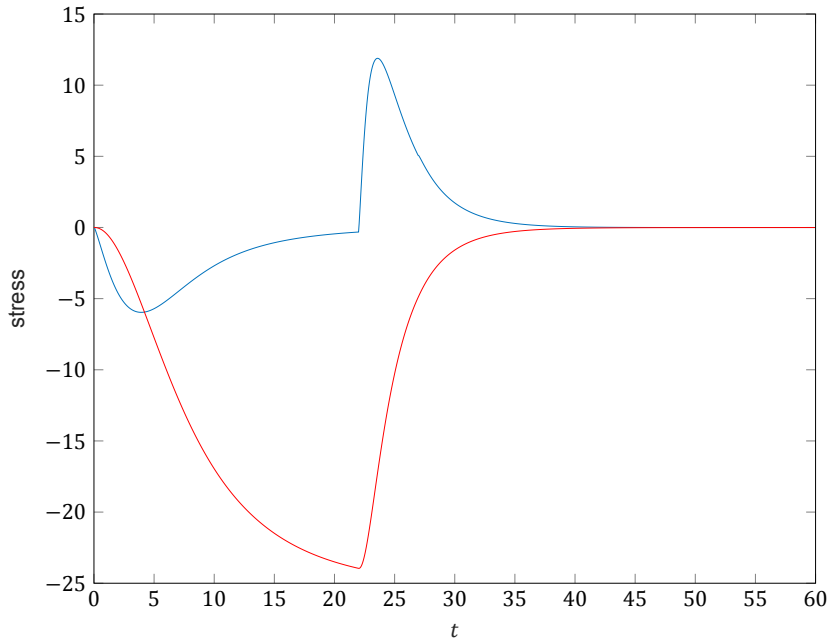

Figure 6.11: Plot of viscous (blue) and elastic (red) stresses in the center of the tissue versus time, i.e. $x(L/2, t)$ versus t.

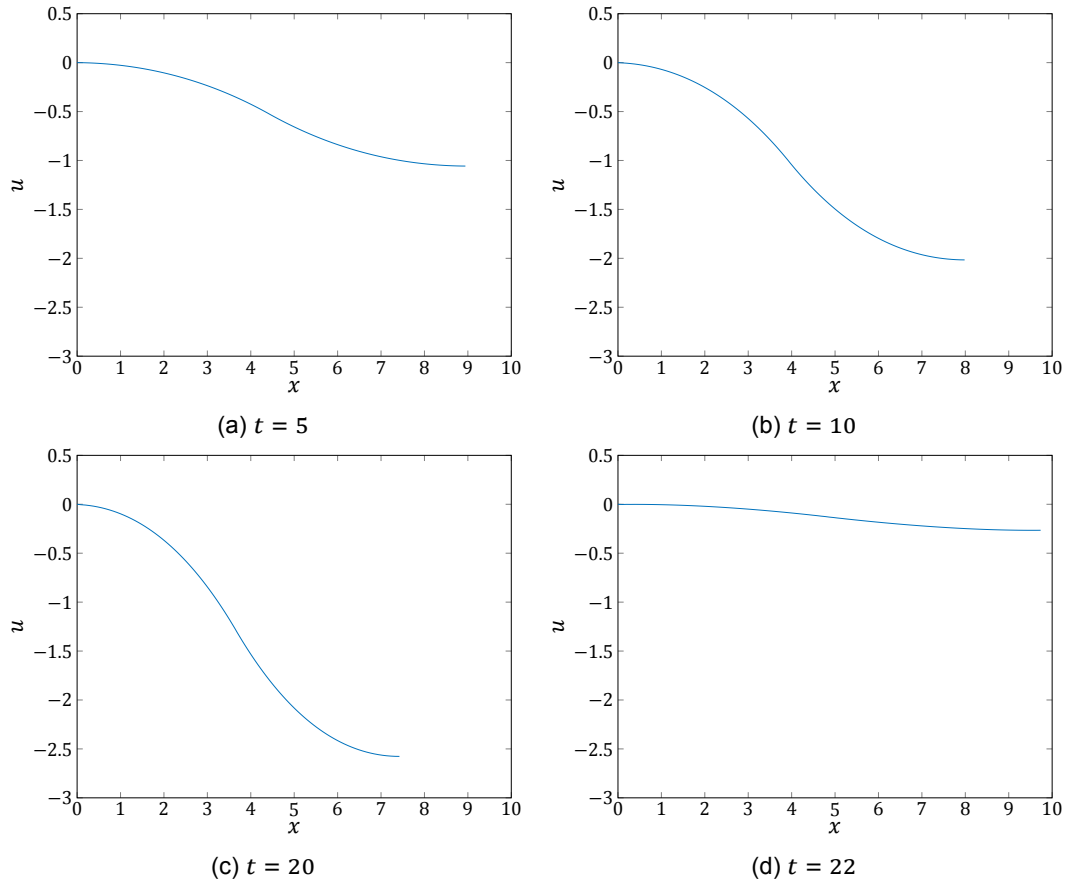

(a) $t = 5$ (b) $t = 10$

(c) $t = 20$ (d) $t = 22$

Figure 6.12: Plots of the displacement profiles u for various values of t.

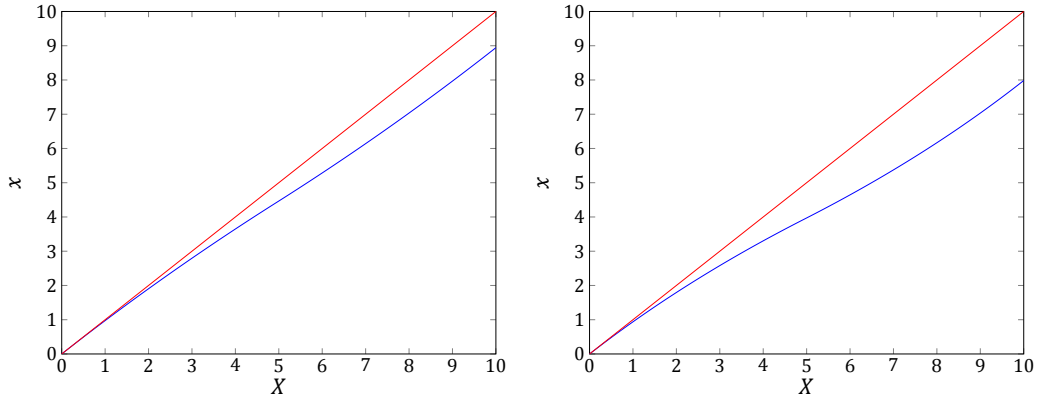

(a) $t = 5$ (b) $t = 10$

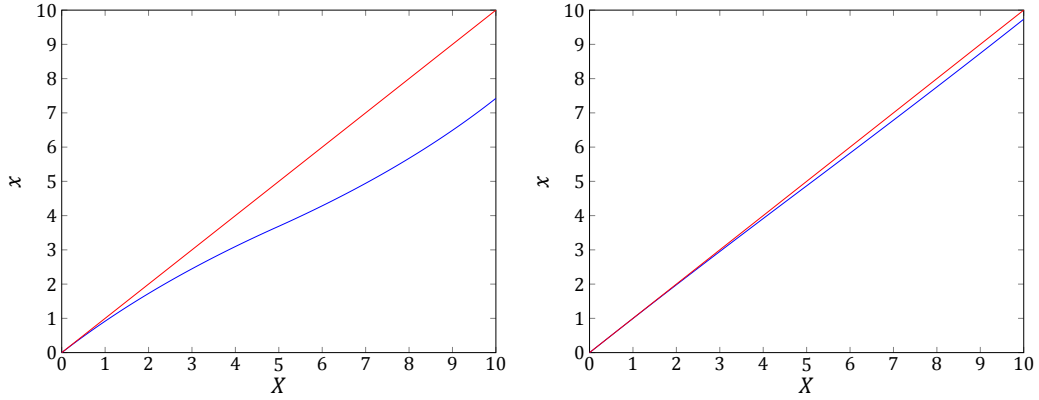

(c) $t = 20$ (d) $t = 22$

Figure 6.13: Plots of (X, x) (blue) and (X, X) as a reference (red) for various values of t.

6.3. A one-dimensional morphoelastic model

In this section we consider model (4.64). We will present plots that show that after contraction the tissue does not fully return to its original length. Furthermore, we will investigate the interaction between the elastic and plastic deformation gradients, and γ.

6.3.1. The right-hand side function g

The function g defines the plastic gradient γ by equation (6.10):

$$\frac{\mathrm{D}\gamma}{\mathrm{D}t} = Fg(x,t). \tag{6.10}$$

We choose $g = \zeta\epsilon$, where $zeta$ is a positive constant. A comparable choice is made in [11]. We justify this expression by imagining a rubber band being stretched. If we elastically deform the rubber band only a bit, it will return to its original shape upon release. However, if we stretch it far enough, it will start to plastically deform. The presumption here is that the plastic deformation occurs linearly with respect to time. Note that our choice for g implies that even small elastic deformations result in plastic deformation, which is not entirely in accordance with the rubber band comparison. However, stating that the rate of change of γ should be approximately proportional to ϵ seems reasonable. This choice for g also allows for an elegant FEM scheme.

6.3.2. Parameters

The parameters for this simulation are almost all the same as in section 6.2. Since plastic deformation affects the total contraction, we have to reconsider the magnitude of the body forces. We have chosen $\bar{F}_b$ and ζ such that the maximal contraction amounts to around 33% (see [8]), and the length of the tissue upon release is around 82% its original value (comparable to [11]). All the parameters for this model can be found in table 6.2.

6.3.3. Analysis of the plots

First off, we consider figure 6.14. It shows that both elastic and plastic deformation are involved in this simulation.

We investigate the interaction between plastic and elastic stress more closely. Consider figure 6.15. We see that in the beginning we have $F \approx \alpha$. Note that we have, by definition:

$$\alpha = 1 - \frac{1}{\epsilon}. \tag{6.11}$$

We see now that we α has a large magnitude, the growth rate of γ will have a large magnitude as well. As the magnitude of γ increases, we see that F and α start to diverge. When the body forces start to decrease, we see that α returns back to 1. This means that $F = \gamma$. This can also be seen in the figure. Physically, this means that only plastic deformation remains once the body forces have fully disappeared. In figure 6.14 we see that plastic deformation causes that the tissues remains contracted after relaxation of the body forces.

Parameter	Value	Unit
E	31	$\mathrm{N/(g\,cm)^{1/2}}$
μ	10^2	(N day)/cm
ρ	1.02	g/cm
$\bar{F}_b$	4.2	(N g)/(cells cm)
ζ	0.05	-
t_{f0}	0.1	days
t_{fm}	20	days
t_{ap}	22	days

Table 6.2: The parameters used for the results in section 6.3.

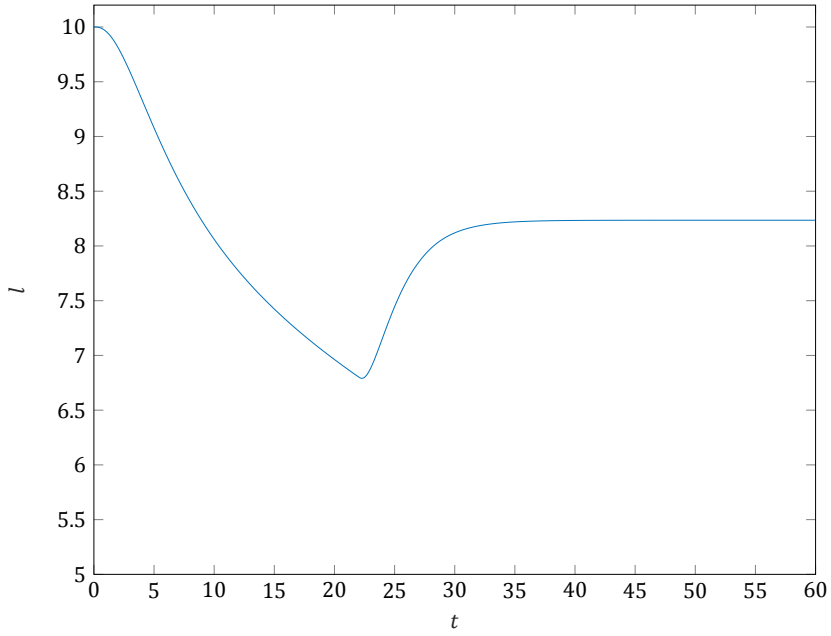

Figure 6.14: Plot of l versus t.

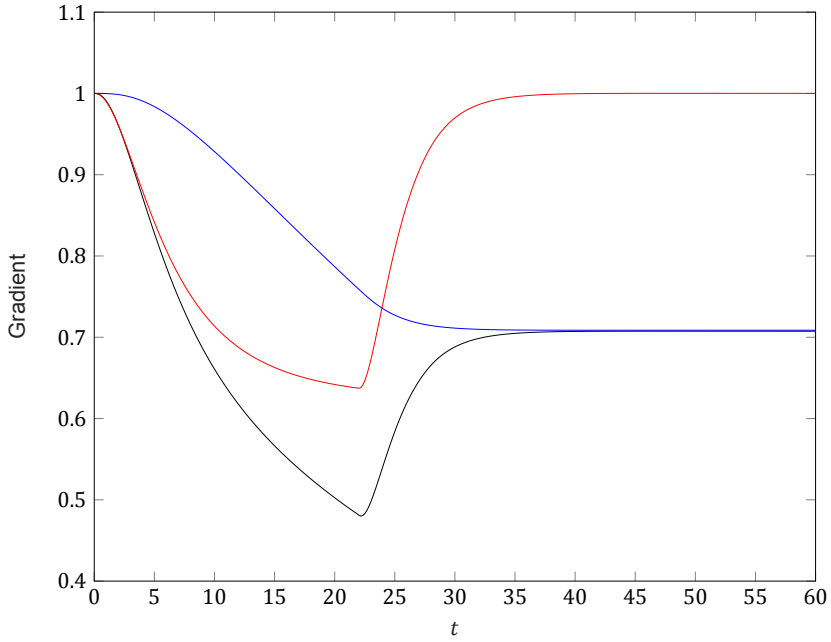

Figure 6.15: Plot of the elastic deformation gradient α (red), plastic deformation gradient γ (blue) and total deformation gradient $F = \alpha\gamma$ (black) versus t.

6.4. Heterogeneity using Karhunen-Loève expansions

In [1] it is stated that scar tissue has approximately 80% of the strength that healthy tissue has. This is just one example of the heterogeneity of human skin. We can imagine that some of the parameters we have used so far are not the exact same value all over the body, and may also vary from person to person. In this section we will lay out a framework that captures heterogeneity and uncertainty, based on so-called *Karhunen-Loève expansions*. Using this framework, we can run the one-dimensional morphoelasticity model with heterogenous, stochastic input. After doing this for multiple inputs, we will present some statistical results.

Parameter	Mean	St. dev.	Unit
E	31	11	$\mathrm{N}/(\mathrm{g\,cm})^{1/2}$
μ	10^2	1	(N day)/cm
ρ	1.02	0.2	g/cm
$\bar{F}_b$	4	2	(N g)/(cells cm)
ζ	0.05	0.02	-

Table 6.3: The means and standard deviations used for the results in section 6.4.

.

6.4.1. Description

For an elaborate description of Karhunen-Loéve expansions the reader can, for example, resort to [19]. The normalized truncated Karhunen-Loève expansion of a zero-mean stochastic process $\hat{u}$ is given by:

$$\hat{u}(X) = \sum_{i=1}^{n_s} \hat{Z}_i \sqrt{\frac{2}{n_s}} \sin\left((2i-1)\frac{\pi}{2L}X\right), \tag{6.12}$$

where $\hat{Z}_i \sim \mathcal{N}(0,1)$, i.e. $\hat{Z}_i$ is standard normally distributed, n_s is the number of terms, and $0 \leq X \leq L$. Let us consider the Young's modulus E. From now this will be a stochastic variable, which we will denote by $\hat{E}$. We can generate a heterogenous realization $E(X)$,

$$\log(E(X)) \sim \mathcal{M} + \mathcal{S}\hat{u}, \tag{6.13}$$

i.e. $E(X)$ is a realization of a *lognormal* distribution with mean $\mathcal{M}$ and standard deviation $\mathcal{S}$, so that:

$$E(X) = \exp(\mathcal{M} + \mathcal{S}\hat{u}(X)). \tag{6.14}$$

If we want $\hat{E}$ to have mean $\bar{E}$ and variance V_E, we need to take:

$$\mathcal{M} = \log\left(\frac{\bar{E}}{\sqrt{1 + V_E/\bar{E}^2}}\right), \tag{6.15}$$

and

$$\mathcal{S} = \sqrt{\log(1 + V_E/\bar{E}^2)}. \tag{6.16}$$

In the same way, we can create heterogeneous, stochastic inputs for $\mu, \rho, \bar{F}_b$, and ζ.

We will base our simulations on the confidence intervals listed in table 6.3.

6.4.2. Statistical results

Using the parameters in table 6.3, 1000 simulations were done. The histograms in figures 6.16 and 6.17 resulted for respectively the maximal contraction and final contraction of the wound.

The empirical cumulative distribution functions (cdf) in figures 6.18 and 6.19 correspond to the histograms in figures 6.16 and 6.17 respectively.

In figure 6.20 we present the mean and 95%-confidence interval for $l(t)$ for each $t \in [0, 60]$.

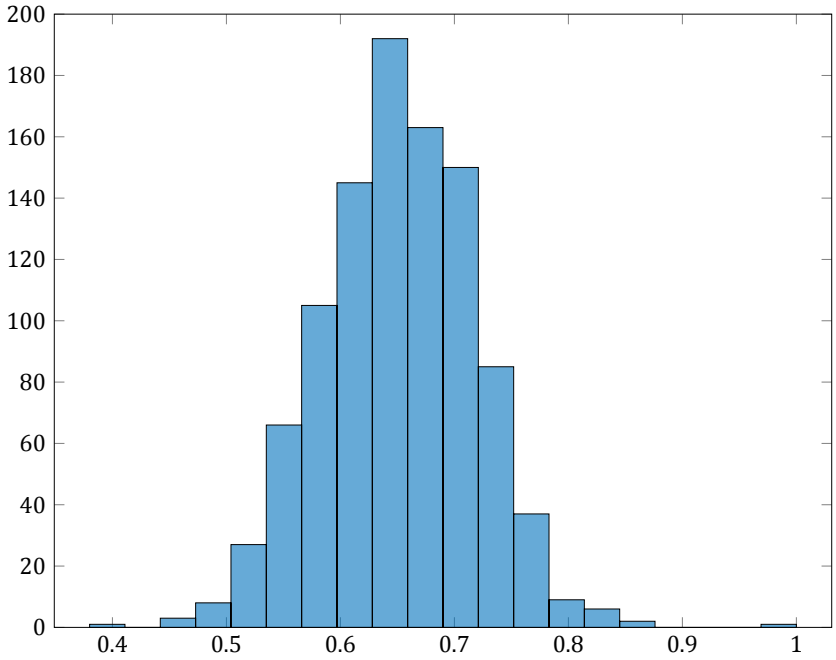

Figure 6.16: A histogram for the maximal contractions.

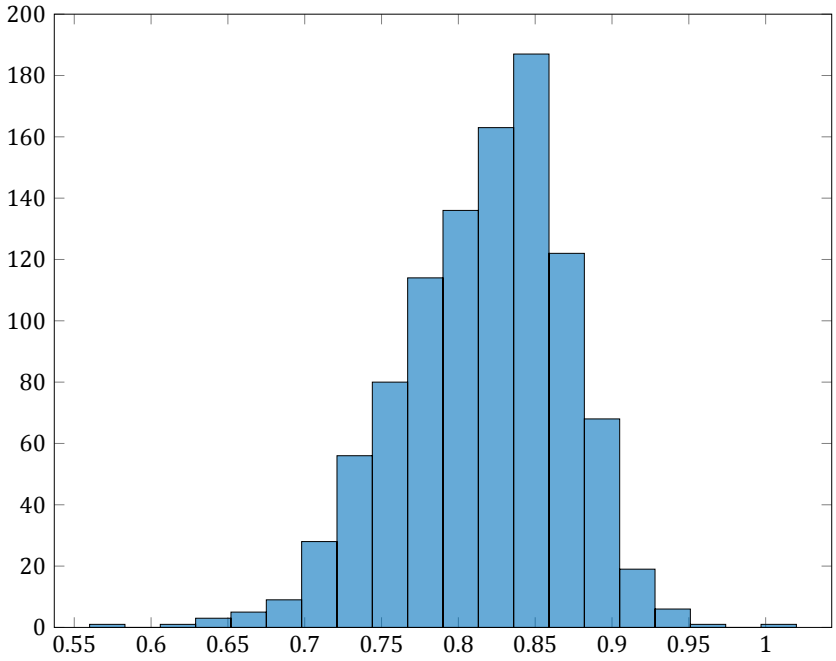

Figure 6.17: A histogram for the final contractions

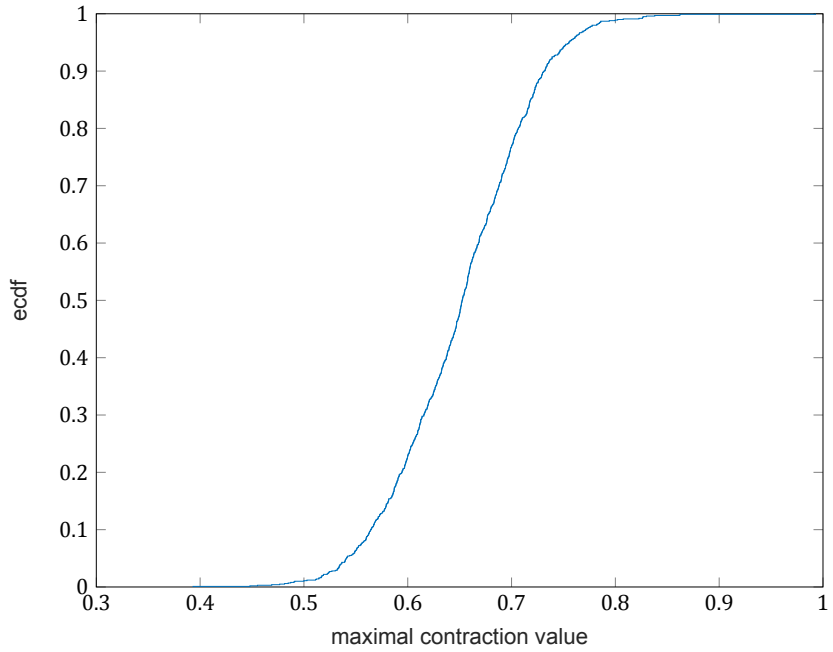

Figure 6.18: Empirical cdf for the maximal contractions.

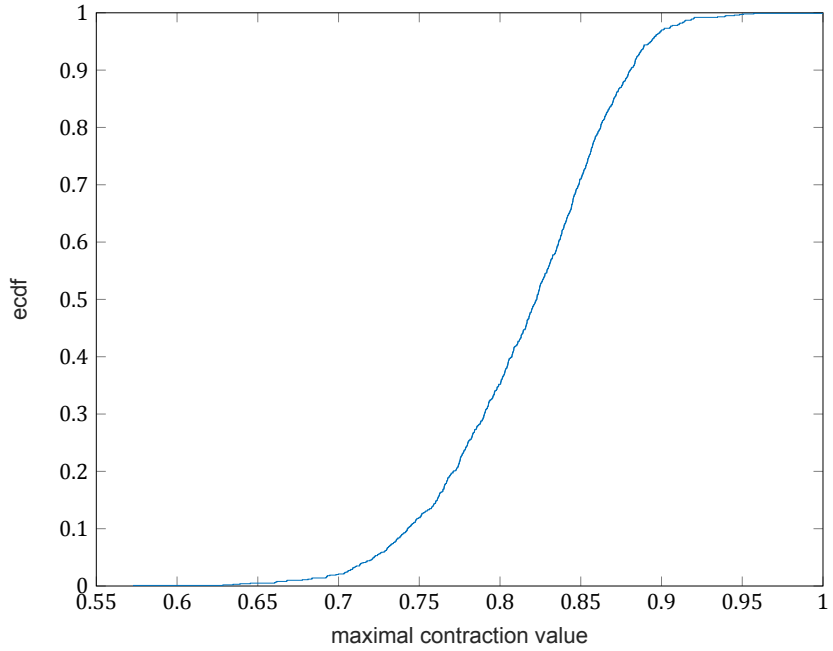

Figure 6.19: Empirical cdf for the final contractions

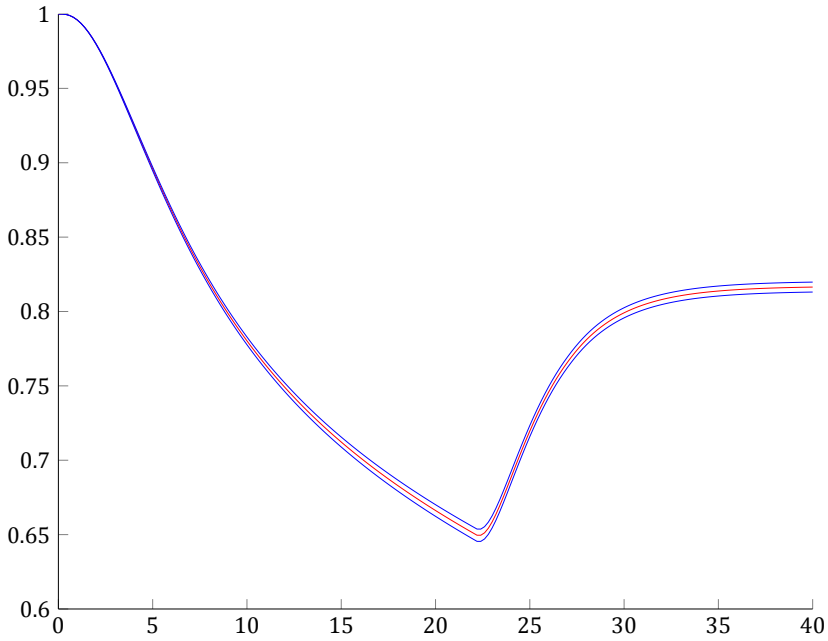

Figure 6.20: Mean (red) and 95%-confidence interval (blue) for $l(t)$ for each t.

6.5. A two-dimensional dynamical viscoelastic model

In this section we will consider model (4.42). From a mechanical point of view, the two-dimensional model is more advanced than the one-dimensional model. For example, we have to deal with shear stress and Poisson's effect. We will present some plots to develop a feel for these phenomena. Additionally, we will look at the deformation of a rectangle, and the evolution of its area in time.

6.5.1. Poisson's effect

To illustrate Poisson's effect, we will run the model with the following body forces:

$$(F_b)_1(x,y) = \begin{cases} \bar{F}_b, & -L/4 \le x \le 0, -L/4 \le y \le L/4, \\ -\bar{F}_b, & 0 < x \le L/4, -L/4 \le y \le L/4, \end{cases} \tag{6.17}$$

$$(F_b)_2 \equiv 0. \tag{6.18}$$

For Poisson's ratio we choose to use the same value as [11], $\nu = 0.48$. The parameters used for this simulation can be found in table 6.4.

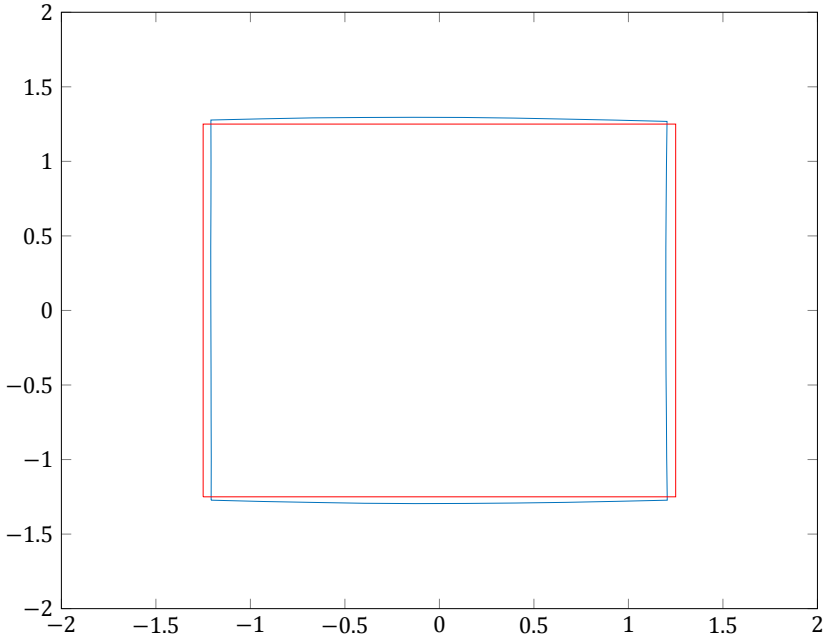

Figure 6.21: Poisson's effect. Original shape in red, and shape at $t = 5$ in blue.

Parameter	Value	Unit
E	31	$\mathrm{N}/(\mathrm{g\,cm})^{1/2}$
μ_1	10^2	(N day)/cm
μ_2	10^2	(N day)/cm
ν	0.49	-
ρ	1.02	g/cm
$\bar{F}_b$	5	(N g)/(cells cm)
t_{f0}	0.1	days
t_{fm}	20	days
t_{ap}	20	days

Table 6.4: The parameters used for the results in section 6.5

6.5.2. Shear stress

To illustrate shear stress, we will run the model with the following body forces:

$$(F_b)_1(x,y) = \begin{cases} \bar{F}_b, & -L/4 \leq x \leq L/4, -L/4 \leq y \leq 0, \\ -\bar{F}_b, & -L/4 \leq x \leq L/4, 0 \leq y \leq L/4, \end{cases} \tag{6.19}$$

$$(F_b)_2(x,y) \equiv 0. \tag{6.20}$$

We use the parameters listed in table 6.4. In figure 6.22 we see the deformation that occurs due to the body forces. In figures 6.23 and 6.24 we see the normal strain in the horizontal direction, and the shear strain.

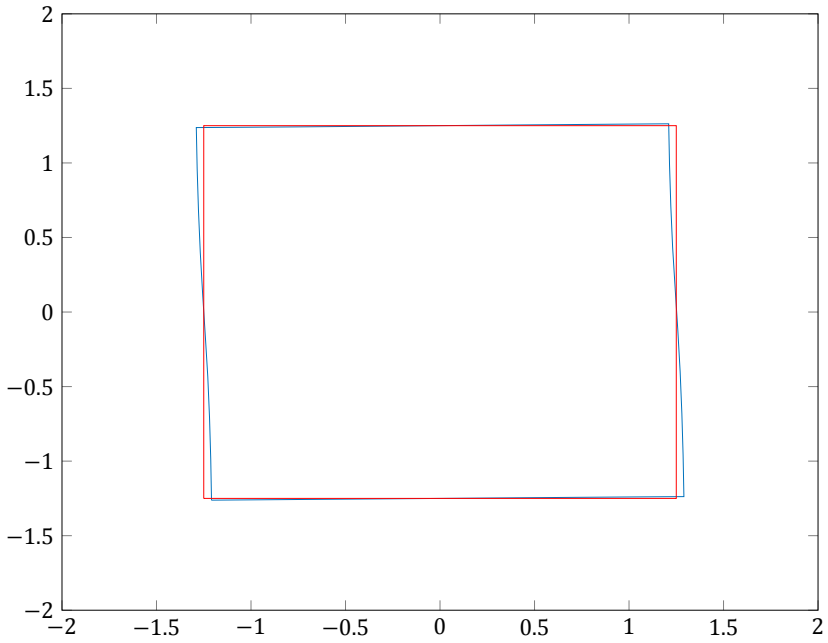

Figure 6.22: Unstrained rectangle (red), and a shape subject to shear deformation at $t = 5$ (blue).

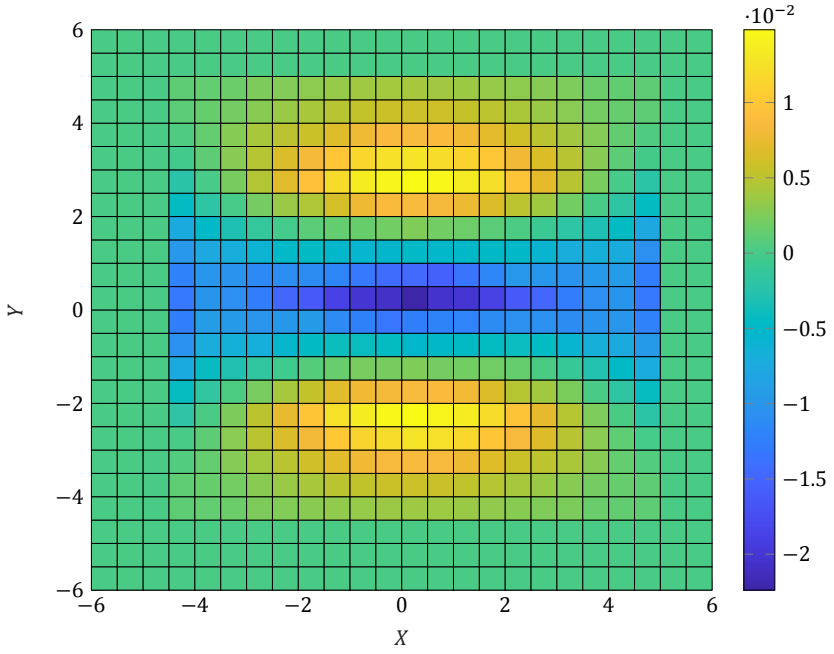

Figure 6.23: Normal strain ϵ_{11} at $t = 5$ under body forces (6.20).

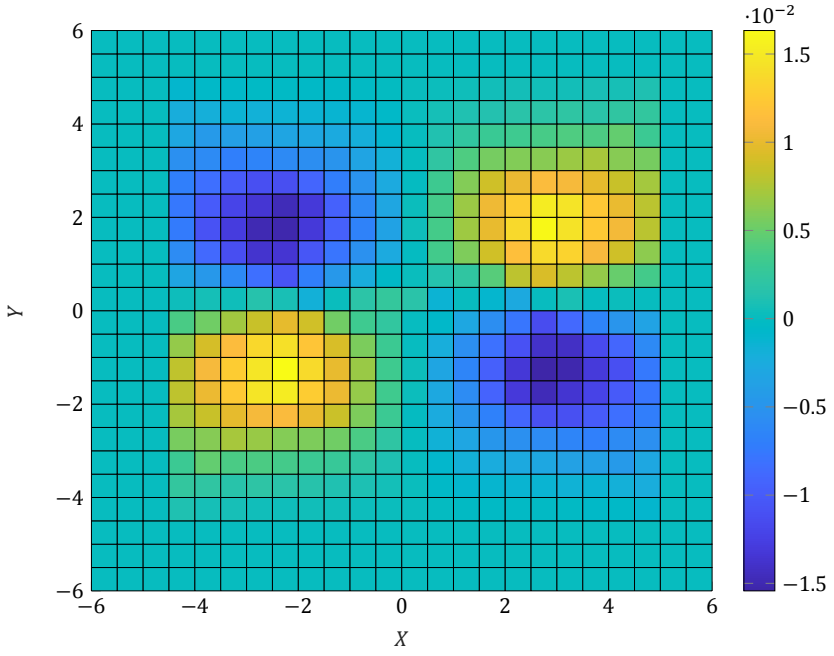

Figure 6.24: Shear strain ϵ_{12} at $t = 5$ under body forces (6.20).

6.6. A two-dimensional morphoelastic model

In this section we will consider model (4.66). Compared to (4.41), this model also involves plastic deformation. In this section we will present results regarding the deformation of a rectangle. We will look at strain values, and the evolution of the area of the rectangle in time.

As explained in 5.2, we have to remesh in order to maintain good accuracy. After experimenting a bit, it turns out that we need to remesh when angles go below 40 degrees. This is a fairly high angle, which means that we have to remesh multiple times.

In figure 6.25 we see a plot the relative area of a rectangle versus time. It can be seen that between $t = 0$ and $t = 20$ the curve is not entirely smooth at some points. This is because at these time points

Parameter	Value	Unit
E	31	$\mathrm{N}/(\mathrm{g\,cm})^{1/2}$
μ_1	10^2	(N day)/cm
μ_2	10^2	(N day)/cm
ν	0.49	-
ρ	1.02	g/cm
$\bar{F}_b$	30	(N g)/(cells cm)
ζ 0.05	-	
t_{f0}	0.1	days
t_{fm}	20	days
t_{ap}	20	days

Table 6.5: The parameters used for the results in section 6.6.

we had to remesh.

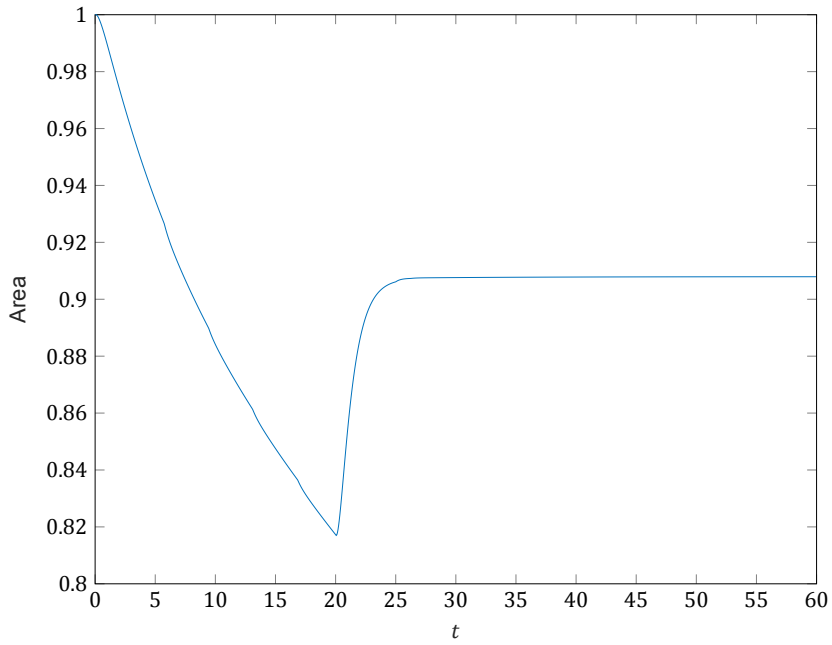

Figure 6.25: Plot of relative area of an initial rectangle versus t.

The parameters used in this section can be found in table 6.5

7

Conclusion, discussion and recommendations

In this thesis we explored some morphoelastic models. The main initial goal was to gain more understanding in these models. We reconstructed the models, starting with rudimentary ones, and ending with a full two-dimensional model.

After the reconstruction of the morphoelastic models, we turned to a novel framework for the incorporation of heterogeneity and stochastics into the one-dimensional model. We were also able to present some statistical results.

Although from a qualitative standpoint the initial goal was hopefully achieved, there are some aspects that could be improved.

Firstly, for a lot of parameters no experimental data is available. In particular, for the fundamental 'morphoelastic parameter' that partially controls the rate of change of plastic deformation, no estimates are available in the literature. Therefore, from a quantitative standpoint, there is a lot of room for improvement.

Secondly, the models could be expanded, to include more relevant wound healing effects. An interesting option could be to include the remodeling of the extra-cellular matrix by fibroblasts. This amounts to constructing an anisotropic model, and a means of incorporating collagen fibre orientation. Also, fibroblast diffusion would need to be included. In [11], diffusion was included. Also, collagen fibre orientation and anisotropy of the tissue are discussed. However, these two phenomena are not included in the two-dimensional model.

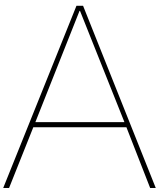

Picard iterations

We will prove here that Picard iterations or *fixed point iterations* converge under the right conditions.

Theorem 2. *Let Ω be a complete metric space and let $f : \Omega \to \Omega$ be a Lipschitz continuous function with Lipschitz constant $\mathbb{L} < 1$. Then f has a unique fixed point, i.e. a point $x \in \Omega$ such that $x = f(x)$. Picard iterations will always converge to this point, i.e. if $x_n := f(x_{n-1})$, then $x_n \to x,\ n \to \infty$.*

Proof. Let $x_0 \in \Omega$ be an initial guess, and let $x_n := f(x_{n-1})$, so that $\{x_n\}_{n\in\mathbb{N}} := \{x_0, x_1, ...\}$ is a sequence of Picard iterations. We have:

$$\begin{aligned} d(x_n, x_{n-1}) &= d(g(x_{n-1}), g(x_{n-2})) \\ &\leq \mathbb{L}d(x_{n-1}, x_{n-2}) \\ &\leq ... \\ &\leq \mathbb{L}^{n-1}d(x_1, x_0). \end{aligned}$$

Since $\mathbb{L} < 1$, we see that $\{x_n\}$ is a Cauchy sequence. Since Ω is complete, it follows that $\{x_n\}$ converges to a limit $x \in \Omega$.

Suppose that x is not a unique fixed point of f. Then apparently there is an initial guess such that the Picard iterations converge to a fixed point $y \neq x$. Since $x = f(x)$ and $y = f(y)$ we then have $d(x, y) = d(f(x), f(y))$, contradicting the Lipschitz condition. So x is unique. □

B

Element integrals

Here we compute the element integrals that are relevant to the derivations in chapter 5. As a reference we used [7].

One-dimensional element integrals

Assume we integrate over an element el. We have:

$$\int_{\mathrm{el}} \phi_m^2 \, \mathrm{d}x = \frac{h}{3}, \tag{B.1}$$

$$\int_{\mathrm{el}} \phi_m \phi_{m+1} \, \mathrm{d}x = \frac{h}{6}, \tag{B.2}$$

$$\int_{\mathrm{el}} \phi_m^3 \, \mathrm{d}x = \frac{h}{4}, \tag{B.3}$$

$$\int_{\mathrm{el}} \phi_{m+1}^2 \phi_m \, \mathrm{d}x = \frac{h}{12}. \tag{B.4}$$

where el is the element with vertices x_m and x_{m+1} and $h = x_{m+1} - x_m$ is the length of the element.

Two-dimensional element integrals

We write $\phi_i(x, y) = \alpha_i + \beta_i x + \gamma_i y$, where α_i, β_i and γ_i are defined as in section 5.2.

An important fact is the following, which was proven by Holand and Bell:

Theorem 3. *If $\phi_1, \dots, \phi_{n+1}$ are linear basis functions on a simplex $S \subset \mathbb{R}^n$, so S has vertices $\mathrm{x}_1, \dots, \mathrm{x}_{n+1}$ and $\phi_i(\mathrm{x}_j) = \delta_{ij}, i, j = 1, \dots, n+1$, then we have:*

$$\int_S \phi_1^{m_1} \cdots \phi_n^{m_{n+1}} \, \mathrm{d}\Omega = \frac{m_1! \cdots m_{n+1}!}{(m_1 + \cdots + m_{n+1} + n)!} |\Delta|, m_1, \dots, m_{n+1} \in \mathbb{N}. \tag{B.5}$$

where $|\Delta|$ is the volume of S multiplied by 2.

Note that in two-dimensional space we are dealing with triangles, and $|\Delta|$ can be computed by doing the following: translate the triangle so that one vertex will be the origin; append zeros to the vectors corresponding to the vertices to make them three-dimensional; compute the cross product of the two vectors defined by the other two - translated - vertices; take the absolute value. An example would be the triangle given by $(1, 1), (1, 2)$ and $(2, 1)$, which would give:

$$|\Delta| = \left|\left((1, 2, 0)^T - (1, 1, 0)^T\right) \times \left((2, 1, 0)^T - (1, 1, 0)^T\right)\right| = 1. \tag{B.6}$$

Assume we integrate over a triangular element el, with vertices $1, 2$ and 3. We have, using the result by Holand and Bell:

$$\int_{\mathrm{el}} \phi_i \phi_j \, \mathrm{d}\Omega = \begin{cases} \frac{1}{24}|\Delta|, & \text{if } i \neq j, \\ \frac{1}{12}|\Delta|, & \text{if } i = j, \end{cases} \tag{B.7}$$

$$\int_{\mathrm{el}} \phi_i \frac{\partial \phi_j}{\partial z} \, \mathrm{d}\Omega = \gamma_j \int_{e_m} \phi_i \, \mathrm{d}\Omega = \frac{1}{6}\gamma_j |\Delta|, \tag{B.8}$$

$$\int_{\mathrm{el}} \phi_i \phi_j \frac{\partial \phi_{j'}}{\partial z} \, \mathrm{d}\Omega = \gamma_{j'} \int_{e_m} \phi_i \phi_j \, \mathrm{d}\Omega = \begin{cases} \frac{1}{24}\gamma_{j'}|\Delta|, & \text{if } i \neq j, \\ \frac{1}{12}\gamma_{j'}|\Delta|, & \text{if } i = j. \end{cases} \tag{B.9}$$

Bibliography

[1] M. Ågren (2016), *Wound Healing Biomaterials*, Woodhead Publishing, ISBN: 9780081006054 0081006055

[2] V. Tiwari (2012), *Burn wound: How it differs from other wounds?*, Indian J Plast Surg., doi: 10.4103/0970-0358.101319

[3] C. Dunkin (2007), *Scarring occurs at a critical depth of skin injury: precise measurement in a graduated dermal scratch in human volunteers*, Plast Reconstr Surg. 119(6):1722-32

[4] E. Rodriguez, A. Hoger and A. McCulloch (1994), *Stress-dependent finite growth in soft elastic tissues*, Journal of biomechanics, 92093-0412

[5] E. Lee and D. Liu (1969), *Elastic-plastic deformation at finite strains*, J Appl Mech

[6] G. Dziuk and C. Elliot (2007), *Finite elements on evolving surfaces*, IMA J Numer Anal 27:262-292

[7] J. van Kan, A. Segal and F. Vermolen (2008), *Numerical Methods in Scientific Computing*, VVSD, ISBN-10 90-71301-50-8

[8] N. Hinrichsen, L. Birk-Sørensen, F. Gottrup and V. Hjortdal (1998), *Wound contraction in an experimental porcine model*, Scandinavian Journal of Plastic and Reconstructive Surgery and Hand Surgery, 32:3, 243-248

[9] T. Hillen and K. Painter (2009), *A user's guide to PDE models for chemotaxis*, J Math Biol 58:183-217

[10] B. Bhushan, W. Tang and S. Ge (2010), *Nanomechanical characterization of skin and skin cream*, Journal of Microscopy 240(2):135-44

[11] D. Koppenol (2017), *Biomedical implications from mathematical models for the simulation of dermal wound healing*

[12] C. Hall (2008), *Modelling of some biological materials using continuum mechanics*

[13] A. Goriely and D. Moulton (2011), *Morphoelasticity: a theory of elastic growth*

[14] S. Menon, C. Hall, S. McCue and D. McElwain (2012), *A model for one-dimensional morphoelasticity and its application to fibroblast-populated collagen lattices*

[15] S. Menon, C. Hall, S. McCue and D.McElwain (2017), *A model for one-dimensional morphoelasticity and its application to fibroblast-populated collagen lattices*

[16] P. Hofmann (2015), *Solid State Physics, an introduction*, Whiley-VCH, ISBN-13: 978-3527412822

[17] J. Stewart (2007), *Single Variable Calculus*, Cengage Learning, ISBN-13: 9780495011699

[18] R. Wasserman (2004), *Tensors and Manifolds, with applications to physics*, Oxford University Press, ISBN: 0198510594 9780198510598

[19] L. Wang (2008), *Karhunen-Loeve Expansions And Their Applications*